Hydraulic Properties of Recycled Pavement Aggregates and Effect of Soil Suction on Resilient Modulus for Pavement Design

By

Kongrat Nokkaew

A dissertation submitted in partial fulfillment of

the requirements for the degree of

Doctor of Philosophy

(Civil and Environmental Engineering)

at the

UNIVERSITY OF WISCONSIN-MADISON

2014

Hydraulic Properties of Recycled Pavement Aggregates and Effect of Soil Suction on Resilient Modulus for Pavement Design

By

Kongrat Nokkaew

A Dissertation submitted in partial fulfillment of

the requirements for the degree of

Doctor of Philosophy

(Civil and Environmental Engineering)

at the

UNIVERSITY OF WISCONSIN-MADISON

2014

Date of final oral examination: 1/8/2014

Month and year degree to be awarded: May 2014

The dissertation is approved by the following members of the Final Oral Committee:

James M. Tinjum, Assistant Professor, Engineering Professional Development
Tuncer B. Edil, Professor, Civil and Environmental Engineering
Craig H. Benson, Professor, Civil and Environmental Engineering
William J. Likos, Associate Professor, Civil and Environmental Engineering
Hussain U. Bahi, Professor, Civil and Environmental Engineering
King-Jau S. Kung, Professor, Soil Science

DEDICATION

To Mam and Dad for unconditional love and support.

ABSTRACT

The successful incorporation of recycled aggregates in pavement design is important for achieving a higher level of sustainability in our transportation network. However, recycled aggregates are non-soil materials and have different unsaturated hydraulic and resilient modulus characteristics. This study investigated the unsaturated hydraulic properties and impact of soil suction on resilient modulus for compacted recycled aggregates used as unbound base course, including recycled asphalt pavement (RAP), recycled concrete aggregate (RCA), and recycled pavement material (RPM). Hydraulic properties and relationships including the soil-water characteristic curve (SWCC) and saturated and unsaturated hydraulic conductivity (K_s and K_ψ), were characterized using a hanging column test coupled with a large-scale testing cell. Regression of the hydraulic parameters from SWCC and K_ψ data for each type of recycled materials was completed. The effect of water repellency on hydraulic properties was evaluated. Development of testing equipment and procedures that incorporate the effect of soil suction during resilient modulus measurement is presented. A mathematical model to predict resilient modulus based on bulk stress, octahedrons shear stress, and soil suction is proposed. In addition, empirical relationships for predicting summary resilient modulus (SRM) via soil suction and SRM at optimum compaction for recycled aggregates are presented. Measured SRM and SWCCs for different types of recycled aggregate were used to evaluate flexible pavement performance according to the approach outlined in the Mechanistic-Empirical Pavement Design Guide (M-EPDG). The impact of environmental effects (including freeze-thaw cycles and changes in temperature) on the resilient modulus of recycled aggregates and subsequent pavement performance are evaluated and presented in this dissertation.

ACKNOWLEDGEMENTS

I would like to thank my advisor, Professor James Tinjum for his support and guidance during my Ph.D. Study at UW-Madison. Professor Tinjum always dedicates his time and effort to my progress and keeps my research connected to practical applications. Professor Tinjum has helped prepare me for entry to the working world. I would like to thank my committee members, Professors Tuncer Edil, Craig Benson, William Likos, King-Jua Kung, and Hussain Bahia for their guidance and for serving as committee members. Without the support and guidance from them, I would not be where I am today.

I am deeply grateful to Xiaodong “Buff” Wang, the manager of UW-Madison’s Soil Mechanics Laboratory, for his technical advice and laboratory assistance throughout this study. I also would like to thank William Lang, the manager of UW-Madison’s Structures and Materials Laboratory and Jackie Bastyr-Cooper, manager of the Environmental Engineering Laboratory, for laboratory assistance and support with material procurement.

I would like to thank all geo-friends at the University of Wisconsin-Madison for their friendship and support. A special thanks to Ron Breitmeyer for his help in understanding and applying unsaturated soil mechanics to my study objectives, Jiannan Chen for his help in sample collection, and Andrew Keene and Ryan Shedivy for their help in setting up the resilient modulus equipment tests and subsequent analysis. I would also like to thank Raul Velasquez for providing the M-EPDG software package and guiding me through the use of this package. This assistance from past and current members of the Transportation Geotechnics Research Group (Ozlem Boyzurt, Andew Keene, Makhaly Ba, Mababa Diagne, Ali Soleimanbaigi, Michael Patinkin, Ben Tanko, and Ben Warrant) is greatly appreciated.

Finally, I would like to thank my family for their unconditional love and support. They mean everything to me. They always understood, encouraged, and believed in my ability. Without them, I would not have been able to succeed in graduate school.

Support for this study was provided by the Ministry of Science and Technology, Thailand, and Kasetsart University at Sakhonakhon, Thailand. I would also like to acknowledge the University of Wisconsin System (Solid Waste Research Program) and the Recycled Material Research Center (RMRC) for their financial assistance used for experimental design and setup and the supply of recycled materials used this study.

TABLE OF CONTENTS

LIST OF TABLES

LIST OF FIGURES

CHAPTER 1: EXCECUTIVE SUMMARY

1.1 INTRODUCTION

The demand to beneficially reuse construction and demolition (C&D) waste has increased in recent decades, which promotes the sustainable use of construction materials. Every year, more than 300 million tons of C&D wastes are produced and generated in the US, many of which can be reused in the base course layer in road construction (CSI 2013; NAPA 2013). C&D waste including recycled asphalt pavement (RAP), recycled concrete aggregate (RCA), and recycled pavement material (RPM) provide proven, high-quality mechanical properties and significant life-cycle benefits when they are used as a substitute for natural aggregates for the base course layer in pavement construction. However, recycled aggregates are non-soil materials and have different resilient modulus and hydraulic characteristics (Bennert et al. 2000; Blankenagel 2006; Bozyurt 2011; Nokkaew 2012). The resilient modulus and hydraulic properties of aggregates are primary input parameters required for the relatively new mechanistic approach to pavement design that predicts the long-term performance of pavement. However, there is limited data available to characterize the hydraulic and resilient modulus characteristic of recycled aggregates and thus provide an assessment of their long-term performance in a pavement system.

This objectives of this dissertation were to (1) comprehensively investigate the hydraulic properties of recycled aggregates including the soil-water characteristic curve (SWCC), saturated and unsaturated hydraulic conductivity (K_s and K_ψ), and water repellency; (2) develop testing equipment and a procedure to incorporate the effect of soil suction during the measurement of resilient modulus; and (3) assess pavement performance when recycled

aggregates are used as an unbound base course. An experimental laboratory program on recycled aggregates was designed and implemented to evaluate the following hypotheses (1) recycled aggregates with different water repellency may result in a change in hydraulic behavior as measured using hanging column testing technquies coupled with a large-scale cell, (2) the effect of moisture on resilient modulus can be described using the soil suction concept (i.e., soil suction affects the state of stress of recycled and natural pavement aggregates and subsequently impacts the modulus); (3) environmental effects such as freeze-thaw cycling and changes in temperature change the behavior of recycled aggregates via changes in the resilient modulus; and (4) long-term performance of pavement can be evaluated using the approach contained in the Mechanistic-Empirical Pavement Design Guide (M-EPDG) using specific inputs for recycled aggregates as measured in this study.

Three papers prepared for publication (one accepted by the Transportation Research Board and two in preparation for submittal) comprise the main chapters in this dissertation:

- Hydraulic properties of recycled aggregates (Chapter 2) – note that an early version of this chapter has been published in the Proceedings of the ASCE Geo Congress (2012)
- Effect of matric suction on resilient modulus for compacted recycled base course (Chapter 3) – accepted for publication in the Journal of the Transportation Research Board
- Performance evaluation for recycled aggregate used as unbound base course per the Mechanistic-Empirical Pavement Design Guide (M-EPDG) (Chapter 4) – prepared for publication in the Road Materials and Pavement Design
- Hydraulic properties of recycled asphalt pavement and recycled concrete aggregate (Appendix A) – published in the Proceedings of the ASCE Geo Congress (2012)

- Effect of matric suction on resilient modulus of compacted aggregate base courses (Appendix B) -- published in the Geotechnical and Geological Engineering

1.2 HYDRAULIC PROPERTIES OF RECYCLED PAVEMENT AGGREGATES

Six RCAs, six RAPs, two RPMs and two conventional aggregates were collected from different geographical regions in the US, and used to characterize the hydraulic properties. The hydrophobicity of recycled and natural base course was characterized by using water drop penetration time (WDPT) and contact angle measurement with ten replication tests (Chapter 2.5.1). Saturated hydraulic conductivity was measured using a rigid-wall, compaction-mold permeameter. The multistep outflow (MSO) method was used to measure the SWCC and K_ψ from specimen aggregates prepared at 95% of maximum dry density according to the modified Proctor test. The tests were conducted using a hanging column test with a large-scale cell fitted with air aspirator (Chapter 2.5.3). The SWCC and K_ψ data were fitted simultaneously using a constitutive function linked to the pore interaction term (L), which may describe tortuosity in aggregate structures (Chapter 2.5.5). A bimodal SWCC was developed using a constitutive function to estimate the hydraulic parameters of bimodal aggregates, such as RCA-Michigan and RCA-Texas.

According to WDPT and contact angle measurement, the WDPTs of studied RCAs and conventional aggregate were lower than 1 s with a contact angle of approximately 0^o, which indicates hydrophobic nature. In contrast, most studied RAPs and RPMs had WDPTs larger than 3600 s and average contact angles larger than 69^o, which are representative of strongly hydrophobic materials. The water repellency affects the K_s and SWCC characteristics. RCAs tended to provide lower K_S (approximately one order of magnitude) in comparison to RAPs and RPMs, although RCAs have higher porosity.

The hanging column test measures suction accurately, especially when lower than 1 kPa, and is thus suitable for the measurement of the SWCC of granular base course where the water in specimen can change rapidly over small, incremental changes in soil suction. However, for K_ψ measurement, the hydraulic impedance of the employed ceramic plate limited the K_ψ when K_ψ was lower than 10^{-7} m/s. Hydrophobic RAPs and RPM tend to provide lower air entry pressure (ψ_a) and steeper SWCC slopes than hydrophilic RCA and conventional base course. As soil suction in the field is directly related to the climatic condition, this may imply that RAP and RPM tend to have lower field water contents in comparison to RCA and conventional aggregates at the same environmental condition. Gap-graded RCAs present with bimodal SWCCs. Bimodal SWCC data for recycled aggregates were fit well using the bimodal van Genuchten equation that is described in Burger and Shackelford (2001).

RAP and RPM with hydrophobic properties tended to have an 'n' parameter (described in van Genuchten 1980) that was higher than n parameters measured for hydrophilic RCA and conventional aggregates. The pore interaction term (L), was measured as a positive and negative in this study, depending on the recycled aggregate evaluated. In comparing RAPs, RCAs, and RPMs with similar grain size distributions, increasing contact angles from hydrophobic base course resulted in decreasing ψ_a and decreasing slope in the SWCC. These findings indicate that water repellency properties directly impact the shape of the SWCC. Because of their ability to repel water, RAPs and RPMs have inherent properties that may benefit their incorporation into base course, particularly where moisture susceptibility is of concern and/or relevant.

1.3 EFFECT OF SOIL SUCTION ON RESILIENT MODULUS FOR COMPACTED RECYCLED BASE COURSE

Selected recycled aggregates (including RAP from Wisconsin, RAC from Wisconsin, RPM from Michigan, and conventional crushed stone) were used to characterize the inter-dependency of soil suction and resilient modulus. Resilient modulus tests were conducted in accordance with NCHRP 1-28A Procedure Ia. Equipment modifications allowed for an applied and control ψ ranging from 1.5 kPa to 65 kPa during testing (Chapter 3.5.1, and Chapter 3.5.2). A mathematical model is proposed that incorporates parameters from the SWCC to predict summary resilient modulus (SRM); i.e., the in-service M_r at representative field stress state (Chapter 3.5.4). An empirical relationship for predicting SRM based on soil suction and SRM at optimum compaction for recycled aggregates is developed and presented in this chapter.

The relationship of M_r along the desorption path of the SWCC (which was experimentally measured) was used to develop a mathematic model for predicting M_r based on bulk stress, octahedral shear stress, and soil suction. For the base course aggregates evaluated in this study, SRM decreased with decreasing degree of saturation. RAP-WI provided the highest SRM, while limestone-WI provided the lowest SRM. These findings support previous research (Bennert et al. 2000; Guthri et al. 2007; Carmago et al. 2008) that recycled base course (RAP, RPM, and RCA) provides high values of SRM, and are suitable for use as unbound base course.

SRM values for the base courses tended to increase with increasing matric suction. A proposed mechanistic model provided a strong fit between SRM and suction for test specimens within the range of measured soil suction (1 kPa to 100 kPa; that is, the range common for in-service aggregates), with R^2 ranging from 0.83 to 0.98. A consistent relationship between normalized SRM with the SRM at the optimum water content (SRM/SRM_{opt}) and degree of

saturation could not be developed at this time. The SRM ratio for different types of base course forms a single linear relationship with logarithmic soil suction within a narrow range (± 0.1 SRM/SRM_{opt}).

1.4 CHAPTER 4: PERPORMANCE EVAUATION FOR RECYCLED AGGREGATE USED AS UNBOUND BASE COURSE PER THE MECHANISTIC-EMPIRICAL PAVEMENT DESIGN GUIDE (M-EPDG)

Measured M_r and SWCCs for different types of recycled aggregate were used to evaluate flexible pavement performance by using the Mechanistic-Empirical Pavement Design Guide (M-EPDG). The M-EPDG incorporates variation of material properties, traffic input, climate, and environmental effects into structural pavement design. Distresses (including longitudinal cracking, alligator cracking, total rutting, and international roughness index, IRI) predicted from M-EPDG after 20 years of service life were compared against the quality of recycled base course. The effect of freez-thaw cycling on pavement performance was evaluated by using a relationship between the number of freeze-thaw cycles and resilient modulus for recycled aggregate that was developed by Bozyurt (2011). The impact of temperature on pavement performance was also assessed using a relationship between temperature and resilient modulus that was developed by Shedivy (2012).

In characterizing the resilient modulus for recycled materials including RAPs, RCAs, and RPMs, the RPMs tended to provide higher SRM when compared to control aggregates. The M-EPDG uses M_r as a primary parameter to predict the varying forms and levels of distresses. Thus, consistent with recycled aggregates having higher as-compacted resilient moduli, each distress prediction of a pavement by the M-EPDG using recycled material tended to be lower than for those pavements using conventional material. The comparison between modulus input Level 1, which requires three fitting parameters (k_1, k_2 and k_3 from the Witczack-Uzan universal

equation), and modulus input level 3, which requires a measured SRM for the analysis, presented significant differences. Using modulus level 3 in the M-EPDG analysis was not conservative for alligator cracking, total rutting, and IRI prediction.

The SWCC predicted from the grain-size distribution within M-EPDG tended to provide higher air entry pressure and a steeper slope for the SWCC when compared to the measured SWCCs obtained through testing with hanging column apparatus. However, the distress predictions were not significantly changed (P-values from the analysis of variance (ANOVA) are larger than 0.43 for all type of distress analyses). This indicates that results from M-EPDG are not necessarily sensitive to the hydraulic properties inputs.

With increasing number of freeze-thaw cycles, the SRMs for RAPs decreased. In contrast, SRM for RCAs actually increased after freeze-thaw cycling. The increase in SRM for RCAs subjected to freeze-thaw cycling is likely due to the self-cementing behavior of adhered mortar in RCAs (Arm 2001). The distress prediction due to freeze and thaw cycles corresponds to the SRM. The predicted distresses decreased with increased SRM. Amongst the forms of distresses predicted within M-EPDG, fatigue cracking was most sensitive to freeze-thaw cycling. Increased temperature reduced the SRMs of RAPs due to viscous behavior of asphalt; however, the predicted distress from M-EPDG did not significantly change the distress prediction for pavements that used RAPs as a base course layer.

1.5 FUTURE WORKS

This study presents a high-quality set of data and supporting analysis that characterizes the hydraulic properties of recycled aggregates (RAPs, RCAs, RPMs) with direct comparison to conventional aggregates, including impacts to resilient modulus and thus pavement distress as

evaluated with the M-EPDG. The following areas are recommended for future study on the hydraulic and structural behavior of recycled aggregates:

1. As the expected in-service life of pavement depends on the ability for base aggregate to drain excessive water from the structure, the hydraulic behavior of recycled aggregates used as base course is important. Current drainage design in pavements is typically based on an analysis of saturated conditions, which thus overestimates hydraulic conductivity. Using an unsaturated flow analysis will provide a more realistic prediction. Also, the drainage capacity of pavement that incorporates recycled material requires further study.
2. Effects due to hysteresis might play an important role in determining the relationship between soil suction and resilient modulus because base course in the field is routinely subjected to moisture cycling from freeze-thaw cycles, wet-dry cycling, and temperature change.
3. Tests on additional test materials for each type of recycled aggregate are recommend to develop stronger statistical relationships between soil suction and resilient modulus.
4. The strain-dependent modulus degradation curve should be developed for each type of unsaturated recycled aggregate.
5. Plastic deformation behavior of recycled aggregate is important for predicting rutting for flexible pavements. RAP composed of asphalt binder tends to provide high plastic deformation in comparison to other base course materials when subjected to traffic loading. Accordingly, calibration factors due to plastic deformation should be incorporated in mechanistic pavement design.

1.6 REFERENCES

Arm, M. (2001). “Self-cementing Properties of Crushed Demolished Concrete in Unbound Layers: Results from Triaxial Tests and Field Tests.” *Waste Management*, 235-239.

Bennert, T., Papp Jr., W.J., Maher, A., and Gucunski, N. (2000). “Utilization of Construction and Demolition Debris under Traffic-Type Loading in Base and Subbase Applications,” *Journal of Transportation Research Record,* No. 1714, Transportation Research Board, Washington DC, 33-39.

Blankenagel, B.J., and Guthrie, W.S. (2006). “Laboratory Characterization of Recycled Concrete for Use as Pavement Base Material,” *Journal of Transportation Research. Record,* No. 1952, Transportation Research Board, Washington DC, 21–27.

Bozyurt, O. (2011). “Behavior of Recycled Pavement and Concrete Aggregate as Unbound Road Base,” Master Thesis, University of Wisconsin, Madison, WI.

Burger, C.A., and Shackelford, C.D. (2001). “Soil-Water Characteristic Curves and Dual Porosity of Sand-Diatomaceous Earth Mixtures,” *Journal of Geotechnical and Geoenvironmental Engineering*., Vol. 38, No.1, 53-56.

Carmago, F., Benson, C.H., and Edil, T.B. (2012). “An Assessment of Resilient Modulus Testing: Internal and External Deflection Measurements,” *Geotechnical Testing Journal*, Vol. 35, No. 6, 2012, 837-844.

CSI (2013). “Recycling Concrete,” Cement Sustainability Initiative, Conches-Geneva, Swisserland (http://www.wbcsdcement.org/pdf/CSI-RecyclingConcrete-FullReport.pdf)

Guthri, S. W., Cooley, D., and Eggett, D. L. (2007). “Effects of Reclaimed Asphalt Pavement on Mechanical Properties of Base Materials.” *Journal of the Transportation Research Board,* No.2005, Washington, DC, 44-52.

NAPA (2013). “Asphalt: Greener than Ever,” National Asphalt Pavement Association and Federal Highway Administration, Washington, D.C. (http://www.asphaltpavement.org)

Nokkaew, K., Tinjum, J.M., and Benson, C.H. (2012). “Hydraulic Properties of Recycled Asphalt Pavement and Recycled Concrete Aggregate,” *In GeoCongress 2012*, ASCE, Oakland, CA, 1476-1485.

Shedivy, R.F. (2012). “The Effect of Climatic Condition and Brick Content on Recycled Asphalt Pavement and Recycled Concrete Aggregate as Unbound Road Base,” Master Thesis, University of Wisconsin, Madison, WI.

CHAPTER 2: HYDRAULIC PROPERTIES OF RECYCLED AGRREGATES

2.1 ABSTRACT

Unsaturated and saturated hydraulic properties were characterized for six compacted recycled concrete aggregates (RCA), six recycled asphalt pavements (RAP), two recycled pavement aggregates (RPM), Minnesota class 5 aggregate, and Wisconsin limestone used as base course. Tested materials were derived from different highway construction projects across the US. Saturated hydraulic conductivities (K_s) were conducted on tested specimens using constant head, rigid-wall permeameter. Desorption Soil-water characteristic curves (SWCC) were measured using hanging columns with large-scale testing cells (305-mm inner diameter and 76-mm height) fitted with air aspirators. The unsaturated hydraulic conductivity curve $K(\psi)$ was measured using the multistep outflow method (MSO). Hydraulic parameters for each recycled base course were determined using the Mualem-van Genuchten model based on non-linear regression on SWCC and $K(\psi)$ data. The degree of water repellencies (hydrophobicity) of recycled and natural aggregate was quantified using water drop penetration time (WDPT) and contact angle measurement. RAP and RPM behaved as strong hydrophobic materials while RCA and conventional aggregate were hydrophilic. Hanging column test data provided precise measurement at low-suction (<1 kPa), which is required for base course. Most studied base courses exhibited unimodal SWCCs, except two gap-graded RCAs, which were bimodal. The hydraulic parameters from the van Genuchten (1980) model are summarized. Hydrophobic base course with high contact angle tended to provide high drainage for suctions < 75 kPA (the range evaluated in this study) This may imply that RAP and RPM should be used as a base course when the moisture susceptibility is of significant concern.

2.2 INTRODUCTION

Growth in roadway construction and rehabilitation in the United States has increased the demand of virgin aggregate, with increased energy consumption in the crushing process and transportation of the material (Lee et al. 2010). The United States Geological Survey (USGS 2011) reported that 1.16 billion metric ton (Gt) of crushed stone was produced in the United State in 2010, and 80% was used as industrial construction aggregate, mostly for highway and road construction and maintenance. However, the limitation of high-quality natural aggregate sources, stricter environment regulation, and restrictive land use policies have dramatically raised the price of natural aggregate (APA 2009).

Beneficial reuse of construction and demolition (C&D) waste offers a viable alternative to natural aggregate and also reduces the amount of landfilled material (Poon et al. 2006; Aatheesan et al. 2008). C&D wastes can be generated from different sources (e.g., concrete, brick, steel, timber, asphalt concrete) (Rahardjo et al. 2010). Among C&D wastes, materials from recycling of the road surface—including recycled concrete aggregate (RCA), recycled asphalt pavement (RAP), and recycled pavement material (RPM) —are the most widely generated and used each year. RCA is crushed concrete obtained from demolished concrete, RAP is aggregate derived from asphalt pavement, and RPM originates from crushed asphalt surface in addition to the underlying base course materials. USGS (2011) reported that 13.4 Mt of RCA and 11.4 Mt of RAP and RPM were produced in 48 states across the US, and recycled material usage is increasing each year.

RCA, RAP and RPM are proven to provide excellent mechanical properties and significant life-cycle benefits as a mixture or full replacement for natural base course (Bennert et al. 2000; Blankenagel and Guthrie 2006; Guthie et al. 2007; Boyzurt 2011). The hydraulic properties of base course, such as the saturated hydraulic conductivity (K_s), affect the long-term

performance and service life of pavement (Cedergren 1988; Cedergren 1994). Although most pavements are unsaturated for the vast majority of their lifespan, the unsaturated hydraulic properties, including soil-water characteristic curves (SWCC) and unsaturated hydraulic conductivity curves (K(ψ)), of recycled aggregates have not been thoroughly investigated. Water entering into the pavement structure can increase pore pressures and consequently reduce the strength and stiffness of the base course, leading to pavement distress (Huang 2004). The Mechanistic-Empirical Pavement Design Guide (M-EPDG) incorporates the impact of moisture for conventional base course in the pavement structure by adjusting resilient modulus as a function of degree of saturation (NCHRP 2004). However, RCA, RAP, and RPM are generated from non-soil material and may provide varying degrees of wettability (hydrophobicity), which then may result in changes in hydraulic properties.

Natural aggregates are typically hydrophilic. Similar in nature, RCA is comprised of a high number of small pores and, combined with mortar paste providing an additional degree of absorption, is hydrophilic (Tam et al. 2004; Vivian et al. 2005). RAP and RPM have a tendency to be strongly hydrophobic due to asphalt coatings on the aggregate surfaces (Pease 2010; Rahardjo et al. 2010). The degree of hydrophobicity affects the SWCC via capillary phenomena for granular materials (Dekker et al. 1994; Dekker et al. 1998; Bauters et al. 2000). Accordingly, the hydraulic response to change in suction for recycled material with different absorption characteristics may be different (in comparison to natural aggregates).

The objectives of this study were to measure and characterize the SWCC, K_s, and $K(\psi)$ relationship for compacted RCAs, RAPs, RPMs used as base course for pavements. Tested aggregates were obtained from varying states across the US. The SWCC was measured using a hanging column apparatus fitted with air aspirator. K_s was determined using a rigid-wall permeable mold, while $K(\psi)$ was measured using the multistep outflow method (MSO). The

hydraulic parameters for studied materials were determined from regression of van Genuchten's (1980) model (VG model) based on measured SWCC and $K(\psi)$ data. The effect of hydrophobicity on hydraulic properties is discussed. Experimental results from recycled materials are compared to Class 5 aggregate (a conventional base course used in Minnesota), and crushed limestone from Wisconsin.

2.3 BACKGROUND

2.3.1 SWCC and $\mathrm{K}(\psi)$ Constitutive Model

One of the most widely used models for predicting the SWCC is the van Genuchten (1980) fitting equation (VG). The VG equation is a smooth, sigmoidal curve that is suitable for various types of soil and which provides fitting parameters with physical meaning. The VG equation for the SWCC is:

$$\Theta = \frac{(\theta-\theta_r)}{(\theta_s-\theta_r)} = [1+[\alpha\psi]^n]^{-m} \quad \text{(Eq. 2.1)}$$

where Θ is normalized volumetric water content, θ is volumetric water content, θ_r and θ_s are residual and saturated volumetric water contents, ψ is soil suction, α (> 0) is related to the inverse of air-entry pressure, n (> 1) relates to pore size distribution, and m is defined as 1 - 1/ n in this study.

$K(\psi)$ is the relationship between hydraulic conductivity (K) and soil suction. $K(\psi)$ can be predicted based on SWCC parameters using the Mualem-van Genuchten model (MVG) as:

$$\mathrm{K}(\psi) = K_o S_e^L \left[1-\left(1-S_e^{1/m}\right)^m\right]^2 \quad \text{(Eq. 2.2)}$$

where L is the pore-interaction term, which is related to pore-size distribution and tortuosity of soil textures. K_o is the hydraulic conductivity at saturation that is obtained from regression.

Mualem (1976) investigated 45 data sets from soil samples and found that L can be either negative or positive, and the optimal value of L is 0.5. If K_s is not known, then K_o is usually assumed to be K_s.

2.3.2 Bimodal SWCC

The general shape of the SWCC for base courses is S-shaped with low air-entry pressure (ψ_a) (Rahardjo et al. 2010). The air-entry pressure is the soil suction at which water first starts to drain from large pores. For gap-graded aggregate, bimodal grain-size and pore-size distributions are usually exhibited. In this case, discontinuity in the shape of the SWCC is typically observed. Aggregates commonly have two distinct pore-size distributions; one for macroscopic porosity (inter-granular pores) and another for microscopic porosity (intra-granular pores) (Smettem and Kirkby 1990; Zhang and Chen 2005; Fredlund 2000). A bimodal SWCC has two continuous S-shaped portions of the curve and a double ψ_a.

The curve fit of a bimodal SWCC may be developed from a unimodal SWCC function from the van Genuchten model (Burger and Shackerford 2001a; Burger and Shackerford 2001b). The bimodal SWCC is separated into microscopic and macroscopic regions by an inflexion or match point, which is described by Burger and Shackerford (2001b). The SWCC of bimodal soil can be developed using the unimodal formulation of the VG SWCC, as follows:

$$\theta = \begin{cases} \theta_r + (\theta_j - \theta_r)\left[1 + [\alpha'\psi]^{\beta'}\right]^{-(1-1/\beta')}; & \psi_j < \psi \\ \theta_j + (\theta_s - \theta_j)\left[1 + [\alpha\psi]^{\beta}\right]^{-(1-1/\beta)}; & \psi \le \psi_j \end{cases} \quad \text{(Eq. 2.3)}$$

where α' and β' are fitting parameters for the microscopic portion, and α and β are fitting parameters for the macroscopic portion. ψ_j and θ_j correspond to ψ and θ at the matching point, or the point that separates micro-and macro-flow behavior.

2.3.3 Effect of Hydrophobicity on Hydraulic Properties

Recycled and natural pavement aggregates are generated from different material types (e.g., recycled asphalt, recycled concrete, and natural rock such as granite, limestone, and dolomite). Thus, hydrophobicity, the ability to repel water from particle surface, varies depending on the surface properties of the aggregates. Buaters et al. (2000) indicated that hydrophobicity affects soil suction via the contact angle, which is defined as the angle between the solid-water interface (α_o) as shown in Figure. 2.1. A perfectly hydrophobic soil has a contact angle of 180^o, while the contact angle of a perfectly hydrophilic material tends towards 0^o (Letely et al. 2000). The contact angle is a dynamic property that depends on the energy state of water in soil. The contact angle on a dry surface (α_o) is representative of the contact angle of soil (Bauters et al. 2000).

The effect of hydrophobicity of soil on unsaturated hydraulic properties can be described via the contact angle by capillary phenomenon, as shown in Figure 2.2 (Hillel 1998; Lu and Likos 2004). The contact angle can change the effective soil suction, thus impacting the shape of the SWCC. The soil suction (ψ) at a specific pore radius (r) is a function of surface tension (σ) in kN/m^3 and α according to the Kelvin equation:

$$\psi = -\frac{\sigma}{\rho_w g R} \quad \text{(Eq. 2.4)}$$

$$R = \frac{r}{cos\alpha_o} \quad \text{(Eq. 2.5)}$$

where R is the radius of the meniscus in m, ρ_w is the density of water in kg/m^3, g is the gravitational acceleration in m/s^2, and r is the pore radius in m.

For perfectly hydrophilic material, α_o tends to be approximately 0^o, thus generating negative pressure per Eq. 2.4 and Eq. 2.5. In contrast, strongly hydrophobic material with α_o

larger than 90^{o} will generate positive pore pressure. As a result, hydrophobic and hydrophilic aggregate with similar soil texture will have different SWCC and flow characteristic. Details of the impact of hydrophobicity on the SWCC and hydraulic conductivity are presented in July et al. (1991), Bauters et al. (2000), and Bachmann et al. (2007).

2.4 MATERIALS

2.4.1 Physical Properties

Six RCAs, six RAPs, two RPMs and two conventional aggregates were collected from different construction sites or quarries in states across the US. The materials were named according to the state of material origin; for example, RCA-WI is RCA obtained from Wisconsin. All specimens were non-plastic, coarse-grained material with fines content less than 5% except RCA-CO, Class 5-MN, and limestone-WI as shown in Table 2.1. The grain-size distributions of recycled and natural aggregates were characterized based on ASTM D 422. All study materials have been used as base course in roadway construction. The gradation curves were classified following ASTM D 2487. The specific gravity (G_s), porosity (n), dry unit weight (γ_d), coefficient of uniformity (C_u), and coefficient of curvature (C_c), percent gravel, percent sand, and percent fines are summarized in Table 2.1.

2.4.2 Percent of Mortar/Asphalt Content, Percent of Absorption and Hydrophobicity

Mortar content of RCA was determined by immersing 500 g of specimen in 10% HCl solution for 24 h. The specimens were then sieved through a 5-mm sieve and the loss calculated (Gokce et al. 2001). Asphalt content of the RAPs and RPMs was determined per ASTM D 6307. The percent absorption is an important property that is an index for the durability of base course subjected to freezing climates. The percent absorption of each recycled and conventional granular used in this study was determined by immersing dry aggregate in water

and measuring the weight difference between the saturated and dry condition in accordance with ASTM C127-07.

2.5 METHODS

2.5.1 Hydrophobicity Characterization

The hydrophobicity of recycled and natural base course was characterized by using water drop penetration time (WDPT) and contact angle measurement with ten replication tests. The WDPT is the time needed for a water drop to completely infiltrate the material upon placement at the surface of soil or porous material (Dekker 1998). Higher WDPT indicates greater degree of hydrophobicity. In general, soil can be classified as repellent when a drop of water does not instantaneously infiltrate the soil surface (Letey et al. 2000). Contact angle was measured by analyzing a high-resolution photo of a drop of water placed on an air-dry aggregate surface.

2.5.2 K_s Measurement

Saturated hydraulic conductivity was conducted following ASTM D5856, Measurement of Hydraulic Conductivity of Porous Material using a Rigid-Wall, Compaction-Mold Permeameter. Rigid-Wall Permeameters were used to simulate the low confining stress typical in a base course. The head loss in the permeameter and side-wall leakage were negligible during K_s measurement. The specimens were compacted at optimum water content and 95% of the maximum dry density. Tap water was used for all tests. A geotextile were placed at the top and bottom of each specimen to prevent washing of fine particles during the test. The head was kept constant with a Marriott bottle. Hydraulic gradients ranging from 1 to 5 were used depending on each material with test time ranging from 5 min to 20 min per test. K_s for each

specimen was computed from five consecutive K_s measurements. Also, the ratio of outflow was measured to confirm saturation of specimens.

2.5.3 Material Preparation

Specimens were prepared at 95% of maximum dry density of the modified Proctor effort (ASTM D 1557), which is representative of specifications for base course layers in the field. Specimens were prepared at saturated volumetric water content θ_s, which was calculated from the desired dry unit weight and measured G_s. Oven-dry soil was mixed with the calculated amount of water and hydrated for 24 h in a closed contained. The specimens were compacted in the testing cell in four lifts using a hand tamper. The number of tamps per layer was varied to achieve the target density. After compaction, the specimens were saturated from the bottom and assumed to be saturated when measured K varied less than 10% between five consecutive measurement.

Hanging columns (ASTM D6836 – Method A) fitted with air (suction) aspirators were used to measure the SWCCs. Details of the experimental set up are presented in Nokkaew et al. (2012) and Breitmeyer and Benson (2011). The hanging column test is comprised of three main parts: the testing cell, an outflow measurement, and a suction-supply apparatus. Large-scale cylindrical specimens (305-mm inner diameter and 76-mm height) were used to reduce potential scale effects and better represent field conditions for compacted base course. The outflow was measured using a cylinder column with an accuracy of 1.1 cm^3. Suction was supplied using hanging column by adjusting the elevation of two reservoirs to the hanging column, and soil suction was measured with a manometer with an accuracy of ±0.02 kPa (2 mm of water). Hanging columns can provide suction in the range of 0.05 kPa to 80 kPa (limitation due to water cavity). In most situations, the ceiling height limits the applied suction. For this

study, suction higher than 25 kPa was supplied to the specimens using air aspirators with accuracy of ±0.2 kPa.

2.5.4 Hanging Column Test

Unsaturated hydraulic conductivity curves were measured using the multistep outflow method (MSO). The MSO measured K_ψ based on the unsteady method using one-dimensional flow analysis. The assumptions for the MSO include: (i) the material is homogeneous, (ii) gravity gradient and impedance of ceramic plate are negligible, (iii) the suction is linear with water content, and (iv) K_ψ for each suction step is constant (Benson and Gribb 1997). The K_ψ can be calculated by the following relationship:

$$K_\psi = D_\psi \frac{\Delta\theta}{\Delta\psi} \quad \text{(Eq. 2.6)}$$

where $\Delta\theta$ is change of volumetric water content due to an incremental change in soil suction, $\Delta\psi$ (m). Water diffusivity, D_ψ (m^2/s), can be determined by the analytical solution proposed by Gardner (1956):

$$ln\left(\frac{V_\infty - V_t}{V_\infty}\right) = ln\left(\frac{8}{\pi^2}\right) - D_\psi \frac{\pi^2 t}{4L^2} \quad \text{(Eq. 2.7)}$$

where V_t is outflow volume (m^3) at time, t, V_∞ is outflow volume (m^3) at equilibrium (m^3), and L is specimen length (m).

The influence of impedance in the ceramic plate was accounted for by determining the unsaturated hydraulic conductivity of the plate. In this study, a high-flow ceramic plate with air-entry pressure of 100 kPa was used for conducting the MSO.

2.5.5 Regression Method

The data from measured SWCCs from the hanging column test and measured K_ψ from the MSO for each unimodal material was fit to Eq. 2.1 and Eq. 2.2, respectively. Least squares methodology was used in the parameter regression analysis. The objective function $O_w(p)$ that was minimized for SWCC regression can be written by:

$$O_K(p) = \frac{1}{\bar{\theta}^2}\sum_{i=1}^{N}[\theta_i - \theta'_i]^2 + \frac{1}{(\overline{logK_i})^2}\sum_{i=1}^{N_k}[logK_i - logK'_i]^2 \quad \text{(Eq. 2.8)}$$

where $\bar{\theta}$ is the average volumetric water content and θ_i and θ'_i are the measured and predicted volumetric water content, respectively. N is the number of SWCC data points derived from hanging column testing, and p represents parameter vectors (θ_r, θ_s, α, n, L). The K_o was assumed to be K_s (Mualem 1976) . $\overline{logK_i}$ is the average K_ψ in logarithmic scale, K_i and K'_i are the measured and predicted K_ψ, respectively, and N_k is the number of K_ψ data points obtained from the MSO.

2.6 RESULTS

2.6.1 Mortar/Asphalt Content, Percent of Absorption and Hydrophobicity

The mortar/asphalt content, percent absorption, WDPT, and average α_o are summarized in Table 2.2. The mortar content of RCA ranged between 37% and 45%. The asphalt contents of RAP and RPM ranged between 4.3% and 6.2%. High surface area due to small pores in cement mortar paste (Tam et al. 2008; Vivian et al. 2005) contributed RCA percent of absorption (5.0% to 5.8% by weight), while RAPs and RPMs composed of hydrophobic asphalt coated surface had percent of absorption between 0.6% and 3.0%. The conventional aggregate (Limestone-WI) had percent absorption 2.5%.

The hydrophobicity characteristic of studied base course was quantified using WDPT and α_o determination. The average WDPT of RCAs and conventional aggregates was less than 1 s except RCA-CA, which had WDPT of 4.8 s. Thus, α_o was 0° for RCA and conventional aggregates. For studied materials with WDPT greater than 3600 s, the drop of water did not infiltrate to the soil and evaporated. The average α_o of RAP ranged between 69° and 101°, whereas the α_o of RPMs was between 83° and 96°. According to Bauters et al. (2000), RCA and natural aggregate are classified as wettable or hydrophilic materials, while RAP and RPM are classified as slightly to severely, severely, or extremely hydrophobic materials. Most RAPs and RPMs except RAP-CO and RPM-NJ exhibited extremely hydrophobic behavior (Table 2.2).

2.6.2 Saturated Hydraulic Conductivity

Saturated hydraulic conductivity values measured with constant head, rigid-wall molds are presented in Figure 2.3. K_s for the various base courses varied over three orders of magnitude. RCAs exhibited the highest porosities, ranging from 0.26 to 0.30, while porosities of RAPs and RPMs ranged between 0.16 and 0.22 (See Table 2.1). Even at these higher porosities, RCAs tended to provide lower K_s than RAPs and RPMs, possibly because of their higher fines content. For conventional base course, K_s of limestone-WI was greater by three orders of magnitude than Class 5-MN because of the much higher gravel percentage. RAP-MN and Class 5-MN had the lowest values of K_s (less than 3×10^{-6} m/s), likely because of low gravel content and higher fines content.

2.6.3 Soil-Water Characteristic Curve

Soil-water characteristic curves for RCAs, RAPs, RPMs, and conventional aggregates were all measured with the hanging column test and large-scale testing cells. Specimens were prepared at saturation and then dried by applying soil suction to 75 kPa, which was the

maximum capacity of the air aspirator used in this study. The SWCCs of RCAs, RAPs, RPMs, and conventional aggregate are presented in Figure 2.4. The hanging column test can measure suction accurately, especially when lower than 1 kPa, which is suitable for SWCC measurement for granular base course where water in the specimen can change rapidly in response to small changes in soil suction (Li et al. 2009). Unimodal SWCC data were fitted with the VG model. The SWCCs of most studied materials were unimodal (S-shaped) except RCA-MI and RCA-TX, which presented as bimodal SWCCs. For the unimodal base courses, the VG model provided a tight fit (R^2 > 0.97 per least squares regression for all study aggregates). Overall, SWCCs determined from hanging column testing provided almost complete S-shapes for SWCC for RAPs. However, for RCAs and conventional aggregates, the complete curve was not measured and other techniques that can measure soil suction larger than 80 kPa, such as the pressure plate test, would be required where a complete SWCC and accurate data for the residual water content is desired.

The air-entry pressure was determined as the intersection of two constructed lines—one parallel to the beginning part of the SWCC and another parallel to the desorption part of the curve—according to methodology presented in Rahradjo (2010). The projection of intersection on matric-suction axis is the air-entry pressure. Table 2.3. summarizes the ψ_a of the recycled and conventional base courses of this study. The distribution in logarithmic scale of ψ_a for each base course is presented as a dot plot, as shown in Figure 2.5 Theoretically, soil with a high percentage of gravel should provide low ψ_a due to their large pores. However, most RCAs except RCA-MI and RCA-TX (which have gravel percentages of 68% and 76% respectively), tended to have average ψ_a greater than that for RAPs. The reason may be because the cement portion in RCA exhibits numerous micro pores in the surface, which tend to absorb more water (Vivian et al. 2004), and the high percentage of fines in RCA may also contribute to high ψ_a.

2.6.4 Soil-Water Characteristic Curve of Bimodal Materials

As shown in Figure 2.6, The SWCCs of RCA-MI and RCA-TX are bimodal. Among the studied materials, only RCA-MI and RCA-TX are gap-graded gravels (see Table 2.1). The pore-size distribution for these gap-graded RCAs thus includes both large pores and small pores, resulting in the bimodal SWCCs. Eq. 2.3 was used to fit the bimodal data. ψ_j and θ_j were selected at the inflection point where the macroscopic porosity is assumed to have completely drained and the microscopic porosity starts to drain (Burger and Shackelford 2001b). The data in the macroscopic and microscopic regions were fitted separately with the unimodal VG fitting equation as described in Burger and Shackelford (2001a). The bimodal SWCC parameters for both macroscopic and microscopic porosity are summarized in Table 2.4.

A bimodal soil exhibits two air-entry pressures, air-entry pressure for macroscopic porosity (ψ_d) and microscopic porosity (ψ'_d). As shown in Figure 2.6, ψ_d occurs immediately after the application of suction to the specimen (0.02 kPa for RCA-MI and 0.15 kPa for RCA-TX) due to their large pores. The second air-entry pressure (ψ'_d) occurs when water in the microscopic porosity zone starts to desaturate. Table 2.4 summarizes ψ_d and ψ'_d for RCA-MI and RCA-TX.

2.6.5 Hydraulic Conductivity Characteristics

The measured unsaturated hydraulic conductivity curves from the MSO for RCAs, RAPs, RPMs, and conventional aggregates are presented in Figure 2.7. The $K(\psi)$ curves for RCA-MI and RCA-TX, which exhibited bimodal SWCCs, are not presented. Because the saturated hydraulic conductivity of the ceramic plate was 8.6×10^{-8} m/s, measured K_ψ higher than 8.6×10^{-8} m/s from the MSO was not used for regression for the hydraulic parameters. As hydraulic parameters were optimized simultaneously from Eq. 2.1 and Eq. 2.2, the $K(\psi)$ curves are influenced by the SWCC curve. The hydraulic conductivities at the starting point (K_o) were

assumed to be K_s (Mualem 1976) After passing ψ_a, the hydraulic conductivity decreased rapidly. For all test materials, hydraulic conductivity was reduced by four orders in logarithmic scale from K_s to the K_ψ measured at a soil suction at 100 kPa. The shape of the $K(\psi)$ relationship follows the shape of the SWCC. Increased soil suction reduces the area of flow in the matrix, and creates a more tortuous flow path, resulting in a decrease in hydraulic conductivity (Vanapli et al. 1996). The $K(\psi)$ relationship is important for an accurate unsaturated flow analysis and thus for predicting the efficiency of drainage in the pavement structure (Stormont 2005)

2.6.6 Fitting Parameters for Hydraulic Properties

The fitted hydraulic parameters for unimodal SWCCs of recycled and conventional aggregates are summarized in Table 2.3. Dot plots that summarize the distribution of VG's parameters α, n, and m and pore interaction term L of RCA, RAP, RPM and conventional aggregate (CB) are presented in Figure 2.8. van Genuchten's α is the inverse of ψ_a. From Figure 2.8(a), VG's α for RAP tended to be greatest compared to other materials although the studied RAPs had higher density and porosity than RCA (See Table 2.2). This may be because the RAPs were strongly hydrophobic materials with the ability to repel water from their structures. RCA, RPM, and conventional aggregate exhibited low α (< 1 kPa^{-1}). RPM was also a hydrophobic material, likely due to their asphalt coatings. However, two of the studied RPMs had low α. The reason may be that these RPMs had hydrophilic materials from the underlying base course and subgrade.

The VG's n parameter affected the slope of the desorption part of the SWCC. As shown in Figure 2.8(b), hydrophobic RAP and RPM tend to have n values higher than hydrophilic RCA and conventional aggregates, indicating an ability to drain water from their structures. Figure 2.7(c) presents the VG pore interaction term, L, for each type of aggregate. Generally, L is

assumed to be 0.5 for predicting $K(\psi)$ (Mualem's 1976) when only SWCC data are available. However, in this study, VG's L ranged widely for the recycled and conventional aggregates. van Genuchten's L was positive (>0) for RCAs, RPMs, and conventional aggregates. However, for RAPs, the pore interaction term was both positive and negative.

2.6.7 Effect of Hydrophobicity on Hydraulic Properties of Base Course

The impact of hydrophobicity on the SWCC can be demonstrated via calculations involving the contact angle of the studied base courses. Figure 2.8 demonstrates the effect of the contact angle on the SWCC. Soil-water characteristic curves were plotted with the assumption that the contact angle was constant with suction. SWCCs at contact angles of 0^o, 30^o, 50^o, 70^o and 85^o were constructed based on Kelvin's equation (Eq. 2.3 and Eq. 2.4). A typical SWCC of a coarse-grained soil is presented with a contact angle of 0^o, whereas strongly hydrophobic materials are presented at 85^o. Effective contact angles equal to and larger than 90^o are not demonstrated as they can generate negative suction. As shown in Figure 2.8, increasing the contact angle results in descreases to ψ_a and the residual water content. As a result, materials with high contact angles (hydrophobic) tend to have the ability to repel water from their structure.

To investigate the impact of α_o on the SWCC, RCA-CA, RAP-TX, and RPM-MI are evaluated side-by-side. Figure 2.9 presents SWCCs of RCA-CA, RAP-TX, and RPM-MI—each with a different α_o but the same particle gradation. The degree of saturation was selected to normalize the amount of water. The average α_o from ten replicated tests of RCA-CA, RPM-MI, and RAP-TX are 0^o, 83^o and 96^o, respectively. As summarized in Table 2.2, RAP-TX and RPM-MI are extremely hydrophobic materials. Figure 2.10 presents an example of a water drop on particles of RCA-CA, RAP-TX, and RPM-MI. The α_o on the dry surface of a particle of RCA

tended to be approximately 0°, while RAP-TX and RPM-MI had α_o that were larger than 90°. The shapes of SWCCs are dependent on the contact angles with similar trends as presented in Figure 2.11. Increasing the contact angle results in a decrease in the ψ_a. The slope of the SWCC tends to increase as the contact angle increases. These results imply that materials with a high degree of hydrophobicity tend to behave as barriers to hydraulic flux when soil suction is less than 75 kPa, which is a typical suction in the field for a base course layer (Raimbaut 1986).

2.7 SUMMARY AND CONCLUSIONS

SWCCs and $K(\psi)$ curves of six RCAs, six RAPs, two RPMs, and two conventional base courses were studied using hanging column testing and the MSO. The SWCC and $K(\psi)$ of unimodal recycled and conventional aggregates were fit such that the fits satisfied both VG's SWCC prediction and MVG's K_ψ prediction. The bimodal SWCC were fitted with methodology recommended by Burger and Shackelford (2001a), which is derived from the VG unimodal equation. The degree of hydrophobicity of studied base course was quantified using WDPT and α_o measurement.

Per the classification system proposed by Bauters et al. (2000), RCAs and conventional aggregates were hydrophilic materials, while RAPs and RPMs were strong hydrophobic materials. The K_s of RAPs and RPMs tended to be higher than those of RCA and conventional base course, although RAPs and RPMs tended to have lower porosities than RCA and conventional base course. Gap-graded particle-size distributions for RCA-TX and RCA-MI resulted in bimodal SWCCs. RAP and RPM tended to provide high values for VG's n parameter, which affected the desorption slope of the SWCC.

The unsaturated hydraulic conductivity was measured simultaneously with the hanging column test and incorporation of the MSO method. The shape of the $K(\psi)$ curve corresponded

to the shape of unimodal SWCCs for all studied base courses. The effect of hydrophobicity on the SWCC were investigated via contact angle measurements. An increase in the contact angle of a hydrophobic base course resulted in a decrease in ψ_a and an increase in the slope of the SWCC. This implies that materials with similar grain-size distribution may have different SWCC shapes and corresponding changes in unsaturated hydraulic conductivity in base course.

2.8 ACKNOWLEDGEMENTS

The material evaluated in this study was provided from the TPF-5(129) Recycled Unbound Materials Pool Fund administered by the Minnesota Department of Transportation. Professors Tuncer B. Edil and Craig H. Benson at the University of Wisconsin-Madison (UW-Madison) are thanked for their input**.** The grain size analyses and index properties were provided by Ozlem Bozyurt, a former graduate student in the Department of Civil and Environmental Engineering (CEE) at UW-Madison. The compaction curves were prepared by Dr. Young-Hwan Son, Assistant Professor, Department of Rural Systems Engineering, College of Agriculture and Life Sciences, Seoul National University.

2.9 REFERENCES

ASTM C127, 2012, “Standard Test Method for Density, Relative Density (Specific Gravity), and Absorption of Coarse Aggregate,”*Annual Book of ASTM Standards,* ASTMInternational, West Conshohocken, PA, www.astm.org.

ASTM D1557, 2009. “Standard Method for Laboratory Compaction Characteristics of Soil Using Modified Effort (56,000 ft-lb/ft^3 (2,700 kN-m/m^3),” *Annual Book of ASTM Standards,* ASTM International, West Conshohocken, PA, www.astm.org.

ASTM D2487, 2011, “Standard Practice for Classification of Soils for Engineering Purposes (Unified Soil Classification System) Annual *Book of ASTM Standards,* ASTM International, West Conshohocken, PA, www.astm.org.

ASTM D422, 2007, “Standard Test Method for Particle-Size Analysis of Soils,” *Annual Book of ASTM Standards,* ASTM International, West Conshohocken, PA, www.astm.org.

ASTM D5856, 2007, “Measurement of Hydraulic Conductivity of Porous Material Using a Rigid-Wall, Compaction-Mold Permeameter,”*Annual Book of ASTM Standards,* ASTM International, West Conshohocken, PA, www.astm.org.

ASTM D6037, 1996, “Standard Test Methods for Dry Abrasion Mar Resistance of High Gloss Coatings,”*Annual Book of ASTM* Standards*,* ASTM International, West Conshohocken, PA, www.astm.org.

ASTM D6836, 2008. “Standard test Method for Determination of the Soil Water Characteristic curve for Desorption Using Hanging Column, Pressure Extractor, Chilled Mirror Hygrometer, or Centrifuge,” *Annual Book of ASTM Standards,* ASTM International, West Conshohocken, PA, www.astm.org.

Aatheesan, T., Arulrajah, A., and Wilson, J., 2008, “Beneficial Use of Brick Rubble as Pavement Sub-base Material,” *Advances in Transportation Geotechnics*, pp. 695-697.

ACPA, 2009, “Recycling Concrete Pavements,” Bulletin B043P, American Concrete Pavement Association, Skokie, IL.

Bachmann, J., Deurer, M., and Arye, G. 2007, “Modeling Water Movement in Heterogeous Water-Repellent Soil: 1. Development of a Contact Angle-Deprndent Water-Retention Model,” Vadose Zone J., pp. 436-445.

Bennert, T., Papp Jr, W. J., Maher, A., and Gucunski, N. 2000. “Utilization of Construction and Demolition Debris under Traffic-Type Loading in Base and Subbase Applications,” *Transport. Res. Rec*, No. 1714, pp. 33-39.

Benson, C. and Gribb, M. 1997, Measuring Unsaturated Hydraulic Conductivity in the Laboratory and Field. Unsaturated Soil Engineering Practice, GSP No. 68, ASCE, Houston, S. and Fredlund, C., Eds., pp. 113-168.

Blankenagel, B.J., and Guthrie, W.S. 2006, “Laboratory Characterization of Recycled Concrete for Use as Pavement Base Material.” *Transport. Res. Rec.*, No. 1952, Washington, D.C., 2006, pp. 21–27.

Bozyurt, O., Tinjum, J.M., Son, Y.H., Edil, T.B., and Benson, C.H., "Resilient Modulus of Recycled Asphalt Pavement and Recycled Concrete Aggregate," GeoCongress 2012, American Society of Civil Engineers, GSP No. 225, Oakland, CA, pp. 3901-3910.

Breitmeyer, R.J. and Benson, C.H. 2011. "Measurement of Unsaturated Hydraulic Properties of Maicipal Solid Waste," Geo-Frontiers 2011, ASCE, Dallas, TX, pp. 1433-1441.

Buaters, T.W.J., Steenhuis, T.S., DiCarlo, D.A., Nieber, J.L., Dekker, L.W., Ritsema, C.J., Parlange, J.-Y., and Haverkamp, R. 2000, "Physics of Water Repellent Soils," J. Hydrol., Vol. 231, pp. 233-243.

Burger, C.A., and Shackelford, C.D., 2001(a), "Evaluating dual porosity of pellettized diatomaceous earth using bimodal soil-water characteristic curve function," Can. Geotech. J., Vol. 38(1), pp. 53-56.

Burger, C.A., and Shackelford, C.D., 2001(b), "Soil-Water Characteristic Curves and Dual Porosity of Sand-Diatomaceous Earth Mixtures," J. Geotech. Geoenviron., Vol. 38, No.1, pp. 53-56.

Cedergren, H. R. 1988. "Why All Important Pavement Should Be Well Drained." *Transport. Res. Rec.*, No. 1188, Washington, D.C., pp. 56-62.

Cedergren, 1987, *Drainage of Highway and Airfield Pavements*, second edition, Robert E. Krieger publishing, FL.

Cedergren, H.R. (1994), "America's Pavements: World's Longest Bahtubs," *Civil Engineering. American* Society *of Civil Engineering*, pp. 56-58.

Dekker, L.W., Ritsema, C.J., 1994, "How Water Move in a Water Repellent Sandy Soil. 1. Potential and Actual Repellency. Water *Resour. Res.*, Vol 30, pp. 257-2517.

Dekker, L.W., Ritsema, C.J., Oostindie, K., Boersma, O.H., 1998, "Effect of drying Temperature on the severity of Soil Water Repellency, *Soil Sci*., Vol. 163, pp. 780-796.

FHWA, 2004, "Recycled Concrete Aggregate – Federal Highway Administration National Review," *Federal Highway Administration*, Washington, D.C.

Fredlund, M. D., Fredlund, D. G., and Wilson, G.W., 2000, "An Equation to represent grain-size distribution," *Can. Geotech. J.,* Vol.37. pp. 817-827.

Gardner, W 1956, “Calculation of Capillary Conductivity from Pressure Plate Outflow Data,” *Soil Sci. Amer. Proc.*, Vol 20, pp. 317-320.

Gokce, A. 2001, “Investigation of the Parameters Controlling Frost Resistance of Recycled Aggregate Concrete,” Doctoral Thesis, Nigata University.

Guthrie, W. S., Cooley, D. and Eggett, D. L. 2007. “Effects of Reclaimed Asphalt Pavement on Mechanical Properties of Base Materials,” *Transport. Res. Rec.*, No. 2006, pp. 44-52.

Hallett, P. D., 2007, “An Introduction to Soil Water Repellency” *Proceeding of the 8th International Symposium on Adjuvants Agrochemicals (ISAA2007)*, International Society for Adjuvants (ISAA), Columbus, Ohio, USA, August, 6-9.

Hillel, D., 1998, Environmental *Soil Physics*, Academic Press, San Diego, California.

Huang, Y.H., 2004, *Pavement Analysis and Design*, 2nd edition, Pearson Prentice Hall, Pearson Education Inc., Upper Saddle, New Jersey.

Jury, W.A., Gardner, W.R., Gardner, W.H. 1991, Soil Physics, Wiley, New York.

Lee, J., Edil, T., Tinjum, J., and Benson, C., 2010, “Quantitative Assessment of Environmental and Economic Benefits of Using Recycled Construction Materials in Highway Construction,” *Transport Res Rec: Journal of the Transportation Research Board*, No 2158., Washington, D.C., pp. 138-142.

Letey, J., Carrillo, M.L.K., and Pang, X.P. 2000, “Approaches to Characterize the Degree of Water Repellency*,” J. Hydrol.*, Vol. 231, pp. 61-65.

Li, X., Zhang, L.M., and Li, J. H., 2009, “Development of a modified axis translation technique for measuring SWCCs for gravel soils at very *low* suctions,” *Geotech. Test. J.*, Vol. 32(6), pp. 1-11.

Lu, N. and Likos, W.J., 2004, Unsaturated Soil Mechanics, John Willey and Sons, Hoboken, New Jersey.

NCHRP (2004). “Guide for Mechanistic-Empirical Design of pavement structures: part 2 – Design Inputs.” *ARA, Inc.*, ERES Consultants Division, Champaign, IL.

Mualem, Y. 1976, “A New Model for Predicting the hydraulic Conductivity of Unsaturated Porous Media.” *Water Resour. Res*, Vol.12, pp. 513-522

Nokkaew, K., Tinjum, and J.M., Benson, C. H., “Hydraulic Properties of Recycled Asphalt Pavement and Recycled Concrete Aggregate,” GeoCongress 2012, ASCE, Oakland, CA 2012, pp. 1476-1485.

Pease, R. E. 2010, *Hydraulic Properties of Asphalt Concrete*, Doctoral Dissertation, University of New Mexico, Albuquerque, 191 p.

Poon, C.-S., Qiao, X., and Chan, D., 2006, “The Cause and Influence of Self-Cementing Properties of Fine Recycled Concrete Aggregates on the Properties of Unbound Sub-Base,” *Waste Management,* No.26, pp. 1166-1172.

Rahardjo, H., Vialvong, K., and Leong, E.C. 2010. “Water characteristic curves of recycled materials,” *Geotech. Test. J.*, Vol. 34, No. 1, pp. 1-8.

Raimbaut, G. Cycles , 1986, Annuels d’Humidite dans une Chaussee Souple et son Support. *Bull. de liason des. Loboratories des Ponts et Chaussees, Laboratoire Central de Ponts et Chaussees*, Vol. 145, pp. 79-84.

Schaap, M.G. and Leij F.J. 2000, “Improved Prediction of Unsaturated Hydraulic Conductivity with the Mualem-van Genuchten Model,” *Sci Soc. Am. J., Vol. 64, pp. 843-851.*

Schaap*, M.G.* and *van Genuchten, M. 2005, “A Modified Mualem-van Genuchten Formulation for Improved Description of the Hydraulic Conductivity near Saturation,” Vadose Zone J.,* Vol. 5, pp. 27-34.

Smettem, K.R.J. and *Kirkby*, C., 1990, “Measuring the Hydraulic Properties of a Stable Aggregate Soil,” *J. Hydro.*, Vol. 117, pp. 1-13.

Stormont, J. C., and Zhou, S., *2005*, “Impact of Unsaturated Flow on Pavement Endgedrain Performance,” *Journal of Transportation Engineering*, ASCE., Vol. 131(1), pp. 46-53.

Tam, W.Y.T., Gao, X.F., and Tam, C.M., 2005, “Microstructure analysis of recycled aggregate concrete produced from two-stage mixing approach,” *Cement and Concrete Res.*, Vol. 35, pp. 1195-1203.

Tam, V.W.Y., Gao, X. F., Tam C.M., and Chan, C.J., 2008, “New Approach in Measuring Water Absorption of Recycled Aggregates,” *Constr. Build. Mater.*, Vol. 33, pp. 379-392.

van Genuchten, M. 1980, “A Close-Form Equation for Predicting the Hydraulic *Conductivity* of Unsaturated Soils,” *Soil. Sci. Am. J.*, 44, pp. 892-898.

Vanapali, S.K. Fredlund, D.G., Pufahl, D.E., and Clifton, A.W. 1996, “Model for the prediction of shear strength with respect to soil suction,” Can. Geotech. J. 33, pp. 379-392.

Vivian, W.Y.T, Gao, X.F., and Tam, C.M., 2005, “Microstructural Analysis of Recycled Aggregate Concrete Produced from Two-Stage Mixing Approach,” *Cement and Concret Res.,* Vol.35, pp. 1195-1203.

USGS, 2011, “Mineral Commodity Summaries 2011.” U.S. Geological Survey, January 2011.

Zhang, L. and Chen, Q., 2005, “Predicting Bimodal Soil–Water Characteristic Curves,” *J. Geotech. Geoenviron.*, Vol. 131, No. 5, pp. 666-670.

Table 2.1 Summarized Index Properties, Percent Fines, and Unified Soil Classification (USCS) of Recycled and Natural Aggregates

Material	Index Properties					Percent			USCS
	G_s	n	γ_d (kN/m^3)	C_u	C_c	Gravel	Sand	Fines	Designation
RCA-CA	2.63	0.27	18.8	22	1.4	50.6	47.1	2.3	GW
RCA-CO	2.63	0.3	18	66	1.1	40.9	46.3	12.8	SW
RCA-MI	2.72	0.26	19.8	35	3.9	68.5	28.3	3.2	GP
RCA-MN	2.71	0.3	18.5	21	1.4	31.8	64.9	3.3	SW
RCA-NJ	2.64	0.28	18.7	28	0.3	41.2	54.6	4.3	SP
RCA-TX	2.6	0.27	18.7	38	6	76.3	21.6	2.1	GP
RAP-CO	2.39	0.16	19.6	9	0.7	31.7	67.7	0.6	SP
RAP-MN	2.52	0.2	19.8	7	0.7	26.3	71.2	2.5	SP
RAP-NJ	2.49	0.21	19.3	6	1.3	51	48.3	0.7	GW
RAP-OH	2.46	0.22	18.8	7	1.3	32.1	66.2	1.7	SP
RAP-TX	2.41	0.18	19.3	11	1.1	41.1	44.9	1	GW
RAP-WI	2.46	0.21	19	6	0.9	30.9	68.5	0.6	SP
RPM-MI	2.5	0.17	20.4	17	1.1	43.7	43.6	0.6	GP
RPM-NJ	2.5	0.2	19.5	18	1	46.5	53.1	0.4	GP
Class 5-MN	2.72	0.26	19.1	21	1.4	22.9	67.6	9.5	SW-SM
Limestone-WI	2.58	0.16	21.1	58	4.5	50.7	41	8.3	GP-GM

Table 2.2 Summarized Mortar/Asphalt Content, Percent Absorption, WDPT, Average Contact Angle, and Water Repellency Classification of Studied Materials (Bauters et al. 2000)

Materials	Mortar/Asphalt Content (%)	Absorption (%)	Average WDPT(s)	Contact Angle (^{o})	Description
RCA-CA	37	5	4.8	0	Wettable
RCA-CO	47	5.8	<0.5	0	Wettable
RCA-NJ	-	5.4	<0.5	0	Wettable
RCA-TX	45	5.5	0.8	0	Wettable
RAP-CO	5.9	3	171	69	Slight to severely water repellent
RAP-NJ	5.2	2.1	>3600	101	Extremely water repellent
RAP-OH	6.2	0.6	>3600	-	Extremely water repellent
RAP-TX	4.7	1.3	>3600	96	Extremely water repellent
RPM-MI	5.3	1.7	>3600	83	Extremely water repellent
RPM-NJ	4.3	2.6	960	96	Severely water repellent
Class 5-MN	-	-	<0.5	0	Wettable
Limestone-WI	-	2.5	<0.5	0	Wettable

Table 2.3 Summary of Fitting parameters for Unsaturated Hydraulic Properties, Air-Entry Pressure (ψ_a), and Saturated Hydraulic Conductivity (K_s) of RCAs, RAPs, RPMs, and Conventional Aggregates.

Materials	Fitting Parameters						Ψ_a	K_s
	θ_r	θ_s	α (kPa^{-1})	n	m	L	(kPa)	(m/s)
RCA-CA	0	0.25	1.14	1.11	0.1	0.5	0.50	$1.93x10^{-5}$
RCA-CO	0	0.27	0.36	1.15	0.13	5.24	3.00	$1.57x10^{-5}$
RCA-MI	-	-	-	-	-	-	0.09	$2.62x10^{-5}$
RCA-MN	0.13	0.25	0.2	2.19	0.54	0.48	1.70	$1.78x10^{-5}$
RCA-NJ	0.01	0.31	0.36	1.19	0.16	0.1	1.03	$2.38x10^{-6}$
RCA-TX	-	-	-	-	-	-	0.03	$7.56x10^{-6}$
RAP-CO	0.08	0.24	0.56	1.58	0.37	1.09	1.10	$3.82x10^{-5}$
RAP-MN	0.03	0.2	0.31	1.52	0.34	-0.2	1.03	$1.10x10^{-6}$
RAP-NJ	0.04	0.21	2.02	2.01	0.5	0.51	0.20	$3.69x10^{-4}$
RAP-OH	0	0.26	1.28	1.25	0.2	-0.45	0.35	$5.03x10^{-5}$
RAP-TX	0.01	0.21	1.92	1.42	0.3	0.5	0.16	$3.18x10^{-5}$
RAP-WI	0.02	0.23	2.43	1.57	0.36	-1.1	0.10	$5.19x10^{-5}$
RPM-MI	0.13	0.27	0.7	1.60	0.38	0.09	0.80	$2.31x10^{-4}$
RPM-NJ	0.04	0.19	0.28	1.94	0.48	1.25	1.90	$1.03x10^{-4}$
Class 5-MN	0	0.25	0.06	1.40	0.29	0.78	8.00	$4.62x10^{-7}$
Limestone WI	0	0.21	0.16	1.34	0.25	7.74	1.13	$5.71x10^{-4}$

Table 2.4 van Genuchten Bimodal Fitting Curve Parameters for RCA-MI and RCA-TX

Material	Macroscopic Portion					Microscopic Portion				
	θ_j	θ_s	α (kPa^{-1})	β	ψ_d (kPa)	θ_r	θ_j	α' (kPa^{-1})	β'	ψ'_d (kPa)
RCA-MI	0.2	0.4	9.19	1.5	0.09	0	0.2	0.05	1.3	10
RCA-TX	0.2	0.3	4.76	1.9	0.03	0	0.2	0.15	1.1	3

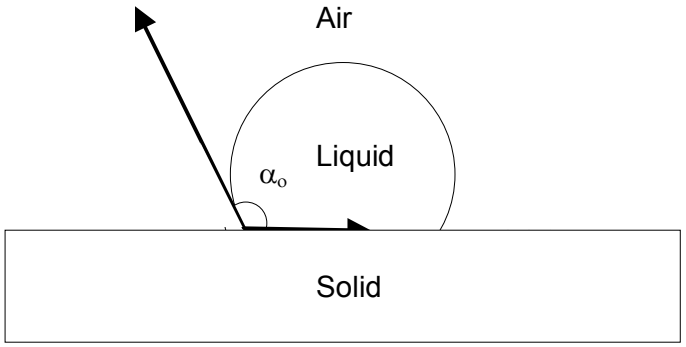

Figure 2.1 Air-Water-Solid Interaction Describing Contact Angle of Water-Air and Solid-Water Interface of Drop of Liquid on Solid Surface

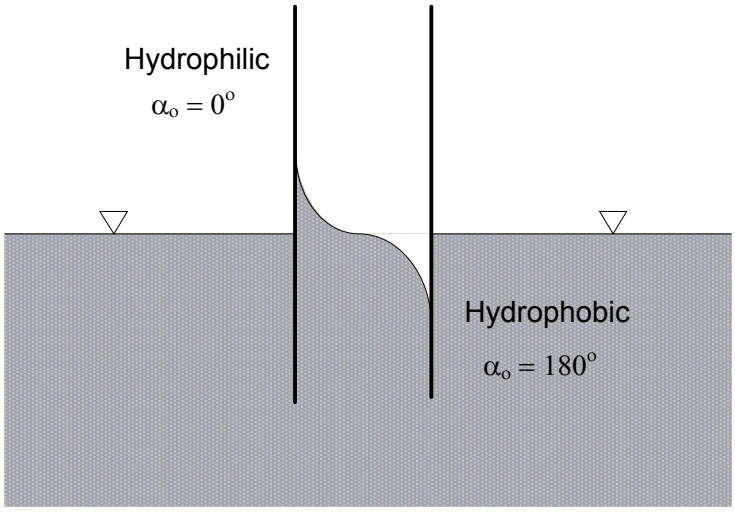

Figure 2.2 Shape of Meniscus for Hydrophilic and Hydrophobic Material

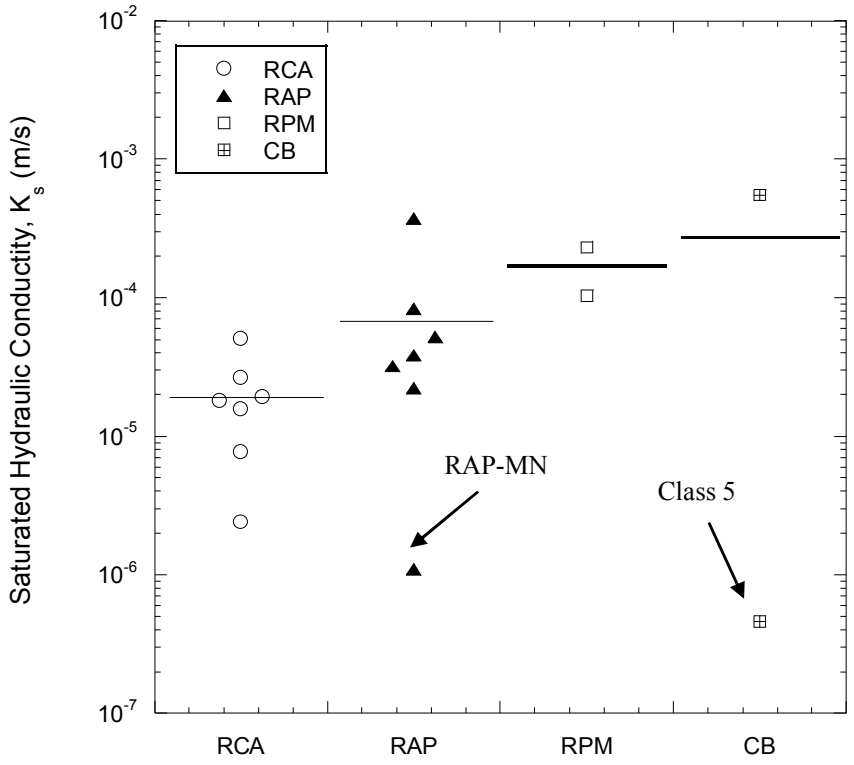

Figure 2.3 Dot plot of K_s for RCAs, RAPs, RPM, and Conventional Base Course (CB), where Bars Represent Mean K_s

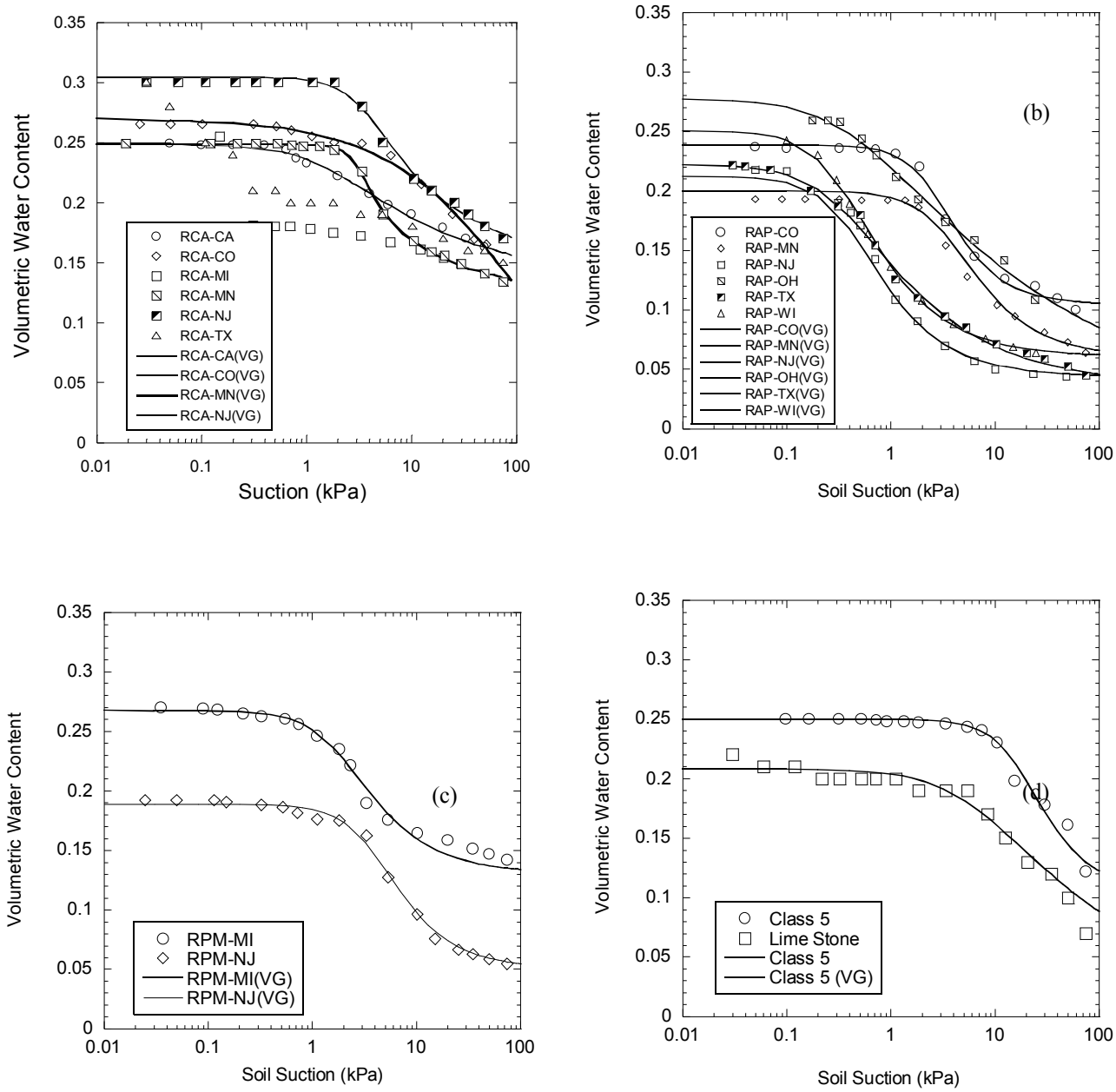

Figure 2.4 Desorption SWCCs of: (a) RCAs, (b) RAPs, (c) RPM, and (d) Conventional Aggregate Fitted with van Genuchten's (1980) Model

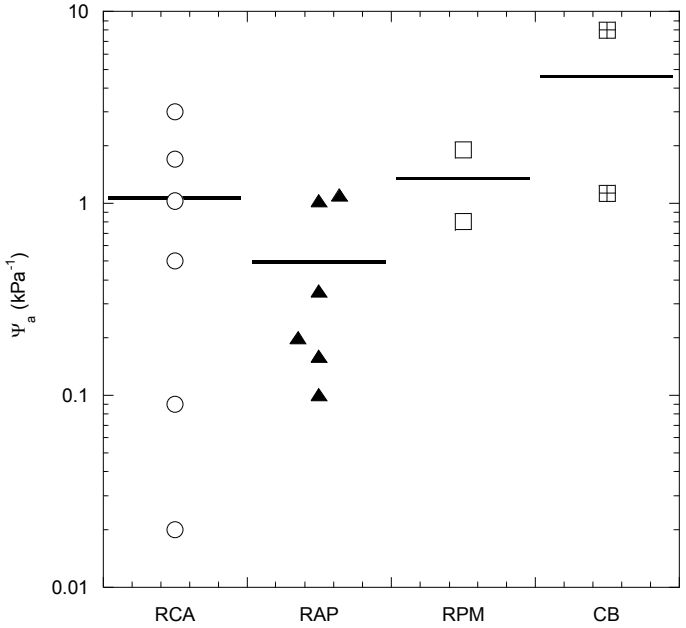

Figure 2.5 Dot plot presents the data distribution of Ψ_a in logarithmic scale for RCA, RAP, RPM, and Conventional aggregate (CB), where bar indicates mean of data

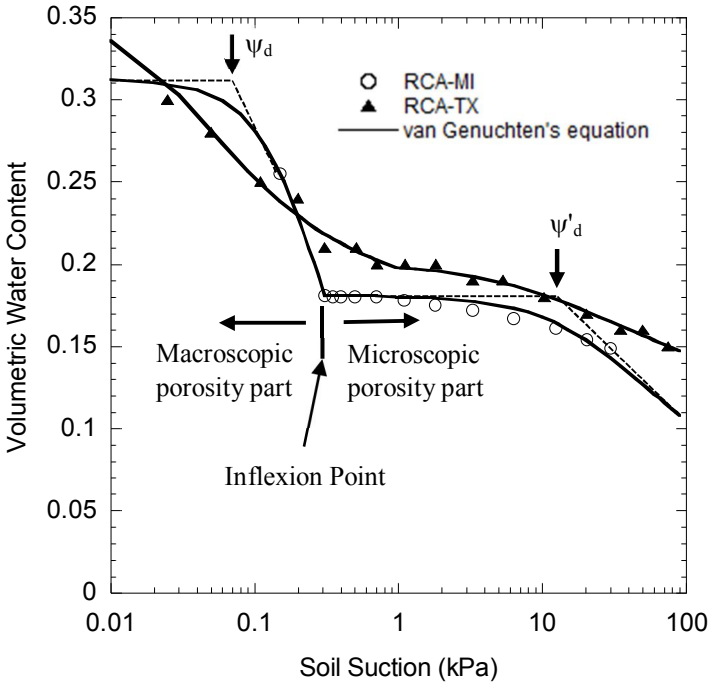

Figure 2.6 Bimodal SWCCs of RCA-MI and RCA-TX Fitted with Equation Developed from van Genuchten's (1980) Model

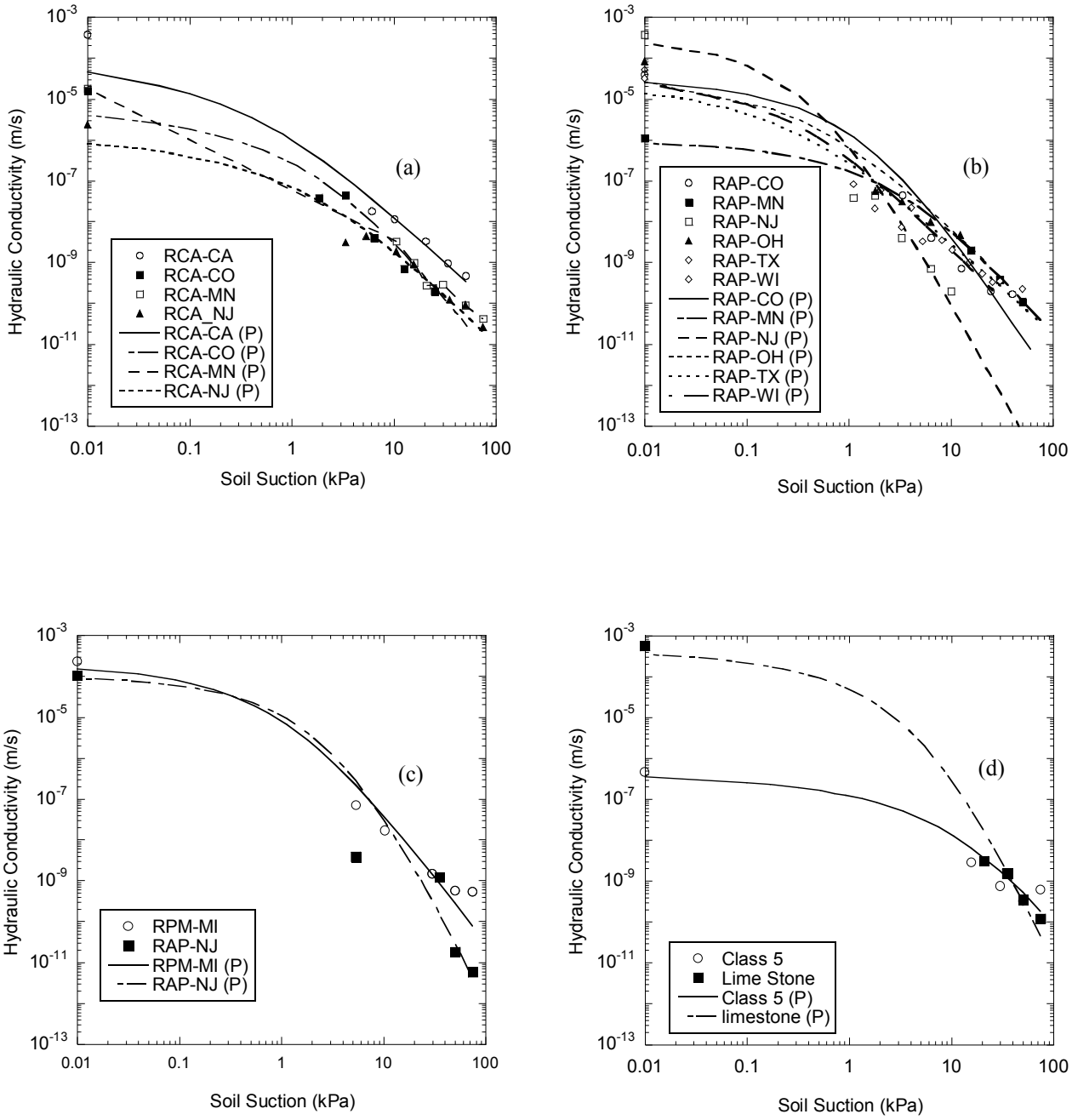

Figure 2.7 Unsaturated Hydraulic Conductivity versus Soil Suction of RCAs, RAPs, RPM and Class 5 fitted by the MVG Model (van Genuchten 1980)

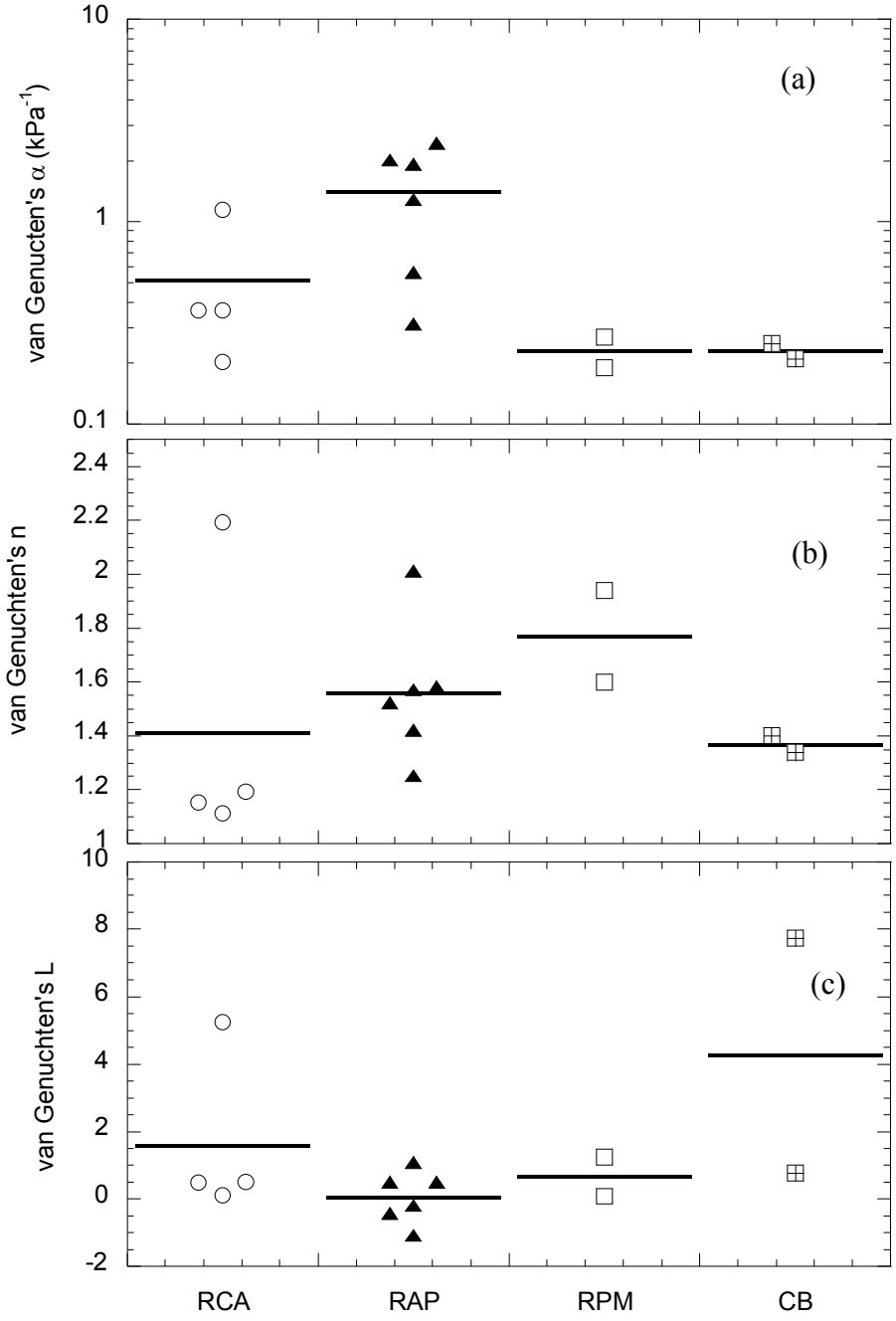

Figure 2.8 Dot Plot Summarizes Data Distribution of (a) van Genuchten's α, (b) van Genuchten's n and Pore Interaction Term L, for unimodal SWCCs of RCA, RAP, RPM and Conventional Aggregate (CB)

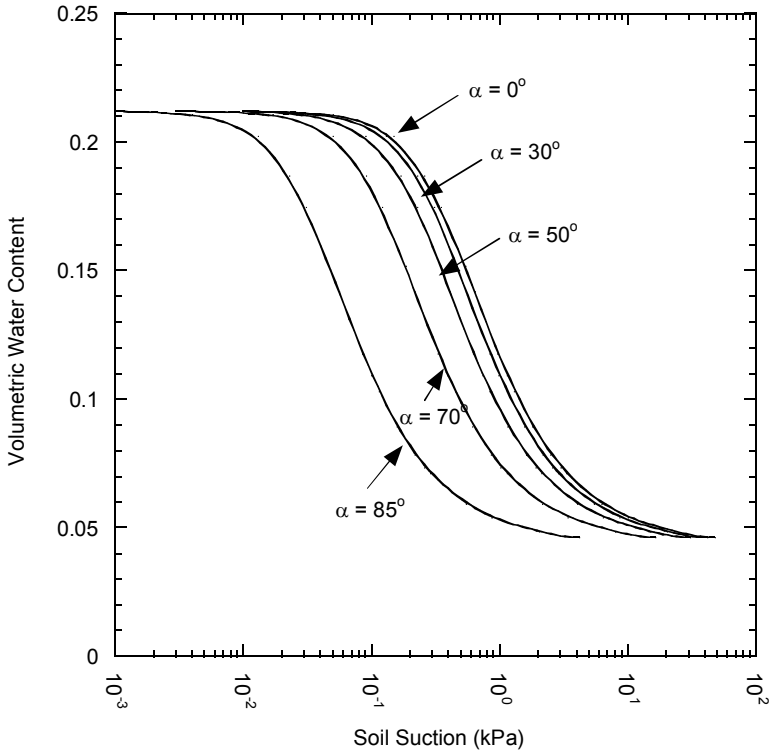

Figure 2.9 Effect of Contact Angle on SWCC

(a) RCA-CA ($\alpha_o \sim 0^o$) (b) RAP-TX ($\alpha_o > 90^o$) (c) RPM-MI ($\alpha_o > 90^o$)

Figure 2.10 Form of Water Drop on RCA-CA, RAP-TX and RPM-MI

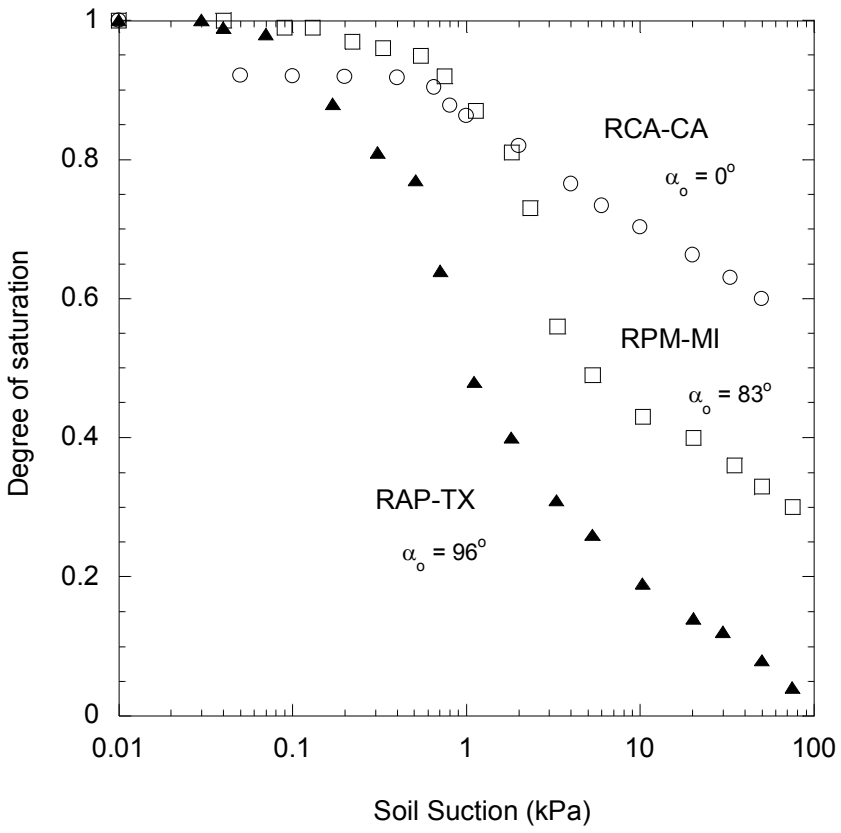

Figure 2.11 SWCC with Different Contact Angles for RCA-CA, RAP-TX, and RPM-MI

CHAPTER 3: EFFECT OF MATRIC SUCTION ON RESILIENT MODULUS FOR COMPACTED RECYCLED BASE COURSE

3.1 ABSTRACT

The demand for recycled material as unbound base course in roadway construction has increased in recent decades because of the excellent mechanical properties of recycled asphalt and inherent life-cycle benefits. However, concerns about post-construction changes in resilient modulus (M_r) due to moisture variation have been expressed. This study investigated the relationship of M_r to soil matric suction (ψ) at an in-service stress state for recycled asphalt pavement (RAP), recycled pavement material (RPM), and recycled concrete aggregate (RCA) with comparisons to crushed limestone as a conventional base course control. Resilient modulus tests were conducted in accordance with NCHRP 1-28A Procedure Ia. Equipment modifications allowed for an applied ψ ranging from 1.5 kPa to 65 kPa during testing. A model is proposed that incorporates parameters from the soil-water characteristic curve (SWCC) to predict a summary resilient modulus (SRM); i.e., the in-service M_r at representative field stress state. The SRM increased with increasing ψ for all compacted base courses studied. An SRM ratio, defined as the ratio of SRM at a particular ψ to the as-compacted SRM at optimum water content was empirically quantified. The modulus ratio increased linearly with logarithmic ψ for studied recycled and natural aggregates. The findings indicate that the M_r-ψ relationship is highly relevant for predicting in-service performance of pavement layers.

3.2 INTRODUCTION

The demand for beneficial reuse of construction and demolition (C&D) waste has increased in recent decades, which promotes the sustainable use of construction materials (Edil 2009; Kilbert 2002). Approximately 6.4 million km of roadway in the US are repaired every 2-5 years and reconstructed every 20-40 years, generating demand for new crushed stone (~1.5 billion metric tons) and millions of metric tons of used asphalt concrete and concrete slab are disposed in landfills each year (FHWA 2004). Using recycled asphalt is a viable solution to reduce demand for natural aggregate and the amount of solid waste produced from roadway construction. The United States Geological Survey (USGS 2011) reported that 11.5 million tons of recycled asphalt and 13.5 million tons of recycled concrete were produced in 48 states across the US in 2012, and more than 80% of recycled material was used by the construction industry.

Recycled asphalt materials used for pavement construction can be classified as recycled asphalt pavement (RAP) and recycled pavement material (RPM). RAP is aggregate derived from asphalt pavement. RPM originates from crushed asphalt surface in addition to the underlying base course material. Recycled concrete aggregate (RCA) is produced from demolition of concrete structures such as roads, runways, and buildings. Using recycled aggregates provides environment-friendly and significant life-cycle benefit for roadway construction because the materials can be reused and produced in place, resulting in reductions in energy and cost due to low transportation needs (Lee et al. 2010). RAP, RPM and RCA have excellent mechanical properties (e.g., high resilient modulus, high durability, and low moisture susceptibility) and are suitable for use as an unbound base course in the pavement structure (Guthrie et al. 2007; Bozyurt 2012).

Past studies have shown that the resilient modulus of unsaturated base course is influenced by moisture (Cracium and Lo 2010,Jong et al 1998). In the field, the resilient modulus of a base course varies in response to change in water content which, in turn, is a function of soil

suction. Matric suction ($\psi = u_a - u_w$, where u_a is pore-air pressure and u_w is pore-water pressure) can be used to understand and model the unsaturated behavior of conventional base course, particularly the M_r (Cracium and Lo 2010). However, since RAP, RPM, and RCA are non-natural aggregate, the variation in M_r with moisture change may trend away from that of natural base courses.

The objective of this study was to evaluate the influence of matric suction on M_r for compacted RAP, RPM and RCA in comparison to conventional crushed limestone in the postcompaction state. A resilient modulus apparatus was modified with suction control to determine the relationship between matric suction and M_r. A model for predicting summary resilient modulus (SRM) from soil suction and the soil-water characteristic curve (SWCC) was established. Additionally, an empirical relationship between normalized SRM to the SRM at optimum water content and soil suction is presented and discussed.

3.3 TEST MATERIALS

Tested materials were named according to their origin. RAP-WI is a commercial product obtained from a road reconstruction project in Sun Prairie, Wisconsin. RPM-MI was provided by the Michigan Department of Transportation (MI-DOT) as part of a Pooled Fund Project and was also sourced from a highway construction project. RCA-WI was from the demolition of building concrete in Madison, Wisconsin, and has been stockpiled for over five years. Limestone-WI that meets the standard specification of Wisconsin Department of Transportation (WI-DOT) for dense-aggregate base course grade 2 (maximum particle size 19 mm) was used as a control. Physical and compaction properties of the materials are presented in Table 1.

3.4 SWCC FOR STUDIED BASE COURSE

3.4.1 SWCC Fitting Equation

A soil-water characteristic curve describes the relationship between water content or degree of saturation and soil suction (Lu and Likos 2004). The typical SWCC of a granular base course is S-shaped (Lu and Likos 2004; Rahardjo et al. 2010). A number of models have been proposed to fit SWCC data. Among these models, the Fredlund and Xing (1994) model is widely used in pavement engineering practice. The Fredlund and Xing model provides a smooth, sigmoidal curve and is defined as:

$$\Theta = \frac{S-S_r}{1-S_r} = \left[1 - \frac{ln\left(1+\frac{\psi}{\psi_r}\right)}{ln\left(1+\frac{10^6}{\psi_r}\right)}\right]\left[\frac{1}{\{ln[e+(\psi/a)^n]\}^m}\right] \quad \text{(Eq. 4.1)}$$

where Θ is normalized degree of saturation; S is degree of saturation; S_r is residual degree of saturation; ψ is soil suction; ψ_r, a, n, and m are fitting parameters; and e is the base of the natural logarithm.

Occasionally, base course associated with two distinct pore-size distributions leads to a bimodal SWCC. In this case, a continuous S-shaped SWCC is observed. In this study, a modified Fredlund and Xing (1994) model for a bimodal SWCC soil was used to fit SWCC data. A bimodal SWCC includes portions that represent the macroscopic pore region and microscopic porosity. Concepts and details of the model are presented in Burger and Shackelford (2001). The bimodal model is defined as:

$$\Theta = \frac{S-S_r}{1-S_r} = \begin{cases} \left[1 - \frac{ln\left(1+\frac{\psi}{\psi_r'}\right)}{ln\left(1+\frac{10^6}{\psi_r'}\right)}\right]\left[\frac{1}{\{ln[e+(\psi/a')^{n'}]\}^{m'}}\right]; & \psi_j < \psi \\ \left[1 - \frac{ln\left(1+\frac{\psi}{\psi_r}\right)}{ln\left(1+\frac{10^6}{\psi_r}\right)}\right]\left[\frac{1}{\{ln[e+(\psi/a)^n]\}^m}\right]; & \psi \leq \psi_j \end{cases} \quad \text{(Eq. 4.2)}$$

where the prime symbols are used to indicate parameters fitted to the microscopic porosity, and regular symbols represent parameters fitted in the macroscopic pore regime. ψ_j represents soil suction at the match point between the macroscopic and microscopic porosity regime.

3.4.2 SWCC for Studied Base Course

Typically, base course is composed primarily of gravel-sized and coarse sand-sized particles which have large pores within the structure. Thus, water content can rapidly drain at low suction (Rahardjo et al. 2010). In this study, desorption SWCCs were measured using a large-scale (305-mm-inner diameter and 76-mm height) hanging column testing apparatus fitted with an air aspirator to provide precise measurement of soil suction ranging from 0.05 kPa to 75 kPa (Nokkaew et al. 2012). The test procedure for SWCC determination followed ASTM D6836. All materials were compacted by hand-tamping in the testing cell at a water content near the optimum water content and at 95% of maximum dry density according to modified Proctor effort (ASTM D1557). Compacted specimens were then saturated using de-aired water.

SWCCs for the compacted base courses are presented in Figure 1. The SWCCs of RAP-WI, RPM-MI, and RCA-WI are characteristically S-shaped and can be fitted with the unimodal Fredlund and Xing model (1994). Limestone-WI exhibits a bimodal SWCC, indicating two distinct pore-size distributions. The SWCC data for Limestone-WI were fit to the bimodal Fredlund and Xing model (1994) as summarized in Eq. 4.2. The soil suction at which water starts to drain is defined as the air entry pressure (ψ_a). The method to determine ψ_a is illustrated in Figure 1. For RAP-WI, RPM-MI, and RCA-WI ψ_a occurs at soil suction < 1 kPa (10 cm of water). Limestone-WI exhibits separate ψ_a corresponding to the macroscopic and microscopic porosity. The first ψ_a (macroscopic pores) was observed at 0.4 kPa, while the second ψ_a (microscopic porosity) was observed at 4.5 kPa. These low ψ_a values imply that base course is generally unsaturated in the field. Optimized SWCC fitting parameters and ψ_a for each material are summarized in Table 2.

3.5 PROCEDURE

3.5.1 Specimen Preparation

All tested base courses classify as Type I material according to NCHRP 1-28A, thus specimen dimensions of 150-mm diameter and 305-mm height are specified (NCHRP 2004). Specimens were prepared at optimum water content and 95% relative compaction (modified Proctor effort) through impact compaction. For consistency, specimens were compacted in six lifts of equal mass and thickness and to within 2% of target density. The number of blows per lift was adjusted to reach the target density. The specimens were secured by covering with a latex membrane.

3.5.2 Saturation and Soil Suction Initialization

Prior to testing, specimens were saturated to remove any residual soil suction resulting from compacting the specimens at optimum water content. De-aired water was supplied to the specimens through a high-flow, high-air-entry ceramic plate mounted in the bottom test platen as shown in Figure 2. A constant water head was maintained using a Marriott bottle under a hydraulic gradient less than 2. Confining air-pressure of 13.8 kPa was supplied to the testing chamber to provide lateral support for specimen during saturation. Specimens were assumed saturated when the hydraulic conductivity was constant, and the volume of outflow water represented more than three pore volumes of flow (PVF). The saturation process required approximately 2 to 3 days for each base course specimen.

After the specimen was saturated, the target soil suction was induced under a desorption process by applying suction using an air aspirator (Figure 2). Since soil suction in the field is usually less than 75 kPa (Raimbaut 1986), six specimens for each compacted base courses were prepared in a series of soil suctions (1.5 kPa, 10 kPa, 20 kPa, 40 kPa, and 65 kPa) that represent the likely range of field conditions. A confining pressure of 13.8 kPa was maintained

during suction conditioning. The target suction was verified by checking the equilibrium volume of outflow water as shown in Figure 3. After 60 hours, outflow from the specimens tended to reach equilibrium. To reach the desired suction, 2 to 4 days of suction conditioning, depending on the tested specimen, was required.

3.5.3 M_r and SRM Determination

Resilient modulus testing was performed at varying states of stress in accordance with NCHRP 1-28A protocol under Procedure Ia for base and subbase materials. Both internal and external linear variable differential transformers (LVDTs) were instrumented for measuring vertical displacement (Figure 2). Internal LVDTs were mounted on clamps at the quarter points around the specimen, while external LVDTs were mounted at the plunger and rested on the top of cell chamber.

Resilient moduli from the last five cycles of each test sequence were averaged to represent M_r for each load sequence. The M_r data for each specimen were fitted to the power function recommended by NCHRP 1-28A:

$$M_r = k_1 p_a \left(\frac{\theta - 3k_6}{p_a}\right)^{k_2} \left(\frac{\tau_{oct}}{p_a} + k_7\right)^{k_3} \quad \text{(Eq. 4.3)}$$

where k_1, k_2, k_3, k_6, k_7 are fitting parameters; p_a is atmospheric pressure (101 kPa); θ is bulk stress in kPa; and τ_{oct} is octahedral shear stress in kPa.

A summary resilient modulus (SRM) for each material was computed. For base course, SRM corresponds to the M_r at bulk stress of 208 kPa and the octahedral shear stress of 48.6 kPa (NCHRP 2004). SRMs for each specimen were measured from both external (SRM_{ext}) and internal LVDT (SRM_{int}). Figure 4 shows the relationship between SRM measured from internal and the SRM ratio (SRM_{int}/SRM_{ext}). The SRM ratio increases consistently with SRM calculated from internal LVDTs. This observation is similar to Sawangsuriya et al. (2009) and Camargo et al. (2008). An SRM computed from internal LVDT is believed to provide better accuracy than an

SRM computed from external LVDTs because displacement measured from an internal LVDT can eliminate the errors resulting from machine compliance and end (bedding) effects (Camargo et al. 2008; Tatsuoka et al. 1995). Thus, only SRMs calculated from internal LVDTs were reported in this study.

3.5.4 M_r Prediction Incorporating Soil Suction

Prediction of M_r for unsaturated pavement layer is employed in mechanistic pavement design (NCHRP 2004; Tatsuoka et al. 1995, Cary et al. 2010). The Mechanistic-Empirical Pavement Design Guide (M-EPDG) addresses the effect of moisture on modulus properties by incorporating an adjusting factor, which calculates the change in modulus at a particular degree of saturation to the optimum degree of saturation. However, using a mechanistic approach, soil suction affects the state of stress of soil and, consequently, changes the modulus. Thus, the influence of soil suction should be addressed in a model that predicts M_r for unsaturated conditions.

Liang et al. (2008) proposed a mathematical model based on the effective stress concept for predicting M_r by considering the effect of moisture variation and by assuming that pore-air pressure is zero. The equation includes effects of bulk stress, octahedral shear stress, and soil suction, which can be described as:

$$M_r = k'_1 P_a \left(\frac{\theta+\chi\psi}{P_a}\right)^{k'_2} \left(\frac{\tau_{oct}}{p_a}+1\right)^{k'_3} \quad \text{(Eq. 4.4)}$$

where k'_1, k'_2, k'_3 = fitting parameters; ψ = soil suction; and other parameters are defined previously.

The parameter χ is Bishop's effective (Lu and Likos 2004) stress parameter, which is defined as the proportion of area (a) contributed by water (a_w), ($\chi = a_w/a$). For unsaturated soil, the parameter χ reflects the proportion of soil suction that contributes to the stress state and

varies between zero (dry soil) to unity (saturated soil). However, determination of the parameter χ is difficult due to lack of unique relationship between degree of saturation and χ (Mitchell and Soga 2005). Liang et al. (2008) calculated the parameter χ by adopting Khalili and Khabbaz's (1998) equation, which assumes that the relationship between χ and soil suction is linear in logarithmic scale when soil suction exceeds ψ_a as:

$$\chi = \left(\frac{\psi_a}{\psi}\right)^{0.55} \quad \text{(Eq. 4.5)}$$

The Liang et al. (2008) model is useful for predicting M_r when incorporating effects of moisture. However, this model cannot predict M_r near saturation when ψ is less than ψ_a and cannot describe unsaturated soil behavior at residual saturation. In addition, a base course may exhibit a bimodal SWCC behavior, which invalidates certain assumptions used by Khalili and Khabbaz (1998). To surpass this limitation, for this study, χ was defined by using a formulation proposed by Vanapalli and Fredlund (2000) as:

$$\chi = \Theta^{\kappa} = \left(\frac{S - S_r}{1 - S_r}\right)^{\kappa} \quad \text{(Eq. 4.6)}$$

where κ is a fitting parameter that provides flexibility to fit χ between measured and prediction values proposed by Vanapalli et al. (2000).

Eq. 4.6 allows for the prediction χ based on SWCC data and the fitting parameter κ, which covers unsaturated behavior from a saturated state to dry state. Hence, Eq. 4.4 can be rewritten as:

$$M_r = k'_1 P_a \left(\frac{\theta + \Theta^{\kappa}\psi}{P_a}\right)^{k'_2} \left(\frac{\tau_{oct}}{p_a} + 1\right)^{k'_3} \quad \text{Eq. 4.7}$$

For base course, an SRM prediction can be developed from Eq. 4.6 by using θ = 208 kPa and τ_{oct} = 48.6 kPa. Because the τ_{oct} value is fixed, the parameter k'_3 can be considered negligible. The SRM prediction incorporates soil suction through:

$$SRM = k_A \left(\frac{208+\theta^{\kappa}\psi}{P_a}\right)^{k_B} \quad \text{Eq. 4.8}$$

where k_A, k_B = fitting paramters; Θ is determined by using Eq. 4.1 for unimodal SWCC soil and Eq. 4.2 for bimodal SWCC soil.

3.6 RESULTS AND ANALYSIS

Fitting parameters regression from Eq. 4.3, summary resilient modulus (SRM), and coefficient of determination for studied RAP, RPM, RCA and crushed limestone under controlled suction and unit weight are presented in Table 3. The fitting parameters were computed based on resilient modulus from 30-sequence loading in according with NCHRP 1-28A protocol. The NCHRP 1-28A equation provide good fitting with R^2 ranging from 0.75 to 1.

3.6.1 SRM-Moisture Relationship for Studied Base Course

SRM variation with degree of saturation for RAP-WI, RPM-MI, and Limestone-WI is shown in Figure 5. SRM tends to decrease with degree of saturation for all studied materials. This trend is similar to that observed by Ba et al. (2013), in which an increase in moisture content led to a reduction in SRM for compacted crushed quartzite, basalt and limestone aggregates used for base courses. The type of materials affected the SRM-degree of saturation relationship. Among the studied base courses, RAP-WI provided the highest SRM, while limestone-WI provides the lowest SRM. These findings support previous researches that recycled base course (RAP, RPM, and RCA) provide high values of SRM, and are suitable for use as unbound base course (Guthrie et al. 2007; Bozyurt 2012). In addition, Figure 5 indicates that RAP, which is a hydrophobic material, tends to have low moisture levels (degree of saturation < 0.5). This implies that RAP may experience less freeze-thaw cycling, although further research is required in this area.

3.6.2 SRM-Moisture Relationship and Validation of Proposed Model

The relationships between SRM and soil suction are presented in Figure 6. SRM values for the base courses tended to increase with increasing matric suction. This finding supports the assumption that soil suction affects the bulk state of stress, which contributes to the modulus of soil. The measured SRMs were fit to the proposed model Eq. 4.8, which incorporates the SWCC function by using a least-squared optimization. The goodness of fit is quantified using coefficient of determination (R^2). Results are compared to the M_r predictions using the model proposed by Liang et al. (2008) as presented in Eq. 4.4.

The results show that the proposed model and the Liang et al. (2008) equation fit the measured SRM well for test specimens within the range of measured soil suction (1 kPa to 100 kPa), with R^2 ranging from 0.83 to 0.98. Both models exhibited similar curve fits at low suction and slightly different fits when matric suction is larger than 60 kPa. Figure 7 is a comparison between predicted and measured SRM using the proposed model and Liang et al. (2008) model for RAP-WI, RPM-MI, RCA-WI, and Limestone-WI. Proposed model and Liang et al. (2008) model provide an R^2 of 0.99 and 0.98, respectively. The proposed model tends to provide better predicted when matric suction is greater than 40 kPa. Typically, the parameter κ is used to adjust the difference between predicted and measured data and ranges, depending on soil type, between 1.0 and 3.0 (Vanapalli 2000). Higher κ results in low SRM at high soil suction. In this study, the best fit κ parameter varied from 0.49 to 2.75. The parameter k_A affects SRM at low suction, whereas the parameter k_B affects the slope of the fitting curve. All fitting parameters are summarized in Figure 6.

3.6.3 Normalized SRM versus Degree of Saturation and Soil Suction

The relationship between normalized SRM with the SRM at the optimum water content (SRM/SRM_{opt}) and degree of saturation is presented in Figure 8. The SRM ratio tended to decrease with degree of saturation for all studied materials. A consistent relationship for SRM ratio and degree of saturation cannot be developed at this time.

Figure 9 presents a relationship between SRM ratio and matric suction. Unlike the SRM ratio and degree of saturation relationship, the SRM ratio for the different types of base course materials form a single linear relationship with logarithmic soil suction within a narrow range (± 0.1 SRM/SRM_{opt}). By using a least-squares regression, SRM ratios can be described empirically with the following single equation:

$$\frac{SRM}{SRM_{opt}} = 0.71 + 0.15log\psi \qquad R^2 = 0.69 \qquad \text{(Eq. 4.9)}$$

This finding suggests that that the effect of moisture on M_r should be captured in terms of matric suction rather than degree of saturation or moisture content. In addition, Figure 8 illustrates that the SRM for compacted base course prepared at the optimum water content is generally greater than the SRM for specimens that is saturated and then dried. Hence, using SRM at optimum compaction without adjusting for deterioration due to environmental conditions may be unconservative.

The linear relationship between soil suction and resilient modulus ratio, Eq. 4.9, is similar to that presented in Ba et al. (2013). However, the slope and y-intersection of modulus ratio-soil suction from Ba et al. (2013) and this study are different. This could be because the types and gradation of test materials between the two studies are dissimilar. In addition, soil suctions from Ba et al. (2013) were obtained indirectly from a separately measured SWCC; whereas, in this study, matric suction was measured directly using an air aspirator with pressure gauge during modulus testing.

3.7 SUMMARY AND CONCLUSIONS

The impact of soil suction on M_r for compacted RAP, RPM, RCA-WI and limestone base course was investigated. Comparison between recycled asphalt and natural aggregate, RAP-WI, RPM-MI, and RCA-WI provides higher SRM than limestone-WI for the entire range of soil suction. These findings provide continued support that recycled base course provide excellent SRM and are suitable for use as unbound base course.

A mechanistic model developed on the principle of unsaturated soil mechanics is proposed to predict SRM via the SWCC function. A resilient modulus test that incorporates matric suction control was developed to test base course specimens at various suctions along the desorption path. The unsaturated mechanical behavior as presented by M_r of base courses (RAP, RPM, RCA and crushed limestone) from saturation to residual moisture was modeled for both unimodal and bimodal SWCC materials. The proposed model fit the test results well (R^2 = 0.80-0.98) over the full range of studied suction (1 kPa to 100 kPa). The proposed model follows a similar trend and is similar in accuracy in comparison to the Liang et al. (23) model. Increases in matric suction led to increases in SRM for all tested specimens.

An SRM ratio-suction relationship was developed. The SRM ratio was defined as SRM at a given suction to SRM at optimum compaction. The calculated SRM ratio for different types of base course materials forms a linear relationship with logarithmic soil suction. In contrast, the relationship between SRM ratio-degree of saturation is unique for each studied base course. Hence, the effect of moisture on M_r or SRM is best described using soil suction instead of degree of saturation or water content.

3.8 ACKNOWLEDGEMENTS

This study was supported by The UW-Solid Waste Grant Program (SWRP). The material evaluated in this study was provided from the TPF-5(129) Recycled Unbound Materials Pool Fund administered by the Minnesota Department of Transportation. The authors acknowledge help and support of the Royal Thai Government during the study.

3.9 REFERENCES

Ba, M., Nokkaew, K., Fall, M., and Tinjum, M. Effect of Matric Suction on Resilient Modulus of Compacted Aggregate Base Course. Geotechnical and Geological Engineering, vol. 3, No. 3, 2013.

Bozyurt, O., Tinjum, J.M., Son, Y.H., Edil, T.B., and Benson, C.H. *In GeoCongress 2012*, ASCE, Oakland, 2012, pp. 3901-3910.

Burger, C.A. and Shackelford, C.D. Soil-Water Characteristic Curves and Dual Porosity of Sand-Diatomaceous Earth Mixtures. *Journal of Geotechnical and Geoenvironmental Engineering*, Vol. 127, No.9, pp. 790-800.

Camargo, F., Benson, C.H., and Edil, T.B. An Assessment of Resilient Modulus Testing: Internal and External Deflection Measurements. *Geotechnical Testing Journal*, Vol. 35, No. 6, 2012, 1995, pp. 837-844.

Cary, C.E., Zapata and C.E. Enhanced Model for Resilient Response of Soil Resulting from Seasonal Changes as Implemented in Mechanistic-Empirical Pavement Design Guide. In *Transportation Research Record No. 2170,* TRB, National Research Council, Washington D.C., 2010, pp. 36-44.

Cracium, O. and Lo, S.C.R. Matric Suction Measurement in Stress Path Cyclic Triaxial Testing of Unbound Granular Base Materials. *Geotechnical Testing Journal*, Vol. 34, No. 1, 2010, pp. 1-8.

Edil, T.B. Geotechnics of Sustainable Construction. *2nd International Conference on New Developments in Soil Mechanics and Geotechnical Engineering*, 2009, North Cyprus, pp. 108-116.

FHWA. Recycled Concrete Aggregate – Federal Highway Administration National Review. Federal Highway Administration, Washington, D.C., 2004.

Fredlund, D.G., and Xing, A. Equation for Soil-Water Characteristic Curve. *Canadian Geotechnical Journal*, Vol. 31, 1994, pp. 521-532.

Gokce, A.Investigation of the Parameters Controlling Frost Resistance of Recycled Aggregate Concrete. Doctoral Thesis, Nigata University,2001, pp. 33-34.

Guthrie, W.S., Cooley, D., and Eggett, D.L. Effects of Reclaimed Asphalt Pavement on Mechanical Properties of Base Materials. In *Transportation Research Record,* TRB, National Research Council, Washington D.C., 2007, pp. 44-52.

Kilbert, C.T. Policy Instruments for a Sustainable Built Environment. *Journal of Land Use & Environmental Law*, Vol. 17, 2002, pp. 379-394.

Lee, J.C., Edil, T. B., Tinjum, J.M., and Benson, C.H. Quantitative Assessment of Environmental and Economic Benefits of Recycled Materials in Highway Construction. In *Transportation. Research Record, No. 2158,* TRB, National Research Council, Washington D.C., 2010 pp. 138-142.

Liang, R.Y., Rabab'ah, H., and Khasawneh, M. Predicting Moisture-Dependent Resilient Modulus of Cohesive Soils Using Soil Suction Concept. *Journal of Transportation Engineering*, Vol. 134, No. 1, 2008, pp. 34-40.

Jong, D.T, Bosscher, P. J., Benson, C.H. Field Assessment of Changes in Pavement Moduli Caused by Freezing and Thawing. In *Transportation Research Record No. 1615,* TRB, National Research Council, Washington D.C., 1998, pp. 41-48.

Khalili, N., and Khabbaz, M.H. A Unique Relationship for χ for the Determination of the Shear Strength of Unsaturated Soils. *Geotechnique*, Vol. 48. No. 5, 1998, pp. 681-687.

Lu, N. and Likos, W. *Unsaturated Soil mechanics*. John Wiley and Sons, Inc., New York, 2004.

Mitchaell, J. k., and Soga, K. Fundamental *of Soil Behavior*. John Wiley and Sons, Inc., New York, 2005.

Nokkaew, K., Tinjum, J.M., and Benson, C. H., "Hydraulic Properties of Recycled Asphalt Pavement and Recycled Concrete Aggregate," *In GeoCongress 2012*, ASCE, Oakland, 2012, pp. 1476-1485.

Rahardjo, H., Vialvong, K., and Leong, E.C. Water Characteristic Curves of Recycled Materials. *Geotechnical Testing Journal*, Vol. 34. No. 1, 2010, pp. 1-8.

Transportation *of the United States*. National Atlas of the United States. from http://nationalatlas.gov/transportation.html. Accessed April 4, 2006

USGS. Mineral Commodity Summaries 2011. U.S. Gological, 2011.

Guide *for Mechnistic-Empirical Design for New and Rehabilitated Pavement Structure*. Final Report, 2004, NCHRP Project 1-37-A. www.trb.org/mepdg/guide.html. Accessed July 23, 2013.

Raimbaut, G. Cycles Annuels d'Humidite dans une Chaussee Souple et son Support. *Bull. de liason des. Loboratories des Ponts et Chaussees, Laboratoire Central de Ponts et Chaussees*, Vol. 145, 1986, pp. 79-84.

Sawangsuriya, A., Edil, T.B., and Benson, C.H. Effect of Suction on Resilient Modulus of Compacted Fine-Grained Subgrade Soils. In *Transportation Research Record No. 2101,* TRB, National Research Council, Washington D.C., 2009, pp. 82-87.

Tatsuoka, F., Teachavorasinskun, S., Dong, J., Kohata, Y., and Sata, T. Important of Measuring local Strains in Cyclic Triaxial tests on Granular Materials. Dynamic Geotechnical: Second Volume, ASTM STP123, ASTM International, West Conshocken, PA, pp. 107-114.

Vanapalli, S.K., and Fredlund, D.G. Comparison of Different Procedures to Predict Unsaturated Soil Shear Strength. Proc., of Sessions of Geo-Denver 2000, Advances in Unsaturated Geotechnics, ASCE, Reston, VA, pp. 195-209.

Vannapalli, S.K., Fredluand, D.G., Pufahl, D.E., and Clifton, A.W. Model for Predicting Shear Strength with respect to soil suction. *Canadian Geotechnical Journal,* Vol. 3, No. 3, 1996, pp. 379-352.

Table 3.1 Physical and Compaction Properties of Studied Materials

Properties	RAP-WI	RPM-MI	RCA-WI	Limestone-WI
USCS designation[1]	SP	SW	GW	GP-GM
AASHTO designation	A-1-a	A-1-b	A-1-a	A-1-a
Percent gravel (>4.75 mm)	35.7	49.3	59.3	50.5
Percent sand (4.75-0.075 mm)	64.8	50.3	39.1	41.5
Percent fines (<0.075 mm)	0.5	0.4	1.6	7.8
Specific gravity, G_s[2]	2.45	2.58	2.65	2.50
Maximum dry unit weight[3] (kN/m^3)	20.6	20.3	19.9	20.2
Optimum water content (%)[3]	6	6.4	7.5	8.1
Percent absorption[2]	1.5	1.7	4.2	2.5
Asphalt[4]/Mortar content[5]	4.3	3.8	21.05	-

Methods: [1] ASTM D422, [2] AASHTO T85, [3] ASTM D1557, [4] ASTM D6307, 5 Gokce (2001)

Table 3.2 Fredlund and Xing (1994) SWCC Parameters for four Base Courses

Parameters	RAP-WI	RPM-MI	RCA-WI	Limestone-WI	
				Macroscopic	Microscopic
α, α' (kPa)	0.29	2.56	2.25	0.65	1.22
m, m'	2.09	1.01	0.84	14.82	15.23
n, n'	0.61	0.68	0.47	3.26	1.1
ψ_r, ψ'_r (kPa)	6047	100	7716	99	100
ψ_a (kPa)	0.1	0.8	0.6	0.4	4.5
R^2	0.99	0.96	0.98	0.98	0.97

Table 3.3 Resilient Modulus Fitting Parameters, Summary Resilient Modulus (SRM), and Coefficient of Determination (R^2) for Recycled and Conventional Base Course under Controlled Suction and Unit Weight

Materials	Suction (kPa)	γ_d (kN/m^3)	Wn (%)	Fitting Parameters					SRM (MPa)	R^2
				K_1	K_2	K_3	K_6	K_7		
RAP-WI	1.5	17.9	6.4	2.6	11.3	-11.8	-1449.4	19.9	453.2	0.86
	10	18.2	4.0	1.4	8.0	-7.1	-1237.1	19.3	490.3	0.90
	20	18.2	3.6	2.3	16.8	-19.3	-1576.1	19.4	460.0	0.88
	40	17.5	3.9	92.1	2.5	-1.8	-172.9	1.3	490.9	0.96
	65	18.3	3.1	0.8	7.4	-6.6	-965.6	12.2	517.6	0.95
Optimum Compaction		18.0	5.7	15.2	7.9	-8.2	-1794.8	22.6	520.1	0.60
RPM-MI	1.5	19.8	9.2	7250.7	1.1	-2.3	-0.1	1.9	225.6	0.97
	10	20.3	6.2	331.5	2.1	-1.8	-64.5	1.0	278.9	1.00
	20	19.9	5.9	238.4	1.8	-1.0	-102.0	1.1	269.7	0.99
	40	19.9	5.0	88.3	3.2	-2.8	-218.1	2.8	294.6	0.88
	65	19.7	4.9	1465.5	1.8	-2.5	-27.6	1.0	358.3	0.94
Optimum Compaction		20.0	6.0	6718.8	0.9	-2.4	0.0	3.9	326.3	0.96
RCA-WI	1.5	19.0	12.6	162.7	2.0	-1.4	-71.5	1.0	166.4	0.95
	10	18.8	10.8	0.6	4.4	-2.1	-269.9	2.5	170.7	0.77
	20	19.2	9.3	1.2	4.2	-2.5	-228.2	1.5	199.2	0.96
	40	19.2	8.5	1.0	4.0	-1.8	-226.3	1.1	232.2	0.87
	65	19.2	8.0	291.0	2.0	-1.6	-78.4	1.0	295.7	0.96
Optimum Compaction		18.7	7.5	837.7	1.5	-1.2	-48.9	1.0	333.2	0.75
Limestone-WI	1.5	21.2	6.0	1088.5	0.68	-0.10	-2.2	23.5	133.2	0.98
	10	20.7	5.8	782.9	0.9	-0.1	-25.0	21.8	139.4	0.88
	20	20.3	5.0	2988.3	1.2	-1.3	-40.1	4.3	167.9	1.00
	40	21.3	3.2	4.2	2.8	-0.6	-281.8	1.4	188.6	0.95
	65	20.8	3.1	849.2	1.2	-1.2	-36.6	1.1	191.1	0.76
Optimum Compaction		20.6	7.3	125.4	3.0	-2.6	-175.7	3.0	173.7	0.93

[6] γ_d = Dry unit weight, [7] w_n = water content after testing

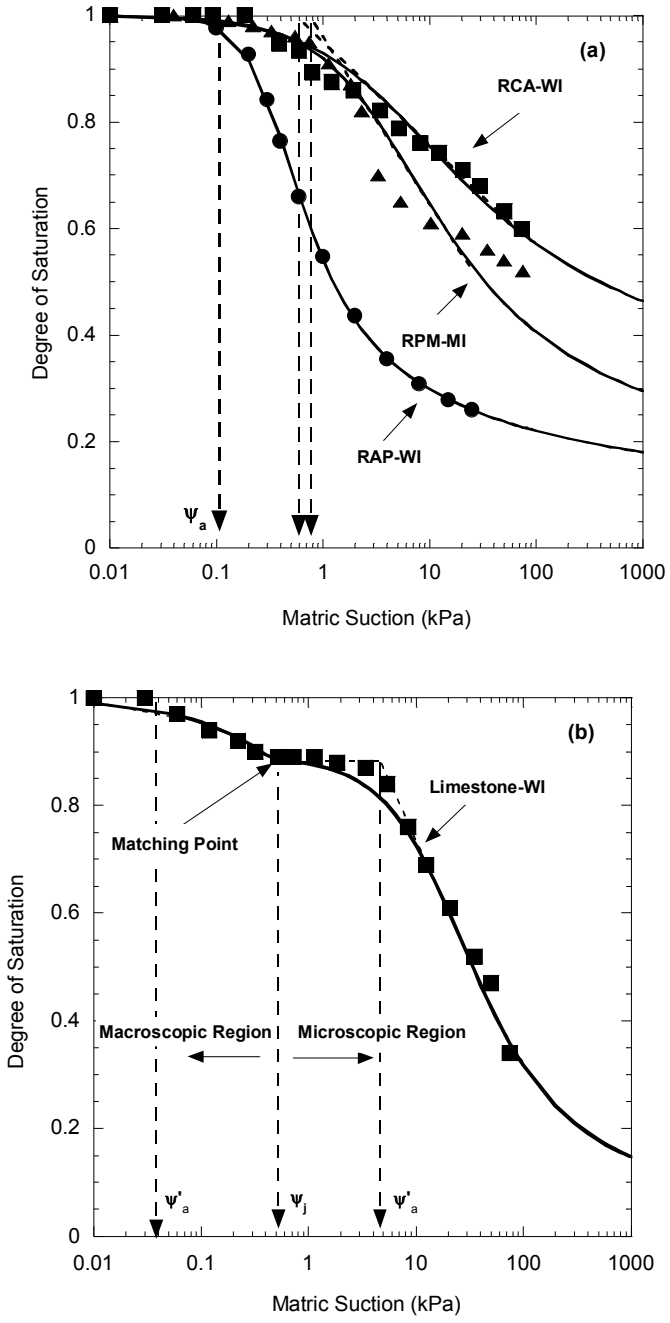

Figure 3.1 SWCCs of Base Courses Compacted near Optimum Water Content and 95% of Maximum Dry Density Using Modified Proctor Effort: (a) RAP-WI, RPM-MI, and RCA-WI Fitted with Unimodal Fredlund and Xing (1994) Model, (b) Limestone-WI Fitted with Bimodal Fredlund and Xing (1994) Model

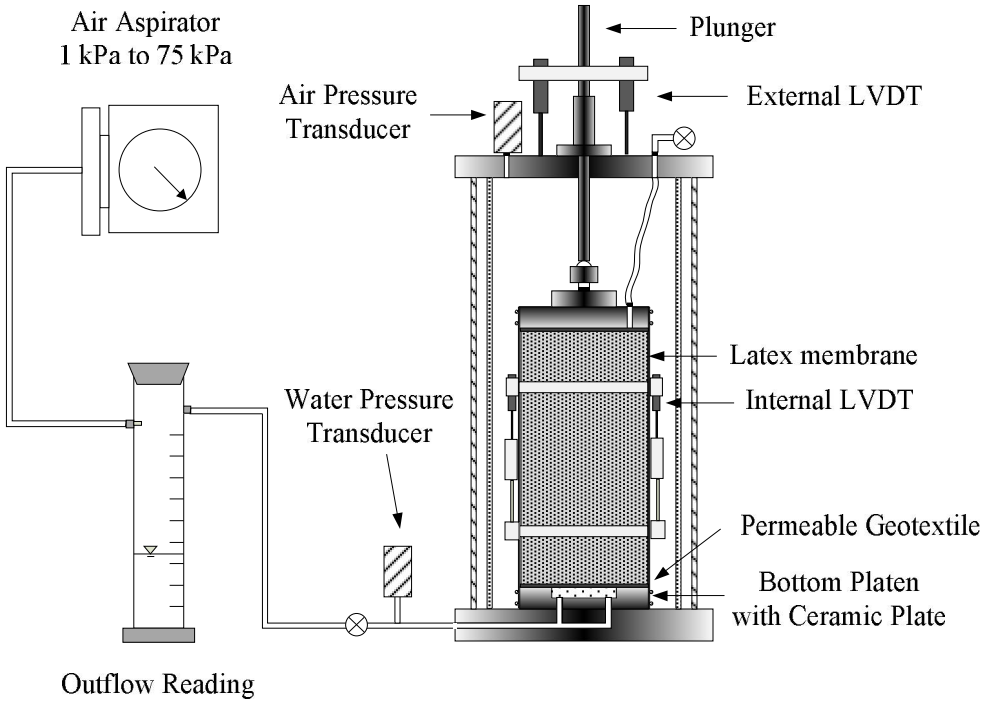

Figure 3.2 Resilient Modulus Testing System with Suction Control

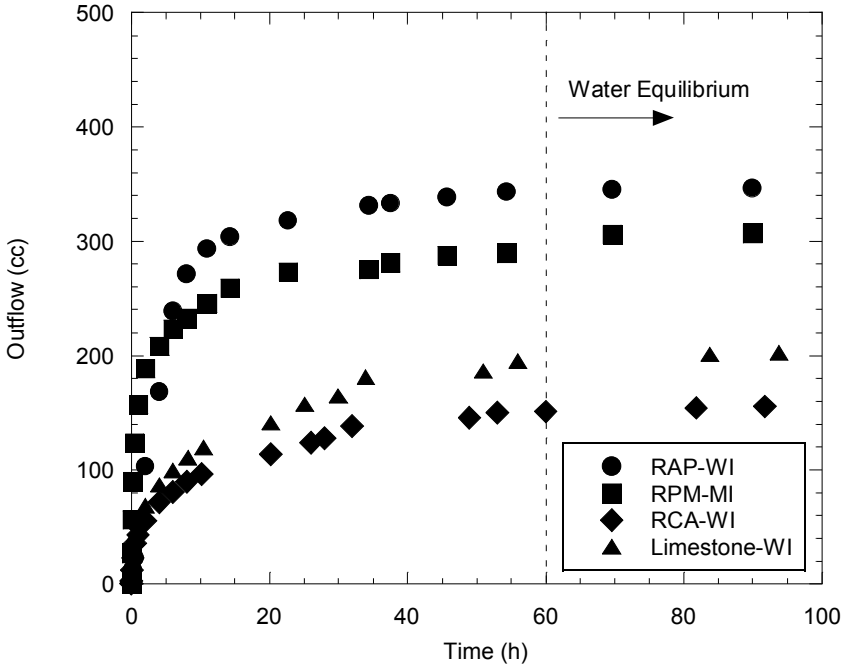

Figure 3.3 Verification of Equilibrium time for Soil Suction Conditioning for an Applied Suction of 10 kPa

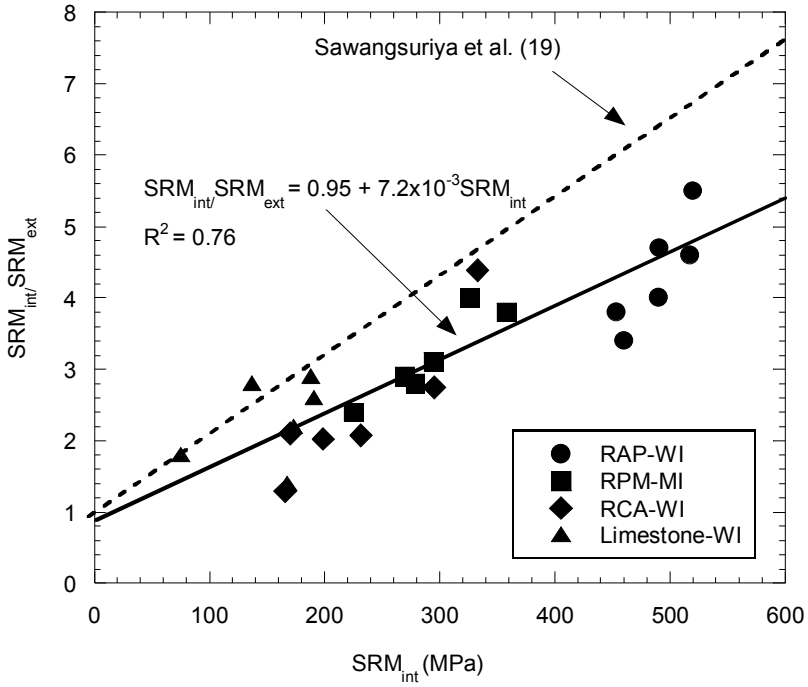

Figure 3.4 Ratio of Internal to External SRM versus Internal SRM

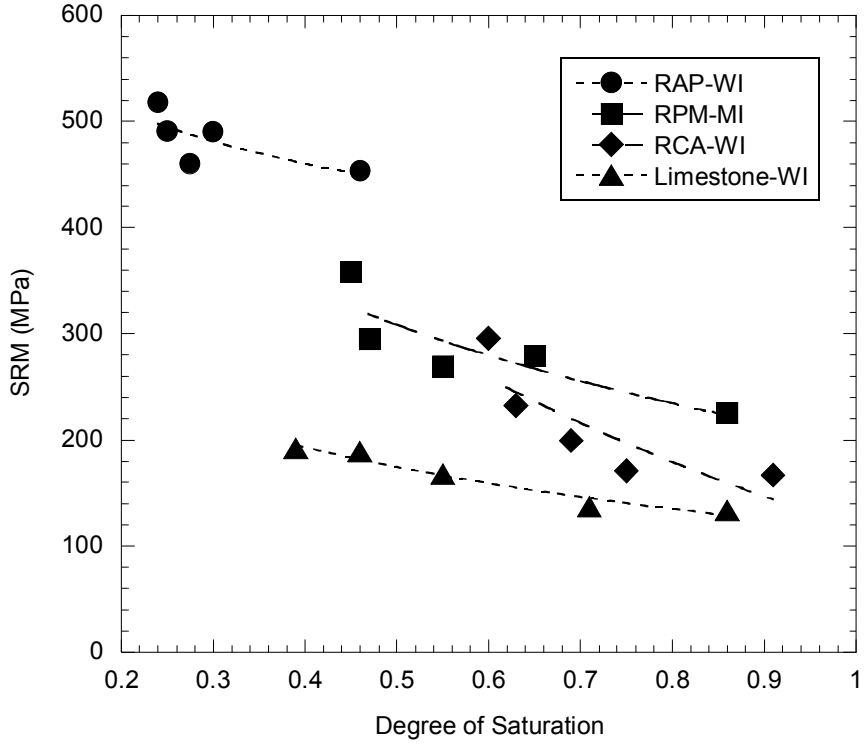

Figure 3.5 SRM Computed Using Internal LVDT versus Degree of Saturation

.

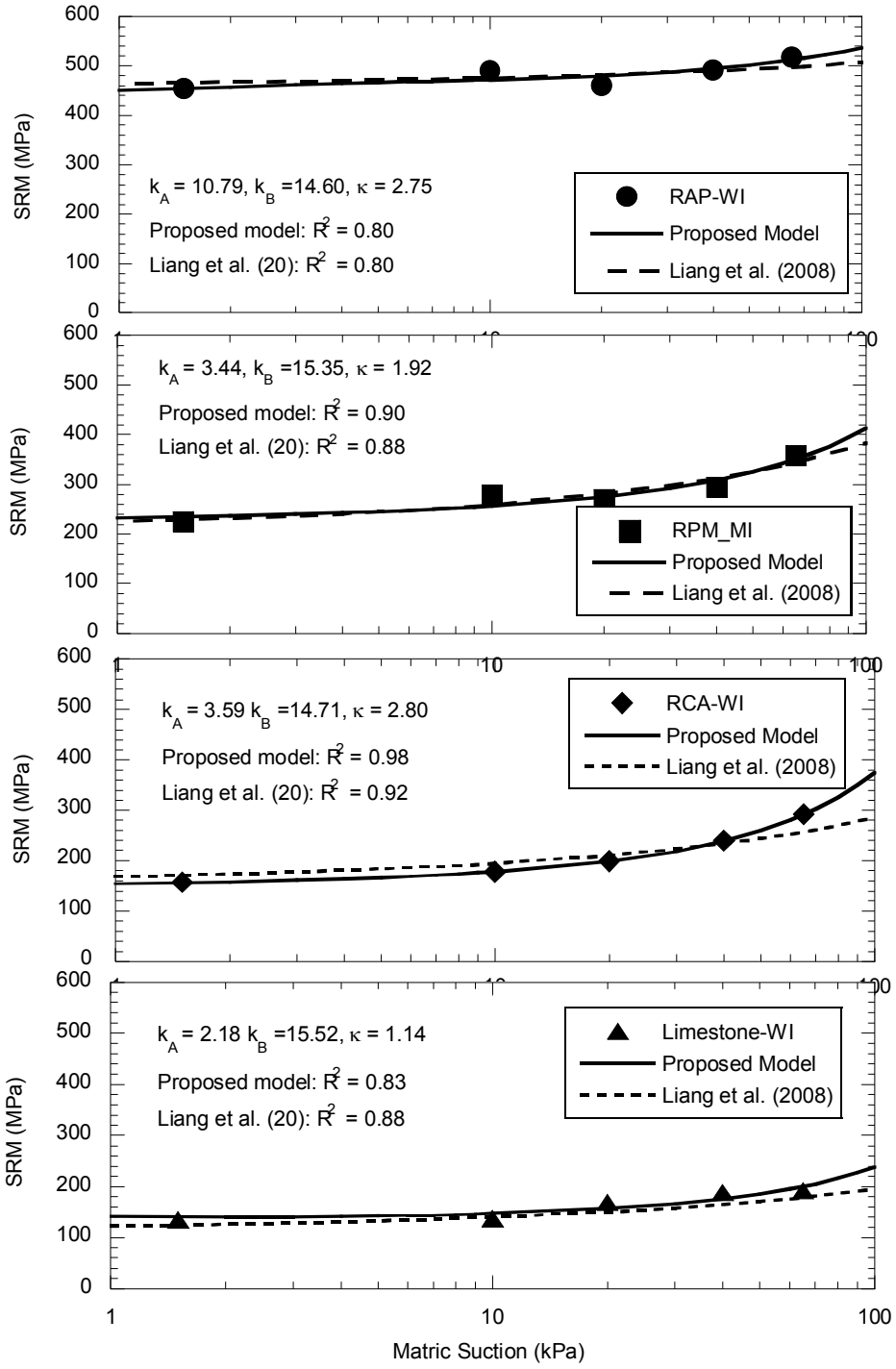

Figure 3.6 Relationship between Soil Suction and SRM for RAP-WI, RPM-MI, RAP-WI, and Limestone-WI

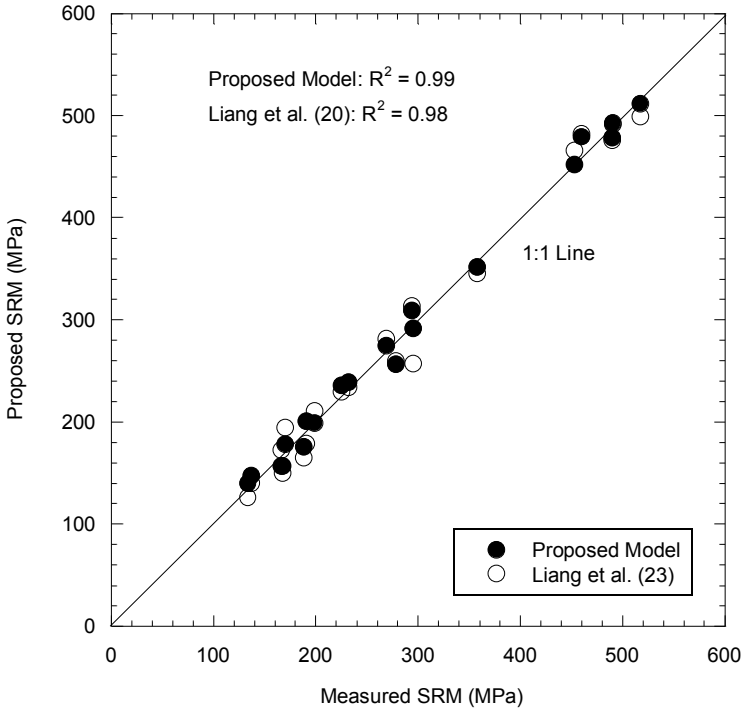

Figure 3.7 Comparison between Predicted versus Measured SRM for RAP-WI, RPM-MI, and Limestone-WI using Proposed Model and Liang et al. (2008)

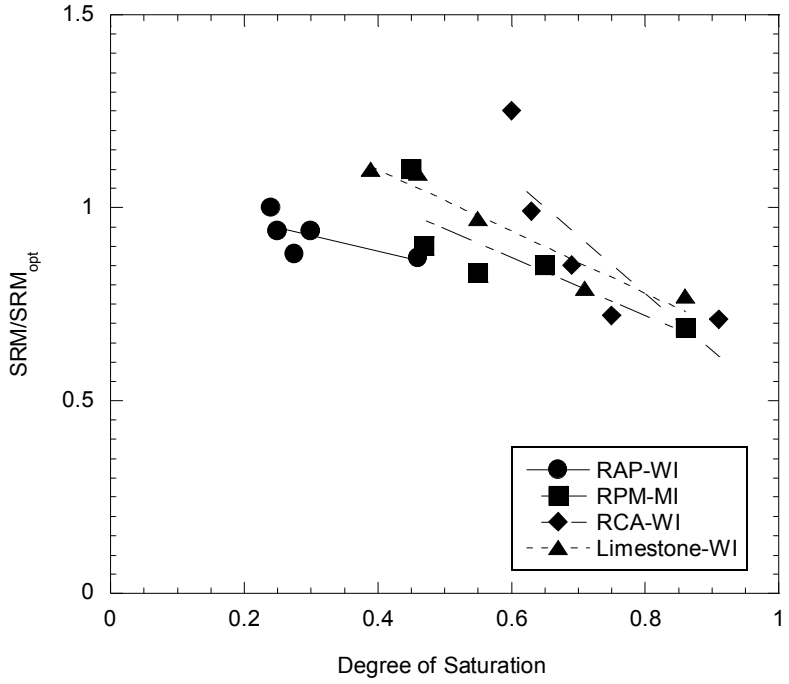

Figure 3.8 SRM Normalized with SRM at Optimum Water Content versus Degree of Saturation

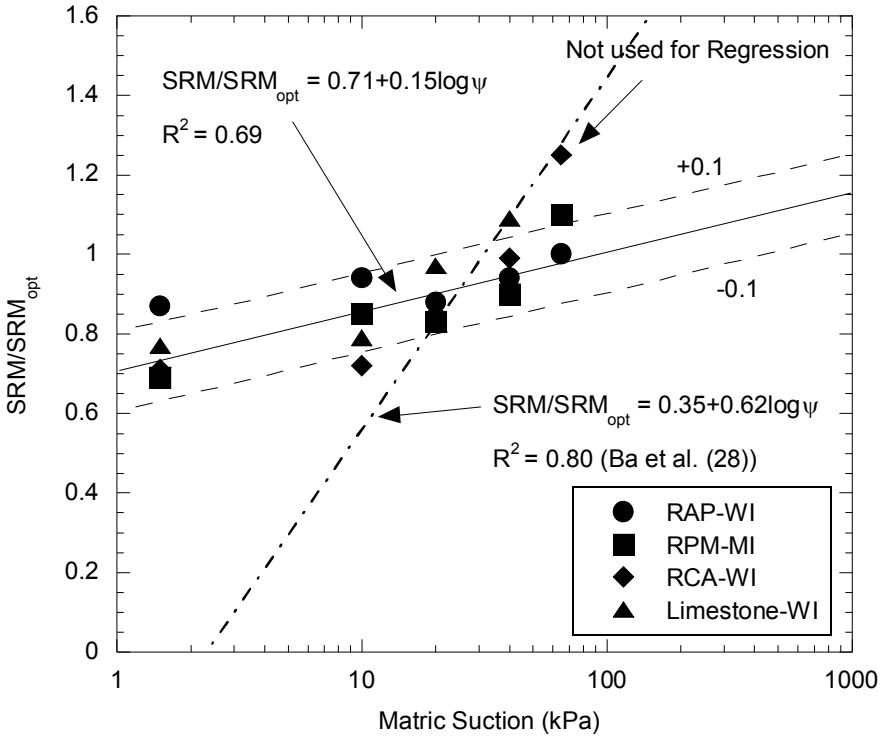

Figure 3.9 SRM Normalized with SRM at Optimum Compaction versus Soil Suction

CHAPTER 4: PERPORMANCE EVAUATION FOR RECYCLED AGGREGATE USED AS UNBOUND BASE COURSE PER THE MECHANISTIC-EMPIRICAL PAVEMENT DESIGN GUIDE (M-EPDG)

4.1 ABSTRACT

The use of recycled asphalt pavement (RAP), recycled concrete aggregate (RCA), and recycled pavement material (RPM) as a base layer have increased in recent decades. However, concerns about long-term performance and durability of the recycled aggregates have not been fully addressed due to their dissimilar hydraulic and resilient modulus characteristics from conventional aggregates. This paper investigates the impact of modulus and hydraulic property inputs for recycled aggregates (previously measured, see Chapters 2 and 3) to the Mechanistic-Empirical Pavement Design Guide (M-EPDG) on distress predictions. In addition, the environmental conditions (including freeze-thaw cycling and the effect of temperature on resilient modulus) that may impact pavement performance were evaluated for selected RAPs and RCAs, and compared to natural aggregate controls. Recycled aggregates tend to provide higher summary resilient modulus (SRM)—the resilient modulus that represents the state of stress in the field—in comparison to the natural aggregates used as controls in this study. As a result, distress predictions from the M-EPDG for recycled materials tend to be lower than those distresses for the natural, crushed aggregates. As evaluated through the analysis of variance (ANOVA), the modulus-level input for the M-EPDG analysis significantly changed the distress predictions, while the hydraulic-level input did not significantly affect the distress prediction. With increasing numbers of freeze-thaw cycles, the SRMs for RAPs decreased. In contrast, SRMs for RCAs actually increased after freeze-thaw cycling. The distress predictions due to freeze-thaw cycles corresponded to the SRM of the studied materials. This finding implies that RCAs would be beneficial for those locations where freeze-thaw cycling is of concern. Although increased

temperature reduces the SRMs of RAPs, the predicted distresses computed from the M-EPDG did not significantly change the distress prediction for flexible pavement.

4.2 INTRODUCTION

Since the rising price and the increased awareness of environmental impact of high-quality virgin aggregate are becoming concerned, a need of sustainable alternatives that can reduce the cost of material without reduced performance is required. Using recycled materials from construction and demolition (C&D waste) is a viable alternative to reduce demand of natural aggregate generation. Every year, more than 300 million tons of C&D wastes are produced and generated in the US, and many of which can be reused as base course layer in road construction (CSI 2013; NAPA 2013). Using C&D waste provides many advantages; 1) reduce the demand of natural crushed stone, a nonrenewable resource, 2) reduce the disposal of waste in landfills, 3) increase the life cycle of pavement material through beneficial reuse, and 4) reduce energy consumption and greenhouse gas emissions by on site reclamation and reuse of C&D waste (Kibert 2002; Edil 2009).

Among C&D waste, recycled concrete aggregate (RCA), recycled asphalt pavement (RAP), and recycled pavement material (RPM) have been most widely used. RCA, RAP and RPM are proved to provide excellence mechanical properties and significant life-cycled benefit suitable to use for unbound base course (Bennert et al. 2000; Blankenagel and Guthrie 2006; Bozyurt 2011). However, recycled aggregates are non-soil materials, and thus do not always have comparable behavior to conventional aggregates. As a result, concerns about pavement performance using recycled materials in the M-EPDG has been raised for designer in pavement design.

Resilient modulus (M_r) and the soil-water characteristic curve (SWCC) are primary inputs for M-EPDG analysis. Obtaining both M_r and SWCC parameters requires costly,

comprehensive, and time-consuming testing; thus, many M-EPDG users may prefer use of default M_r and SWCC parameters as recommended in the M-EPDG. However, RAP and RPM generated from old asphalt surfaces tend to provide high plastic deformation but better drainage in comparison to similar gradations of natural, crushed stone (Shedivy 2012), while RCA has the ability to absorb water due to small pores in the cement mortar (Vivian et al. 2005; Nokkaew 2012). Thus, recommended M_r and predicted SWCC parameters in the M-EPDG, which are developed from a database of natural aggregates, may not be congruent with recycled aggregates. Consequently, pavement distresses predicted from the M-EPDG may not represent realistic values for the pavement design.

Another stated concern with using recycled aggregate is the impact of environmental conditions on the long-term performance of the pavement. Increases in moisture content typically result in reductions to the modulus and thus the stiffness of the pavement. In sub-zero temperatures, moisture in the unbound layer become ice-lenses that rigidly bind the aggregate together, with resultant increases in stiffness (Mitchell 1993; Dawson 2009). However, as the ice lenses thaw, the stiffness of the unbound layer significantly decreases, leading to a general weakening of the unbound layer Previous American Association of State Highway and Transportation Officials (AASHTO) design procedures for pavement (AASHTO 1972; AASHTO 1986; AASHTO 1993) paid limited attention to these environmental effects. However, the current design protocol (M-EPDG) more fully considers the impact of climate and environmental effects through the input parameters needed for structural pavement design (NCHRP 2004).

In response to these concerns, a comprehensive suite of modulus and hydraulic properties were obtained from laboratory testing of RAPs, RCAs, and RPMs from various sources across the US. These measured properties were used to characterize the distress levels of flexible pavement based on the M-EPDG analysis. The main objectives of this study were to (1) investigate the effect of resilient modulus and hydraulic properties of recycled

unbound aggregate on pavement performance and (2) assess the impact of environmental effects, including change in modulus due to freeze-thaw cycling and change in temperature, on pavement distresses for selected conventional pavement structures. The influence of aggregate types and input level (Level 1 versus Level 3) in M-EPDG on pavement distresses is determined for each type of recycled aggregate evaluated in this paper.

4.3 BACKGROUND

4.3.1 The Mechanistic-Empirical Pavement Design Guide

Design practices for pavements have evolved greatly over the decades, starting with the AASHTO Guide for Design of Pavement Structures. The AASHTO design approach was developed based on AASHTO Road Tests that were conducted in the 1950's. Pavement design life was predicted through the structural number and road serviceability based on experimental data from the field and empirical predictions. Serious limitations in the design protocol developed from this empirical approach were addressed in the Workshop of AASTHO (1972). For example, the AASHTO procedure could not integrate changes in truck volume, climate and environmental effects, uniformity of base course and surface course, and pavement rehabilitation. This led to a lack of reliability in this approach to pavement design. The 1986 AASHTO Guide tried to fix the concerns and limitations of the earlier AASTHO guidance documents by incorporating design reliability to reduce the impacts of uniformity of pavement materials, but excessive layer thickness' were often observed (AASHTO 1986; Johaneck and Khazanovich 2010). During the development of 1986 AASHTO Guide, one of the conclusions from the seminar was that future design procedures should rely on mechanistic-empirical design. The life of a pavement could then be predicted by the cumulative distresses (e.g., fatigue, rutting, International Roughness Index (IRI)) over the service life of the pavement. The mechanistic-empirical design procedure was first introduced in the Workshop as a calibration of mechanistic models with performance tied to observations; i.e., empirical correlations. The 1993 AASHTO Guide version included

rehabilitation design and the effect of drainage in the base layer within the design procedure. However, the 1993 AASHTO Guide was an overall minor modification, and the design was still based on the empirical design approach (AASHTO 1993).

In 1996, the *Workshop on Pavement Design*, which was organized by the AASHTO Joint Task Force on Pavement (JTFP), recommended that a new AASHTO mechanistic-empirical pavement design procedure should be used by the year 2002. The workshop also recommended a long-term research project to develop the new mechanistic-empirical design guide, which was later realized as NCHRP Project 1-37A, *Development of the Guide for Design of New and Rehabilitated Pavement Structures*. The Mechanistic-Empirical Pavement Design Guide (M-EPDG) was subsequently introduced in 2002.

The M-EPDG provided a more realistic characterization of in-service pavement performance. The designer can incorporate the effects of traffic volume, climate, subgrade properties, and existing pavement conditions for rehabilitation. A trial design is evaluated by comparing cumulative pavement distresses (e.g., fatigue cracking, alligator cracking, and total rutting) over the service-life target with design reliability (NCHRP 2004; Li et al. 2011). The M-EPDG offers an hierarchical approach to design inputs, which provides the designer with flexibility to choose the design inputs based on the importance of the project and available resources. Three hierarchical levels are employed for traffic materials and environmental inputs:

- Level 1 input provides for the highest level of quality and accuracy and thus has the lowest uncertainty. Level 1 input is typically used for heavily trafficked pavements, such as interstate highways, and requires comprehensive laboratory or field testing. Using level 1 input requires the most resources and time.
- Level 2 input provides an intermediate level of accuracy and would be closest to the typical procedures for previous AASHTO design guidance. Level 2 inputs can be obtained from a limited testing program or estimated through correlations.

- Level 3 input provides the lowest level of accuracy. This level might be used for low-volume roads. Level 3 input typically would be user-selected values without the need for a testing program. Recommended parameters and national default values are provided in the M-EPDG software.

4.3.2 The Enhanced Integrated Climate Model

One of major change in the M-EPDG from previous AASHTO design is that the M-EPDG fully considers changes in temperature and moisture profiles in the pavement structure over the design life through the Enhanced Integrated Climate Model (EICM) (NCHRP 2004; Johaneck and Khazanovich 2010). The EICM integrated three models:

- The two-dimensional drainage infiltration model (ID Model)
- The Climatic-Materials-Structure Model (CMS)
- The CRREL frost heave and thaw settlement model

The EICM is based on the Integrated Climatic Model, developed for the Federal Highway Administration in 1989, but contains several improvements. The Fredlund and Xing (1994) soil-water characteristic curve (SWCC) model replaced the Gardner equation for a better prediction of the SWCC. For M-EPDG level 2 input, the SWCC parameters are estimated by index properties such as grain-size distribution (percent fines and D_{60}) and plasticity index (PI). A prediction of the unsaturated hydraulic conductivity based on the SWCC was also incorporated into the EICM.

The EICM model uses actual climatic data (hourly or monthly) and predicts the following parameters throughout the design life of the pavement structure: temperature, M_r adjustment factors, soil suction, frost and thaw depth, frost heave, and drainage performance (NCHRP 2004; Dawson 2009). The EICM evaluates the change in moisture from a reference condition (equilibrium moisture condition) for the subgrade and unbound layers. The model addresses the

effect of seasonal changes in moisture, and subsequently changes of modulus. Additionally, the model calculates the effect of freeze and thaw via a change to the modulus. For example, a stiffer modulus for frozen soil is applied during freezing periods and a reduced modulus is used in the model to simulate damage during periods of thaw.

4.3.3 Current State-of-Practice of Environmental Effect in the M-EPDG

The effect of stress state, moisture and density variation, and freeze-thaw are accounted for by adjusting the M_r in the M-EPDG. Environmental factors such as soil moisture, suction, and temperature are calculated by sophisticated climate modeling. The M_r at any time can be expressed as:

$$M_r = F_{env} M_{Ropt} \quad \text{(Eq. 4.1)}$$

where the factor F_{env} is an adjustment factor due to environmental effects, and M_{ropt} is the M_r at the maximum dry density and optimum water content at any state of stress.

The M-EPDG developed the function used for adjusting the M_r based on the effect of moisture for course- and fine-grained soil. The M_r is determined by:

$$log \frac{M_R}{M_{Ropt}} = a + \frac{b-a}{1+EXP\left(ln\frac{-b}{a} + k_m(S-S_{opt})\right)} \quad \text{(Eq.4.2)}$$

where M_R/M_{Ropt} = Resilient modulus ratio

a = Minimum of $log\left(M_R/M_{Ropt}\right)$

b = Maximum of $log\left(M_R/M_{Ropt}\right)$

k_m = regression parameter

$(S - S_r)$= Variation in degree of saturation expressed in decimal

The a, b, and k_m parameters for coarse-grained soil are -0.31, 0.3, and 6.82, respectively. The degree of saturation shown in the Eq. 4.2 is determined automatically by the

EICM software. A pedo-transfer function within M-EPDG is used to predict the SWCC based on the gradation curve and index properties of the soil as an alternative to direct measurement.

The effect of freezing and thawing is also considered in the M-EPDG by adjusting M_r. A frozen M_r is applied automatically if the calculated temperature from the EICM is lower than 0 ^{o}C for the subgrade or other unbound layerss. The default frozen M_r for coarse-grained soil, fine-grained soil, and clay are 2.1 GPa, 1.4 GPa, and 0.7 GPA, respectively. For thawed material, the M_r reduction factor ranges between 0.4 and 0.85 and is applied according to the potential for frost susceptibility as recommended in NCHRP (2004).

4.4 RESILENT MODULUS AND HYDRAULIC PROPERTIES OF RECYCLED AGGREGATES

Thirteen recycled materials and two conventional base courses were used in this study. Recycled materials include six RCAs, five RAPs, two RPMs. The recycled aggregates were collected from various states across the US and represent gradations used in practice. The two conventional base courses are Minnesota Class 5 aggregate (Class 5-MN) and crushed limestone from Wisonsin (Limestone-WI). These natural aggregate controls are used to compare their hydraulic and mechanical performance against that of the recycled materials.

All materials were targeted to be broadly, well-graded material with a low PI, thus providing the high strength and durability properties suitable for base course. Classified by AASTHO (ASTM D3282), the recycled and conventional base courses are A-1-a or A-1-b, which are well-graded granular materials suitable for use as base course. Studied materials were compacted at optimum water content and 95% of maximum dry density according to ASTM D1557.

4.4.1 Resilient Modulus

The mechanical performance of a pavement system depends mainly on the stiffness of the subsurface layers. In pavement design, M_r is a required parameter for the M-EPDG analysis

provides a measurement of pavement response to traffic loads. Various factors affect the M_r including loading conditions, moisture, angularity, particle-size distribution, and plasticity (Lekarp 2010). However, the most important factors are the stress conditions, including bulk stress (θ) and octahedron shear stress (τ_{oct}). A variety of mechanistic models have been proposed to express the M_r of as a function of stress state. Among these models, the Witczak-Uzan universal model has been widely accepted to provide a high-accuracy M_r prediction by combining the effects of confining stress and octahedron shear stress (NCHRP 2004; Uzan 1985; Witzak and Uzan 1988). The Witczak-Uzan model was adopted in the M-EPDG and requires three fitting parameters, as follows:

$$M_r = k_1 p_a \left(\frac{\theta}{p_a}\right)^{k_2} \left(\frac{\tau_{oct}}{p_a} + 1\right)^{k_3}) \quad \text{(Eq. 4.3)}$$

where θ = bulk stress = $\sigma_1 + 2\sigma_3$ (for cylindrical specimens)

σ_1, σ_3 = major and minor principal stress

τ_{oct} = octahedron shear stress

= $\frac{\sqrt{2}}{3}(\sigma_1 - \sigma_3)$ (for cylindrical specimens)

p_a = atmosphearic pressure = 100 kPa = 14.7 psi)

k_1, k_2, k_3 = regression parameters

The M_r test in this study was conducted immediately after sample compaction. According to NCHRP 1-28A protocol, the sample was subjected to 1,000 load cycles for preconditioning, followed by 30 load sequences. The M_r was calculated by averaging a pair of internal LVDTs to reduce the effects from bedding and machine compliance (Sawangsuriya et al. 2009; Camargo et al. 2012). M_r from the last 5 cycles of each test sequence are averaged to represent the M_r for each load sequence. A summary resilient modulus (SRM), which represents the stress state in the field, is required for M-EPDG level 3 input and is calculated according to section 10.3.3.9

of NCHRP 1-28A. For base course, the SRM is the M_r at a bulk stress of 208 kPa, and octahedron shear stress at 48.6 kPa.

4.4.2 Hydraulic Properties

The measured SWCC data form large-scale hanging column tests for the studied recycled aggregates and natural aggregate controls were fitted to the Fredlund and Xing (1994) model. The estimated suction (ψ) at equilibrium condition was used to predict the degree of saturation. The Fredlund and Xing (1994) equation provides a sigmoidal curve that is representative of different types of soil for matric suctions ranging from 0 to 1 GPa and was thus adopted for use in the EICM. The model requires four fitting parameters as defined by

$$\theta = C(\psi)\frac{\theta_s}{\left\{ln\left[e+(\psi/a_f)^{b_f}\right]\right\}^{c_f}} \quad \text{(Eq. 4.4)}$$

$$C(\psi) = \left[1 - \frac{ln\left(1+\frac{\psi}{h_{rf}}\right)}{ln\left(1+\frac{1\,000\,000}{h_{rf}}\right)}\right] \quad \text{(Eq. 4.5)}$$

where θ is volumetric water content, θ_s is saturated volumetric water content, ψ is suction in kPa, and a_f (kPa), b_f, c_f, and h_{rf}(kPa) are fitting parameters. $C(\psi)$ is the adjusting function that forces θ to zero at 1 GPa.

For data input level 2, the M-EPDG provides a_f, b_f, c_f and h_{rf} estimation based on D_{60}, P_{200} (percent fines), and PI per the following relationships:

$$a_f = 0.00364(P_{200}PI)^{3.35} + 4(P_{200}PI) + 11 \quad \text{(Eq. 4.6)}$$

$$\frac{b_f}{c_f} = -2.313(P_{200}PI)^{0.14} + 5 \quad \text{(Eq. 4.7)}$$

$$c_f = 0.0514(P_{200}PI)^{0.465} + 0.5 \quad \text{(Eq. 4.8)}$$

$$\frac{h_r}{a_f} = 32.44e^{0.0186(P_{200}PI)} \quad \text{(Eq. 4.9)}$$

where P_{200} is percent passing standard sieve No. 200 and PI refers to plasticity index. The M-EPDG automatically calculate hydraulic parameters when the grain-size distribution and PI are provided.

4.5 RESEARCH METHEDOLOGY

To evaluate the effect of M_r and hydraulic properties for recycled unbound aggregate on pavement performance, a sensivitivity analysis was designed for the M-EPDG analysis. The M-EPDG inputs and variables are summarized in Table 4.1. A conventional pavement structure comprised of an asphalt layer, base course, subbase, and subgrade was selected for pavement simulation. The effect of M_r and hydraulic properties were investigated via longitudinal cracking, alligator cracking, total rutting, and international roughness index (IRI). All distresses were calculated after 20 years. The variation in M_r and pavement distresses were defined via Eq. 4.7. Since the main objective of this research is to evaluable the quality of recycled materials used for unbound base course, only the properties of the base course were changed. The other properties (climate condition, traffic input, thickness of pavement structure, and material properties of other layers) were fixed. Input parameters that are not defined were used as default values recommended in the M-EPDG (input level 3). The 90% of reliability was used in the analysis. The failure criteria were defined as 18% of total area for alligator cracking, 31.6 m/km for longitudinal cracking, 1.9 cm for total rutting, and 2.53 m/km for IRI (NCHRP 2004; Attia and Abdelrahman 2010).

$$Percent\ Modulus\ Change = \left(\frac{modulus\ of\ reference - SRM\ of\ analyzed}{SRM\ of\ reference}\right) x100 \quad \text{(Eq. 4.10)}$$

$$Percent\ Distress\ Change = \left(\frac{distress\ of\ reference - distress\ of\ analyzed}{distress\ of\ reference}\right) x100 \quad \text{(Eq. 4.11)}$$

Although the MEPDG incorporates the effect of freezing and thawing cycles in the analysis by increasing M_r during the freezing period and reducing M_r during the thawing period. However, the impact of freeze-thaw cycles on M_r is not addressed in the M-EPDG model. In addition, the impact of temperature on M_r for RPAs is not be included in the M-EPDG. Thus, the results from Bozyurt (2011) and Shedivy (2012) were used to evaluate environmental effects, including freeze-thaw cycles (F-T cycles) and temperature on pavement performance with selected RAPs, RCAs, and Class 5-MN. Table 4.2 summarizes the environmental variables used for the sensitivity analysis. The SRM for selected recycled aggregates and Class 5-MN were determined at 1 F-T cycle, 5 F-T cycles, 10 F-T cycles, and 20 F-T cycles. The specimens were compacted at optimum water content and 95% of maximum dry density according to the modified Proctor test (ASTM D1557). After compaction, the specimens were secured in the PVC to prevent moisture loss and subjected to the design number of F-T cycles. Pavement distresses for each selected material at varying F-T cycles were predicted using the M-EPDG. The effects of temperature on M_r of the RAP were evaluated using NCHRP 1-28a protocols at 7, 23, 35, and 50 °C. Also, pavement distresses for each selected material at different F-T cycles were predicted using the M-EPDG.

4.6 RESULTS AND DISCUSSIONS

4.6.1 Effect of Resilient Modulus Input Level

The fitting parameters for M_r for fifteen different types of aggregates were regressed based on the Witczack-Uzan universal model with the resulting SRM and R^2 values summarized in Table 4.3. The universal model requires three fitting parameters (k_1, k_2, and k_3) for the M_r prediction. Among the three fitting parameters, k_1 is the most significant contributor to the M_r of aggregates (Pan et al. 2006). The k_2 parameter relates to bulk stress (θ) and affects the M_r of aggregates directly with a positive k_2 that wasobserved for all tested specimens. In contrast, the

k_3 parameter indicates the effect of octahedron shear stress (τ_{oct}) and was inversely correlated to M_r as indicted by negative values. SRM represents the M_r of aggregate at the field stress state and was higher for the RAPs, RCAs, and RPMs of this study in comparison to the natural aggregate controls. This indicates that recycled aggregates are stiffer than commonly used conventional aggregates. The high R^2, ranging from 0.71 to 0.97, indicated the goodness of prediction of the Witczack-Uzan universal model. The SRM for each material is a primary input for the analysis of M-EPDG with level 3 input. Recycled materials including RAPs, RCAs, and RPMs tended to provide higher SRM when compared to control aggregates.

Figure 4.1(a) is the relationship between θ and M_r predicted by the Witczack-Uzan universal model of select RAP-CO, RCA-CO, RPMI, and Class 5-MN aggregates. The M_r increased with θ for all aggregates. M_r at varying stress state behaves differently. At low θ (i.e., θ = 208 MPa as required for calculation of the SRM), the M_r varied from 157 MPa for Class 5-MN to 387 MPa for RAP-CO, and the M_r increased dramatically when θ was increased to 1,000 MPa (140% for Class 5 to 267% for RCA-CO). Figure 4.1(b) shows the relationship between τ_{oct} and M_r for the recycled aggregates. As shown in Fig. 4.1(b), the M_r decreased as τ_{oct} increases. The τ_{oct} decreased by 52% (Class 5-MN) to 66.5% (RCA-CO) when τ_{oct} changed from 48.6 kPa to 500 kPa.

Resilient modulus is a primary input to the M-EPDG and affects all of the distress predictions (NCHRP 2004). Many different types of distresses are associated with flexible pavement. Longitudinal cracking (sometimes called surface-down fatigue) results from excessive tension strains at the surface and is due to wheel load. Aging of the HMA surface mixture is believed to contribute to crack propagation. Alligator cracking, or fatigue cracking, results from elastic deflection in the pavement layer. Alligator cracking is related to tensile strains at the bottom of bound layers (Huang 2004). Rutting is a surface displacement in the wheel path that results from plastic deformation of all pavement layers and the subgrade. The International

Roughness Index (IRI) reflect smoothness of drive and is an important index that indicates road serviceability (Huang 1993; Al-Omari and Darter 1994; NCHRP 2004). The IRI in the M-EPDG is computed by the calculated distresses, including rutting, longitudinal cracking, and alligator cracking.

The cumulative pavement distresses or damages over time were calculated. Figures 4.2 to Figure 4.5 present the results computed from modulus input level 1 (k_1, k_2, and k_3) compared to those of modulus level 3 (SRM) at distresses after 20 years. For results calculated from modulus input level 3, the M_r was fixed to the SRM over the full analysis period. As SRM increases, all types of longitudinal cracking and alligator cracking decrease exponentially. For total rutting and the IRI, the distresses decrease slightly with increase in SRM. For modulus input level 1, change of M_r due to state of stress was included in the M-EPDG analysis. Because of the complicated stress state-M_r relationship, a consistent trend could not be developed when data input level 1 was implied. Based on the analysis of variance (ANOVA), distresses calculated from modulus input level 1 are significantly different in comparison to distresses calculated with data input level 3 ($F > F_{critical}$ for all types of distress predictions). Using modulus level 3, distresses predictions were not conservative for alligator cracking prediction as seen in Figure 4.3.

4.6.2 Effect of Hydraulic Input Level

In a pavement structure, moisture affects the modulus and, in turn, moisture levels are controlled by soil suction. Moisture can also affect soil structure through the destruction of cementation that may exist between soil particles (Lekarp et al. 2000; Mittchell 1993). Fredlund and Xing's (1994) fitting parameters are required for hydraulic data input for level 1. Hydraulic fitting parameters (input level 1) determined from large-scale hanging column tests for the studied recycled and conventional materials (see Chapter 2) are summarized in Table 4.4. Details of the regression and measurement techniques is presented in Nokkaew et al. (2012).

The Fredlund and Xing (1994) model provided good prediction for SWCC with R^2 ranging from 0.94 to 1.0 for all aggregates. For hydraulic input level 2, the M-EPDG estimates the SWCC based on grain-size distribution as well as plasticity index (see Eq. 4.6 to Eq. 4.9).

Figure 4.6 presents measured SWCCs of the recycled and control aggregates—including RAP-CO, RCA-CO, RPM-MI, and Class 5-MN—in comparison with the SWCCs predicted by the M-EPDG software. The results show that the Fredlund and Xing (1994) model fit the SWCC data well, with R^2 ranging from 0.99 to 1.00. The SWCC predicted by the M-EPDG tends to provide larger air entry pressure (ψ_a), defined as the soil suction where the largest water-filled voids begin to drain (Fredlund and Rahardjo 1993). After passing the ψ_a, the slope of the SWCC decreases rapidly to a residual degree of saturation, which is the degree of saturation in which an incremental increase in soil suction does not significantly change the degree of saturation.

In general, pavement with RAP, RCA, or RPM as the base course tended to provide lower longitudinal cracking and total rutting than Limestone-WI. A statistical analysis of predicted distresses between hydraulic property data input level 1 and hydraulic property data input level 2 used for the M-EPDG was conducted using ANOVA with a single factor. Results show that the calculated F value was lower than F critical, and p-values were larger than 0.43 for longitudinal cracking, fatigue cracking, total rutting, and the IRI prediction. This indicates that hydraulic property input does not significantly change the distress prediction in the M-EPDG.

Only alligator cracking and total rutting were used to present the impact of hydraulic input level on pavement performance. Figure 4.7 and Figure 4.8 present longitudinal cracking and total rutting after 20 years as predicted by the M-EPDG with hydraulic property data input level 1 and data input level 2. Use of hydraulic property data input Level 2 tended to provide conservative predictions of total rutting.

4.6.3 Effect of Freeze-Thaw Cycling on Pavement Distress with Recycled Aggregates as the Base Course

Freeze-thaw cycling is an environmental factor in cold climates that weakens pavement performance. The frozen, bound layer beneath the pavement can cause a major distress in the form of uneven uplift during freezing. When the temperature increases after a period in which frost penetrates into the pavement sublayers, water from melt ice or snow migrates to large voids created by ice lenses, resulting in loss of support upon thawing (Mitchell 1993). Figure 4.9 presents the change in SRM for several RAPs and Class 5-MN as a result of freeze-thaw cycling. Most of the change in the SRM of the RAPs occurred through five F-T cycles, with relatively small changes thereafter (Bozyurt 2011). Percent of SRM decrease due to F-T cycling ranged between 28% and 32% for the three RAPs that were tested. For Class 5-MN, F-T cycling had a relatively small effect on SRM (7% change after 20 F-T cycles). In contrast to RCAs, as shown in Figure 4.10, F-T cycling decreased the SRM at five F-T cycles, and then the SRM increased thereafter for all studied RCAs. After being subject to 20 F-T cycles, the SRM of RCA-CA, RCA-MI, and RCA-TX increased by 11%, 38%, and 15%, respectively, when compared to 1 F-T cycle. The self-cementing properties of RCA due to adhered mortar are believed to cause the increase in SRM (Arm 2001; Poon 2006; Bozyurt 2011).

Alligator cracking and total rutting are major distresses used to calculate pavement life; thus, these two types of pavement distress were selected to evaluate pavement performance when subject to F-T cycles. The impact of F-T cycles on alligator cracking predicted by the M-EPDG for RAPs and Class 5-MN is illustrated in Figure 4.11. As the SRM of the RAPs decreased with F-T cycles, the alligator cracking after 20 F-T cycles increased between 26% and 38% relative to those of 1-F-T cycle. For Class 5-MN, the number of F-T cycles increased the alligator cracking and, after 20 F-T cycles, the alligator cracking increased 12% relative to 1 F-T cycle. Figure 4.12 presents the effect of F-T cycling on the predicted total rutting for RAPs

and Class 5-MN. As discussed previously, total rutting is not sensitive to the SRM of the base course layer as determined by M-EPDG analysis. However, total rutting changed slightly due to the effect of F-T cycling (5% and 2% increase for total rutting for RAPs and Class 5-MN, respectively).

Freeze-thaw cycling contributed to the resulting distress levels in pavements when RCAs were used as the base course. Figure 4.13 presents the impact of F-T cycles on alligator cracking for selected RCAs. The increase in SRM in the RCAs due to F-T cycling (after 25 F-T cycles) for RCAs (see Fig. xx) contributed to a decrease in alligator cracking of between 4% and 18%. Figure 4.14 presents the impact of F-T cycles on total rutting for RCAs. The decrease in SRM due to F-T cycling in RCAs caused a reduction in rutting that ranged between 1.2% and 3.6%. This finding implies that RCA might be beneficial for use as a base course in areas where F-T cycling is of concern.

4.6.4 Temperature Effect

Temperature plays an important role in the characteristics of the M_r response in RAP because RAP contains asphalt binder, which is a temperature-sensitive material. As temperature increases, asphalt binder becomes less viscous thus causing a change in the modulus (Griffin et al. 1959). Selected RAPs including RAP-CO, RAP-NJ, and RAP-TX were used to determine the effect of temperature on SRM (Shedivy 2012). The results show that the increased temperature resulted in an increase to the rate of strain and also to the reduction in SRM for studied RAPs. Figure 4.15 presents the SRM of RAPs at varying temperatures. In comparing SRM at room temperature (23 ^{o}C) to a temperature 50 ^{o}C, the SRM of RAP-CO and RAP-TX were reduced by 13.8% and 7.6%, respectively. The SRM of RAP-NJ at 35 ^{o}C was reduced by 19.3% in comparison to SRM at 23 ^{o}C. The changes of SRM will affect the pavement performance as predicted in the M-EPDG.

The effect of temperature on alligator cracking predicted by the M-EPDG for RAPs is illustrated in Figure 4.16. Corresponding to the SRM-Temperature relationship, the alligator cracking tended to increase with an increase in temperature. The predicted alligator cracking increased 20.4% and 9.1%, respectively, for RAP-NJ and RAP-TX when the temperature changed from 23 ^{o}C to 50 ^{o}C. The predicted alligator cracking increased 16.8% when the temperature changed from 23 ^{o}C to 50 ^{o}C. Figure 4.17 shows the impact of temperature on total rutting. As temperatures increases, the total rutting increased slightly (between 1% and 4%) for the studied materials. This finding implies that change of SRM in RAP based on temperature does not significantly influence the distress prediction from the M-EPDG analysis.

4.7 CONCLUSIONS

This study investigated the effect of M_r and SWCC input on flexible pavement performance and assessed the impact of environmental effects, including freeze-thaw cycling and changing temperature, on for different RAPs, RCAs and RPMs. The studied materials were obtained from varying geographical sources across the US. The effect of freeze-thaw cycles and changing temperature were obtained from Boyzurt (2011) and Shedivy (2012). The different types of distresses that were evaluated included longitudinal cracking, alligator cracking, total rutting, and IRI, which were all predicted using the M-EPDG analysis. The main findings from this study include:

1. The Witczak-Uzan universal model provided M_r prediction of high accuracy, with R^2 ranging between 0.71 and 0.99 for all studied base course aggregates. The recycled materials (RAPs, RCAs, and RPMs) tended to provide higher SRM when compared to control aggregates.
2. The Fredlund and Xing model provided SWCC predictions of high accuracy, with R^2 ranging between 0.91 and 1.00 for all studied base course aggregates. The SWCC

predicted from grain-size distribution by the M-EPDG tended to provide higher air-entry pressure and a steeper slope for the SWCC prediction.

3. Modulus input level significantly impacted all types of distress predictions. Use of modulus level 3 in the M-EPDG analysis was not conservative for alligator cracking, total rutting, and IRI prediction.
4. Although the SWCC predicted from the M-EPDG differed from measured curves, the distress predictions were not significantly changed. This finding implies that M-EPDG design is not sensitive to the hydraulic property inputs.
5. Freeze-thaw cycling is known to decrease the SRM of RAPs (Bozyurt 201x), but contributes to an increase in SRM for RCAs. The increase of SRMs in RCAs is believed to be due to the self-cementing behavior of the adhered mortar in the RCAs. The distress prediction due to freeze-thaw cycling corresponded to the change in the resulting SRM. Among distress predictions, fatigue cracking was most sensitive to the number of freeze-thaw cycles.
6. Increased temperatures were responsible for only a slight reduction in the SRMs of RAPs. The effect of temperature did not significantly change the distress prediction for pavements that used RAPs as a base course layer in the M-EPDG analysis.

4.8 ACKNOWLEDGEMENTS

The material evaluated in this study was provided from the TPF-5(129) Recycled Unbound Materials Pool Fund administered by the Minnesota Department of Transportation. Ben Tanko assisted with the laboratory work. The grain-size analyses, index properties, and SRM from freeze-thaw cycling were conducted by Ozlem Bozyurt, a past graduate student in the Department of Civil and Environmental Engineering (CEE) at the University of Wisconsin-Madison (UW-Madison). The temperature-SRM relationship was provided by Ryan F. Shedivy, a past graduate student in UW-Madison CEE. Xiaodong Wang (Manager of the UW-Madison Soil

Mechanics Laboratory) and William Lang (Manager of UW-Madison's Structures and Materials Laboratory) assisted with experimental set up for resilient modulus testing.

4.9 REFERENCES

AASHTO (1972) "Interim Guide for the Design of Pavement Structures," American Association of State Highway and Transportation Officials, Washington DC.

AASHTO (1986). "Guide for Design of Pavement Structures," American Association of State Highway and Transportation Officials, Washington DC.

AASHTO (1993). "Guide for Design of Pavement Structures," American Association of State Highbway and Transportation Officials, Washington DC.

Al-Omri, B., and Darter, M.I., "Relationships Between International Rougness Index and Present Serviceability Rating," *Journal of Transportation Research. Record,* No. 1435, Transportation Research Board, Washington DC, 130-136.

Arm, M. (2001). "Self-cementing Properties of Crushed Demolished Concrete in Unbound Layers: Results from Triaxial Tests and Field Tests." *Waste Management*, 235-239.

Attia, M. and Abdelrahman, M. (2010). "Variability in Resilient Modulus of Reclaimed Asphalt Pavement as Base Layer and Its Impact on Flexible Pavement Performance," *Journal of Transportation Research. Record,* No. 2167, Transportation Research Board, Washington DC, 18-29.

Bennert, T., Papp Jr., W.J., Maher, A., and Gucunski, N. (2000). "Utilization of Construction and Demolition Debris under Traffic-Type Loading in Base and Subbase Applications," *Journal of Transportation Research. Record,* No. 1714, Transportation Research Board, Washington DC, 33-39.

Blankenagel, B.J., and Guthrie, W.S. (2006), "Laboratory Characterization of Recycled Concrete for Use as Pavement Base Material," *Journal of Transportation Research. Record,* No. 1952, Transportation Research Board, Washington DC, 21–27.

Bozyurt, O. (2011). "Behavior of Recycled Pavement and Concrete Aggregate as Unbound Road Base," Master Thesis, University of Wisconsin, Madison, WI.

Camargo, F., Benson, C.H., and Edil, T.B. (2012). “An Assesment of Resilient Modulus Testing: Internal and External Defection Measurements,” *Geotechnical Testing Journal*, Vol. 35, No. 6, 837-844.

CSI (2013). “Recycling Concrete,” Cement Sustainability Initiative, Conches-Geneva, Swisserland (http://www.wbcsdcement.org/pdf/CSI-RecyclingConcrete-FullReport.pdf)

Dawson, A. (2008). *Water in Road Structures*, Springer, Berlin, Germany.

Edil, T.B., 2009, “Geotechnics of Sustainable Construction” in *2nd International Conference on New Developments in Soil Mechanics and Geotechnical Engineering*, 28-30 May 2009, Near East University, Nicosia, North Cyprus, 108-116.

Fredlund, D.G. and Rahardjo, H. (1993). *Soil mechanics for unsaturated soils*, Wiley, New York.

Fredlund, D.G., and Xing, A. (l994). “Equations for the Soil–Water Characteristic Curve,” *Canadian Geotechnical Journal*, Vol. 31, No. 3, 521–532.

Griffin, R.L., Simpson, W.C., and Miles, T.K. (1959). “Influence of Composition of paving Asphalt on Viscosity, Viscosity-Temperature Susceptibility, and Durability.” *Journal of Chemical and Engineering Data*, Vol. 4, No. 4, 349-354.

Lekarp, F., Isacsson, U. and Dawson, A., 2000, “State of the Art.I: Resilient Response of Unbound Aggregates,” *Journal of Transportation Engineering,* Vol.126, No.1, Washington, DC, 66-75.

Li, Q., XIAO, D. X., Wang, K. C. P., Hall, K. D., and QIU, Y. (2011). “Mechanistic-Empirical Pavement Design Guide (MEPDG),” *Journal of Modern Transportation*, Vol. 19, No. 2, 114-133.

Kilbert, C.T. (2002), “Policy Instruments for a Sustainable Built Environment,” *Journal of Land Use & Environmental Law*, Vol. 17, 379-394.

Mittchell, J.M (1993). *Fundamental of Soil Behavior*, John Wiley & Son, Inc. New York.

NAPA (2013). “Asphalt: Greener than Ever,” National Asphalt Pavement Association and Federal Highway Administration, Washington, D.C. (http://www.asphaltpavement.org)

NCHRP (2004). “Guide for Mechanistic-Empirical Design of Pavement Structures,” *ARA,* Inc., ERES Consultants Division, Champaign, IL.

Nokkaew, K., Tinjum, J.M., and Benson, C. H. (2012). “Hydraulic Properties of Recycled Asphalt Pavement and Recycled Concrete Aggregate,” *In GeoCongress 2012*, ASCE, Oakland, CA, 1476-1485.

Pan, T., Tutumluer, and Anochie-Boateng, J. (2006). “Aggregate Morphology Affecting Resilient Behavior of Unbound Granular Materials,” *Journal of Transportation Research. Record,* No. 1022, Transportation Research Board, Washington DC, 12-20.

Poon, C.-S., Qiao, X., and Chan, D. (2006). “The Cause and Influence of Self-Cementing Properties of Fine Recycled Concrete Aggregates on the Properties of Unbound Sub-Base” *Waste Management,* No.26, 1166-1172.

Sawangsuriya, A., Edil, T.B., and Benson, C.H. (2009). “Effect of Suction on Resilient Modulus of Compacted Fine-Grained Subgrade Soils. *Journal of Transportation Research. Record,* No. 2101, Transportation Research Board, Washington DC, 82–87.

Shedivy, R. F. (2012). “The Effect of Climatic Condition and Brick Content on Recycled Asphalt Pavement and Recycled Concrete Aggregate as Unbound Road Base,” Master Thesis, University of Wisconsin, Madison, WI.

Uzan, J. (1985). “Characterization of Granular Material,” *Journal of Transportation Research. Record,* No. 1022, Transportation Research Board, Washington DC, 52-59.

Vivian, W.Y.T., Gao, X.F., and Tam, C.M. (2005). “Microstructural Analysis of Recycled Aggregate Concrete Produced from Two-Stage Mixing Approach,” *Cement and Concrete Research.,* Vol. 35, 1195-1203.

Witczak, M.W, and Uzan, J. (1988). The Universal Airport Pavement Design System, Report I of V: Granular Material Characterization. University of Mary Land, College Park.

Table 4.1 Input for All Variables Used in Sensitivity Analysis for Studying Impact of Resilient Modulus and Hydraulic Property Input Level in M-EPDG

Input Category	Input Variable	Number of Variable
Climate Station	Madison, WI	1
Design Traffic Volume	AADTT 1,500	1
Asphalt Concrete Layer	PG 58-34	1
Aggregate Base:	6-RAPs, 5-RCAs, 2-RPMs, 2-Controls	15
	Input Level 1 (k_1, k_2,k_3, a_f, b_f, c_f and ψ_r)	
	Input Level 2 (SRM, Predicted SWCCs)	
	Input Level 3 (SRM)	
Granular Subbase	River Run (Uniform graded sand), SRM = 134 MPa	1
Subgrade	A6 (AASHTO), SRM = 100 MPa	1

Table 4.2 Environmental Variables Used for Sensitivity Analysis

Environmental Effect	Material	Variable	Referenece
Freeze and Thaw Cycles	RAP-CA, RAP-MN, RAP-TX RCA-CA, RCA-MI, RCA-TX, and Class 5	SRM at 1 cycle, 5 cycles, 10 cycles, and 20 Cycles	Bozyurt (2011)
Temperature	RAP-CO, RAP-NJ, RAP-TX,	SRM at 5^{o}C, 15 ^{o}C, 23 ^{o}C,	Shedivy (2012)

Table 4.3 Witczack-Uzan's Fitting Parameters, Summary Resilient Modulus, and Coefficient of Determination (R^2) for Studied Base Course Aggregates

Material Type	Aggregate	K_1 (MPa)	K_2	K_3	M_r (MPa)	R^2
RAP	RAP-CO	16.2	0.63	-0.57	297	0.81
	RAP-MN	19.7	0.73	-0.94	337	0.83
	RAP-NJ	14.1	0.90	-0.90	277	0.93
	RAP-OH	20.5	0.91	-1.28	350	0.92
	RAP-TX	28.6	0.77	-1.06	480	0.92
	RAP-WI	20.6	1.03	-1.30	380	0.94
RCA	RCA-CA	23.5	0.69	-0.96	386	0.71
	RCA-CO	21.6	0.83	-1.00	387	0.81
	RCA-NN	11.8	1.28	-1.76	217	0.85
	RCA-OH	23.7	1.00	-1.57	385	0.77
	RCA-WI	18.1	0.85	-0.91	342	0.82
RPM	RPM_MI	19.5	1.00	-1.23	359	0.88
	RPM-NJ	27.8	0.98	-1.35	482	0.83
Control	Limestone-WI	8.2	1.07	-0.94	180	0.96
	Class 5-MN	13.6	0.55	-1.59	157	0.97

Table 4.4 Fredlund and Xing (1994) Fitting Parameters and Coefficient of Determination (R^2) for Studied Base Course Aggregates

Material Type	Aggregate	Fredlund and Xing (1994) Parameters				R^2
		a_f	b_f	c_f	h_{rf}	
RAP	RAP-CO	1.9	1.5	0.5	97.0	0.99
	RAP-MN	3.0	2.6	0.4	97.0	1.00
	RAP-NJ	2.4	0.4	0.7	97.0	1.00
	RAP-OH	1.7	0.8	0.4	97.0	0.99
	RAP-TX	1.4	0.4	0.7	97.0	1.00
	RAP-WI	2.1	0.3	0.6	97.0	1.00
RCA	RCA-CA	1.4	1.2	0.2	104.8	1.00
	RCA-CO	67.6	0.7	2.2	100.0	0.99
	RCA-MN	2.8	4.9	0.2	97.0	1.00
	RCA-NJ	3.1	2.2	0.3	97.0	1.00
	RCA-WI	1.0	0.8	0.4	97.0	0.98
RPM	RPM-MI	2.4	1.0	0.3	97.1	0.99
	RPM-NJ	2.0	0.4	0.4	97.1	0.99
Control	Limestone-WI	0.8	4.3	0.9	100.0	0.94
	Class 5-MN	1.4	19.6	0.8	97.2	0.99

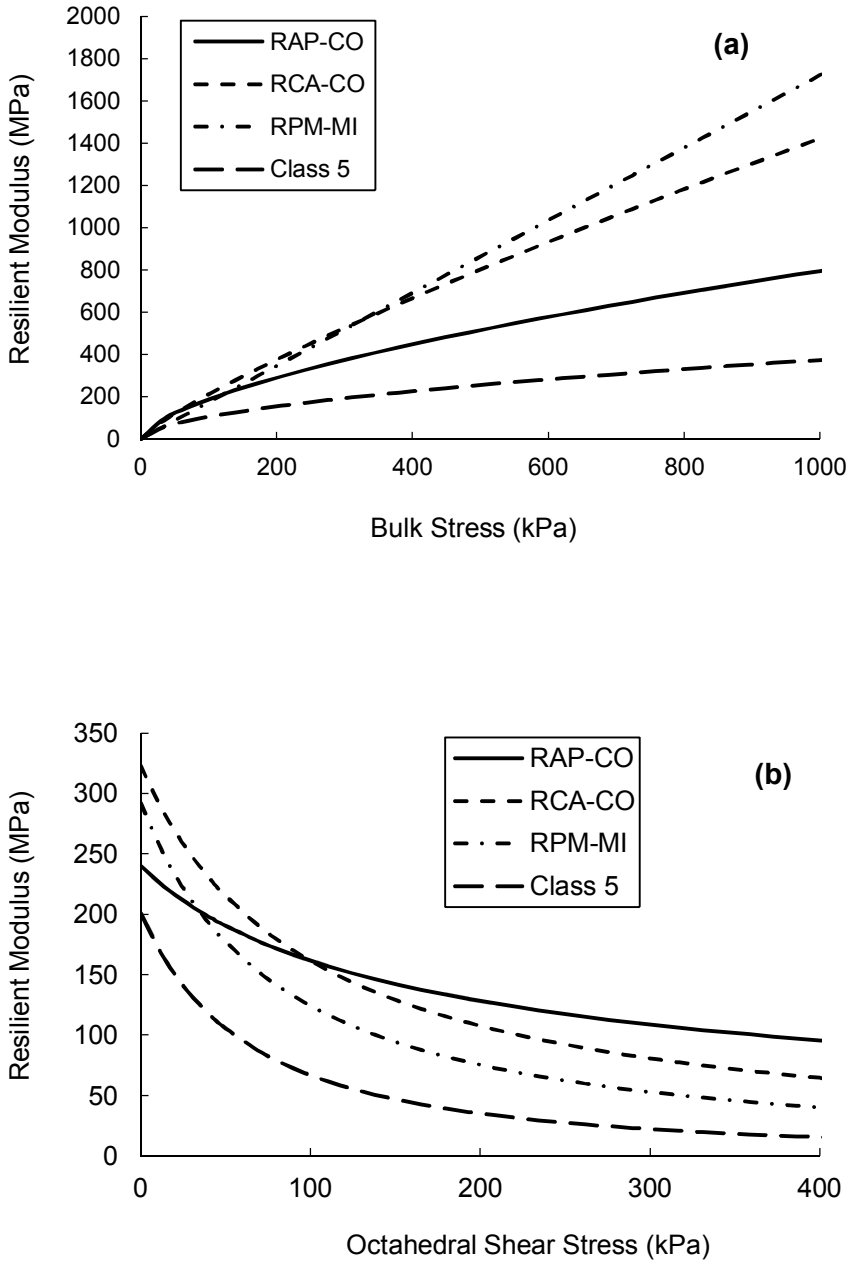

Figure 4.1 Resilient Modulus versus (a) Bulk Stress, (b) Octahedral Shear Stress for RAP-CO, RCA-CO, RPM-MI, and Class 5

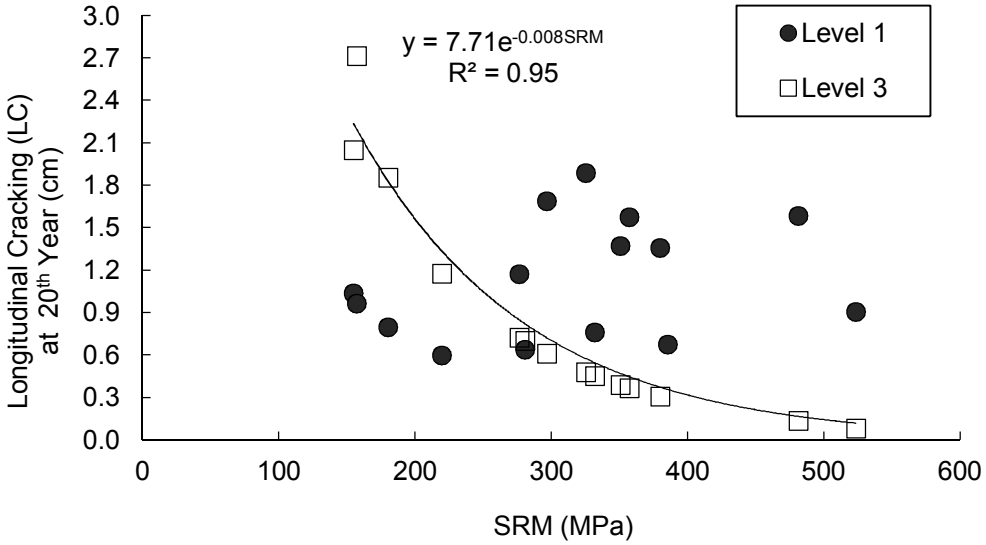

Figure 4.2 Relationship between Summary Resilient Modulus (SRM) and Total Rutting at 20th Year Predicted using M-EPDG

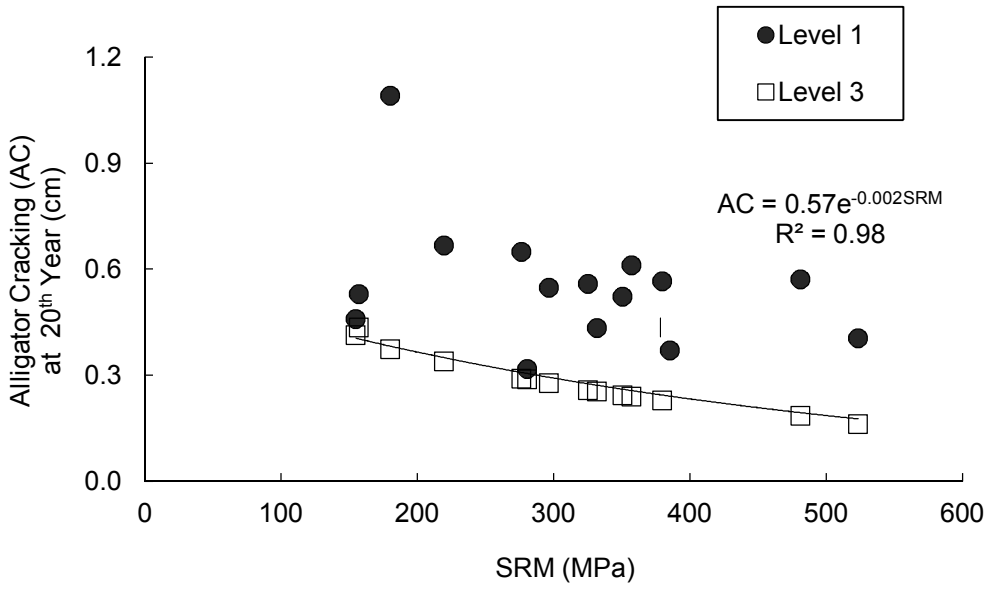

Figure 4.3 Relationship between Summary Resilient Modulus (SRM) and Total Rutting at 20th Year Predicted using M-EPDG

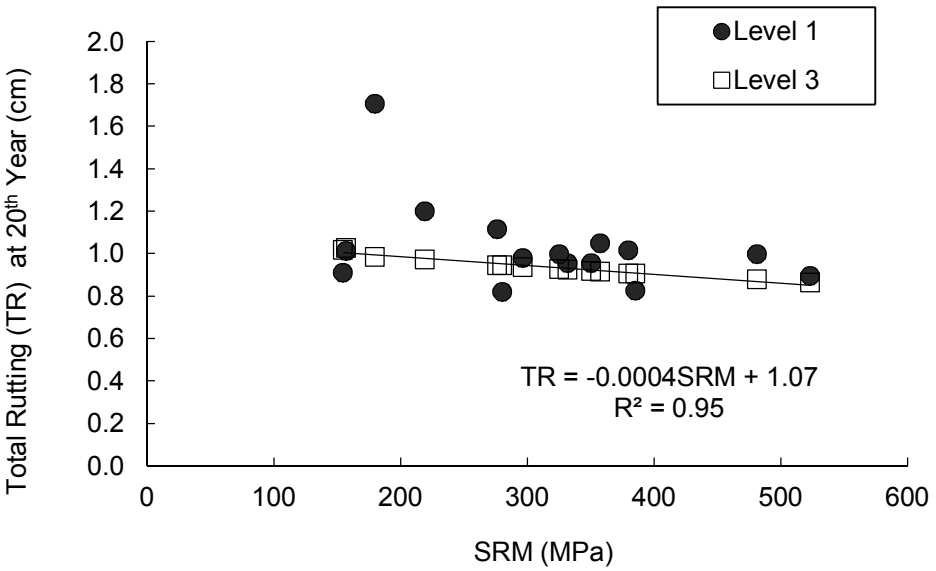

Figure 4.4 Relationship between Summary Resilient Modulus (SRM) and Total Rutting at 20thPredicted using M-EPDG

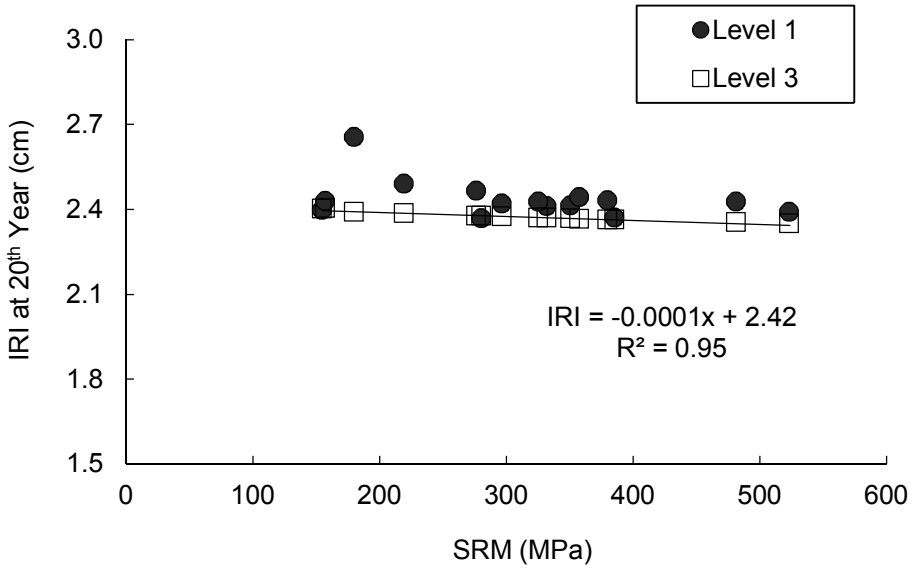

Figure 4.5 Relationship between Summary Resilient Modulus (SRM) and International Roughness Index (IRI) Predicted using M-EPDG

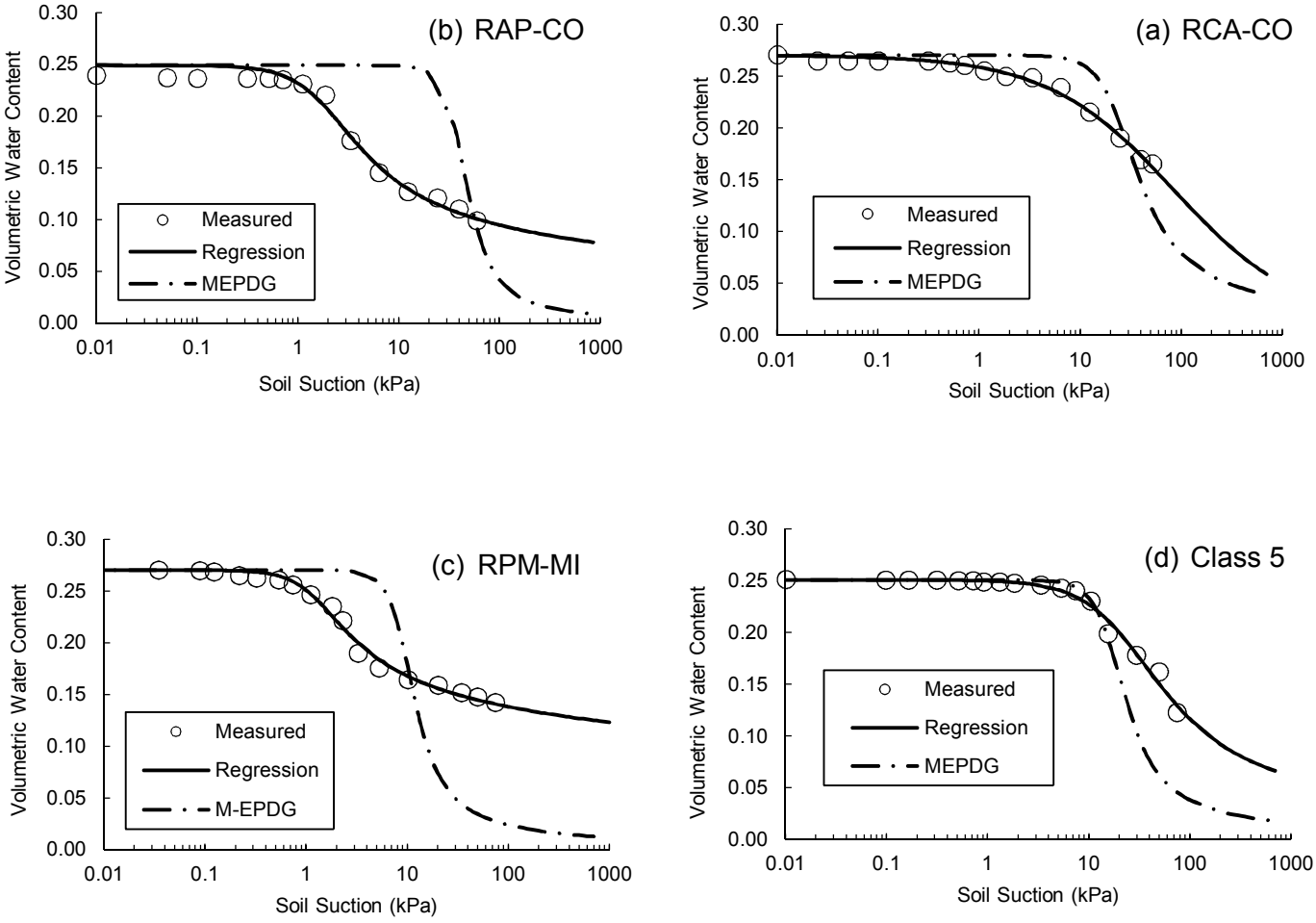

Figure 4.6 Measured Soil-Water Characteristic Curves with Fredlund and Xing (1994) model fit in comparison to M-EPDG prediction for (a) RAP-CO, (b) RCA-CO, (c) RPM-MI, and (d) Class 5-MN

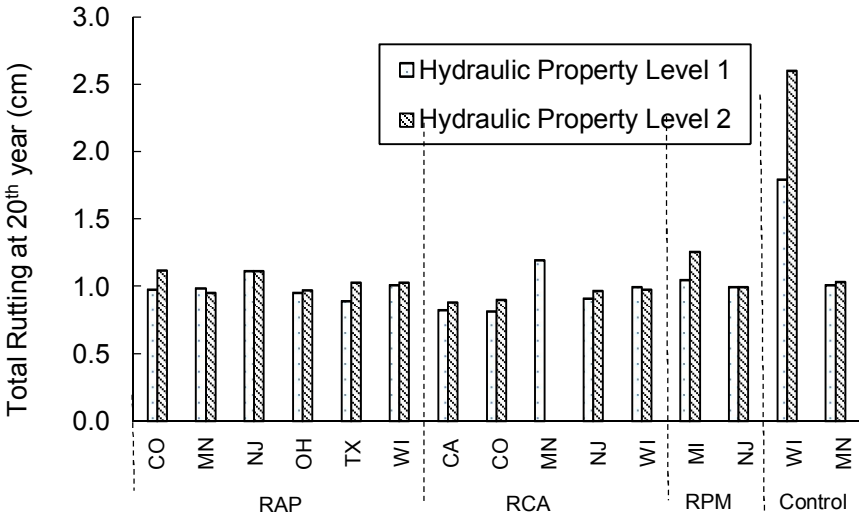

Figure 4.7Impact of Hydraulic Property Level on Total Rutting after 20 Years Predicted Using M-EPDG

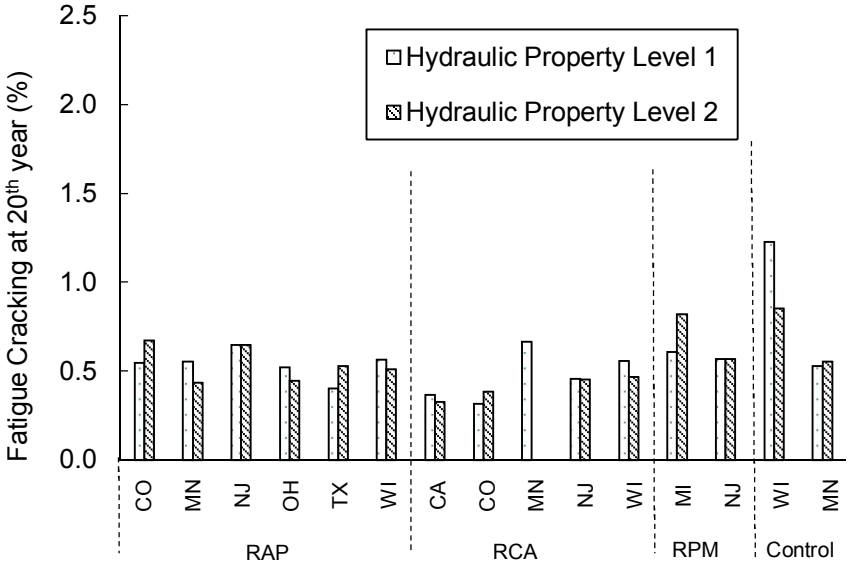

Figure 4.8 Impact of Hydraulic Property Level on Fatigue after 20 Years Predicted Using M-EPDG

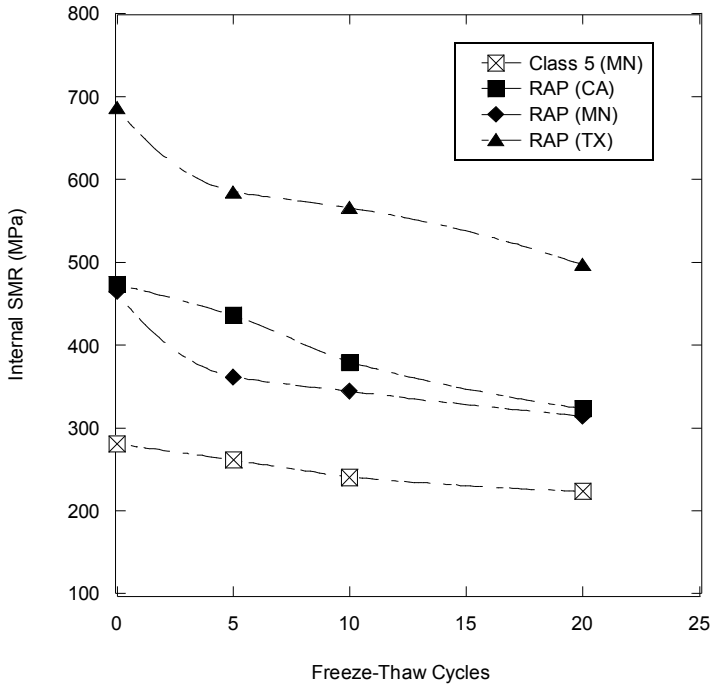

Figure 4.9 Internal Summary Resilient Modulus (SRM) of RAP and Class 5 aggregate after 0, 5, 10 and 20 freeze-thaw cycles

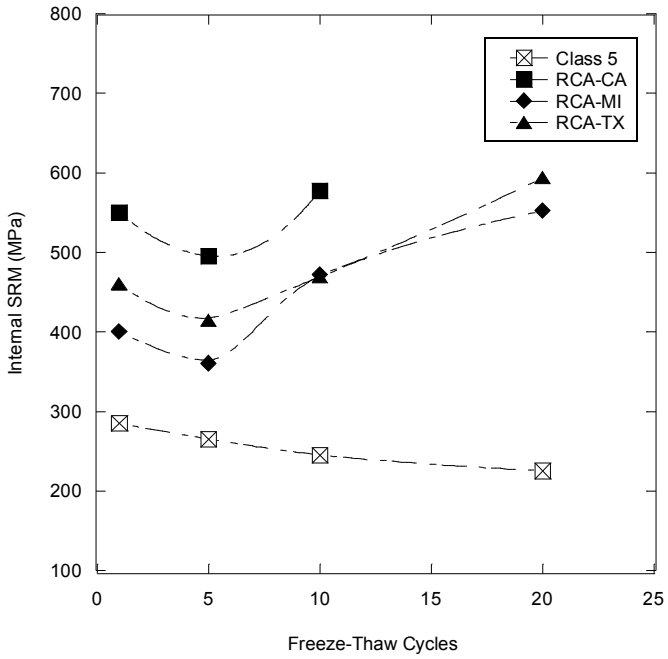

Figure 4.10 Internal Summary Resilient Modulus (SRM) of RCA and Class 5 aggregate after 0, 5, 10 and 20 freeze-thaw cycles

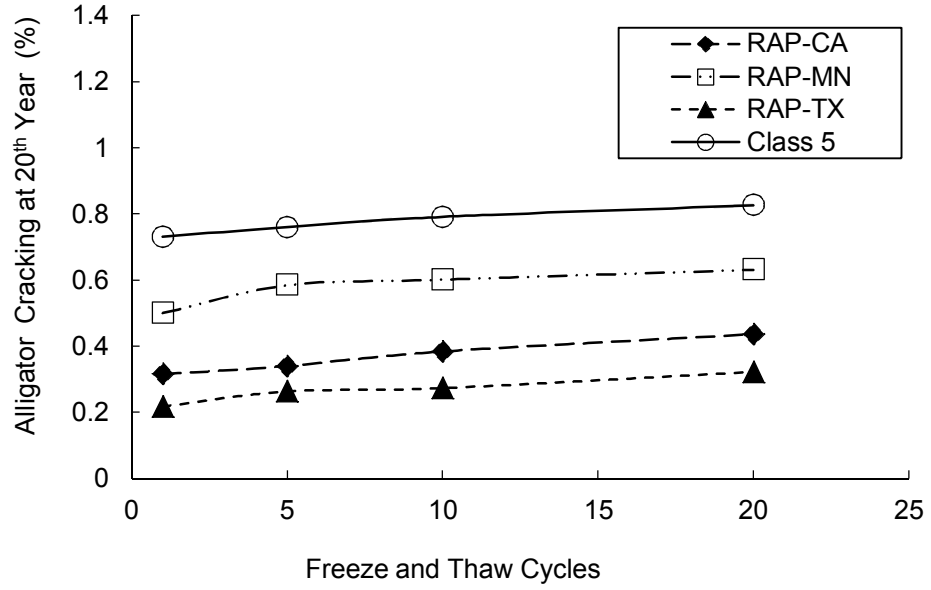

Figure 4.11 Effect of Freeze and Thaw Cycles on Alligator Cracking after 20 Years for Studied RAPs and Class 5-MN

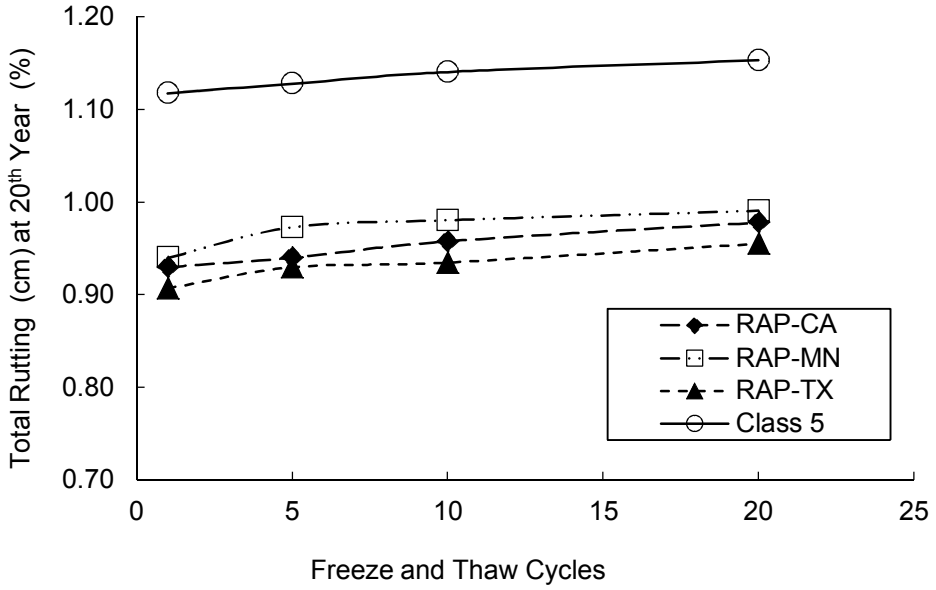

Figure 4.12 Effect of Freeze and Thaw Cycles on Total Rutting after 20 years for Studied RAPs and Class 5-MN

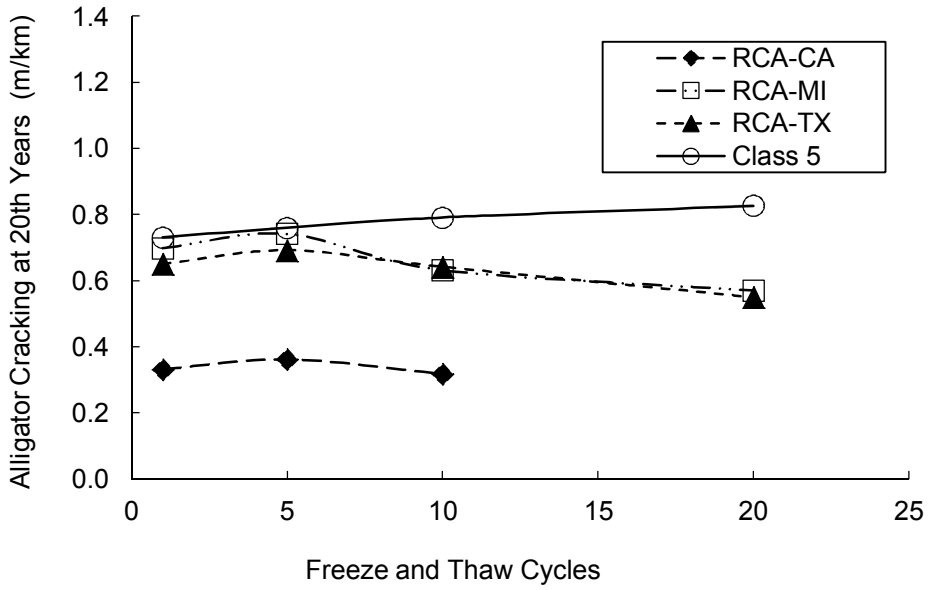

Figure 4.13 Effect of Freeze and Thaw Cycles on Alligators cracking after 20 years for Studied RCAs and Class 5-MN

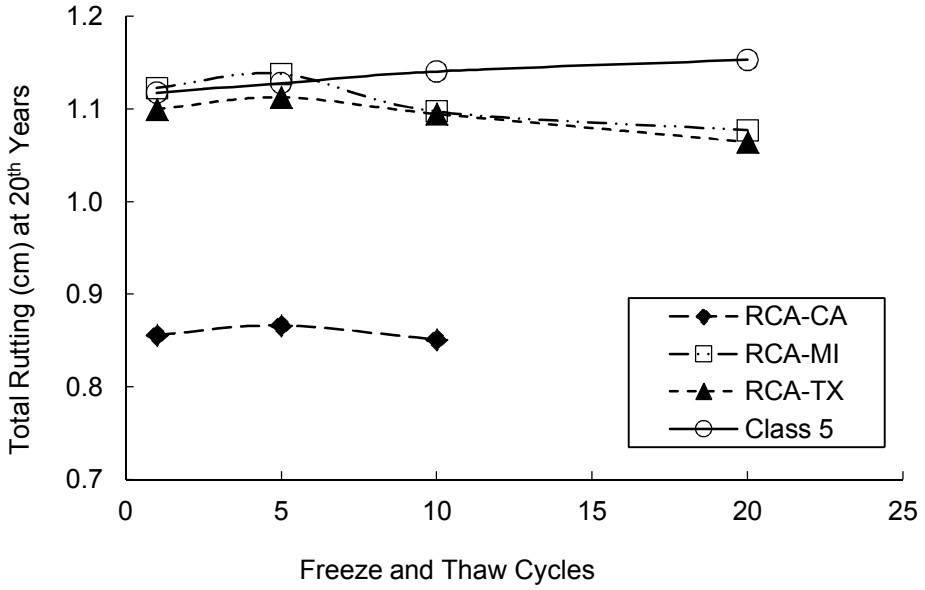

Figure 4.14 Effect of Freeze-Thaw Cycles on Total Rutting after 20 years for Recycled Aggregates and Class 5-MN

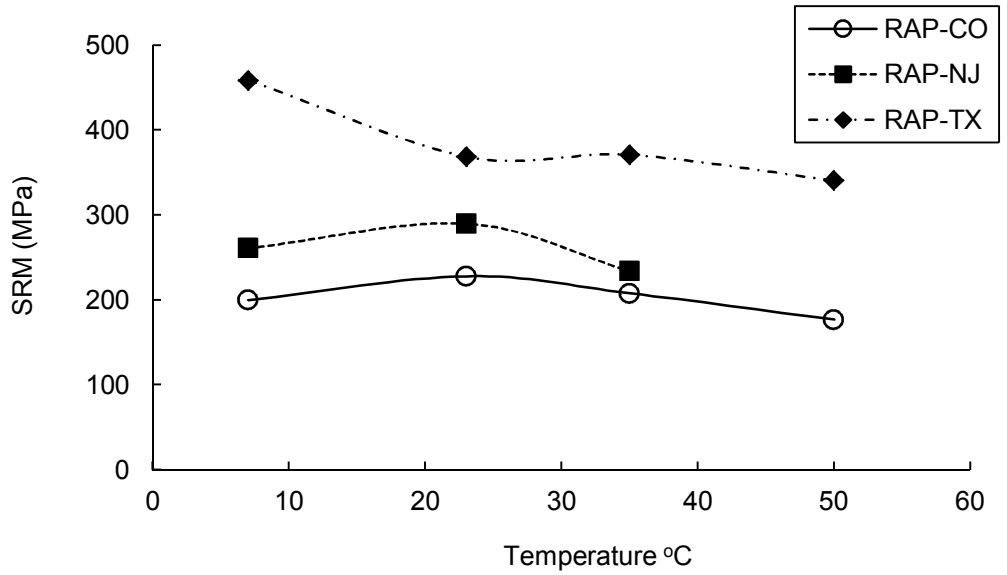

Figure 4.15 Relationship between Temperature and SRM for RAP-CO, RAP-NJ, and RAP-TX

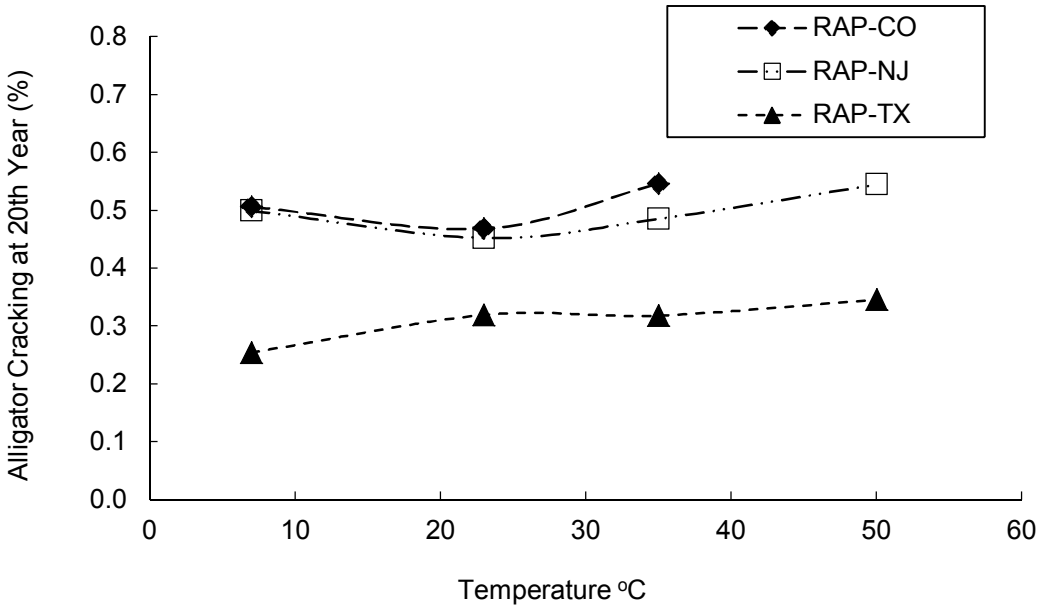

Figure 4.16 Effect of Temperature on Alligator Cracking after 20 years for Studied RCAs and Class 5-MN

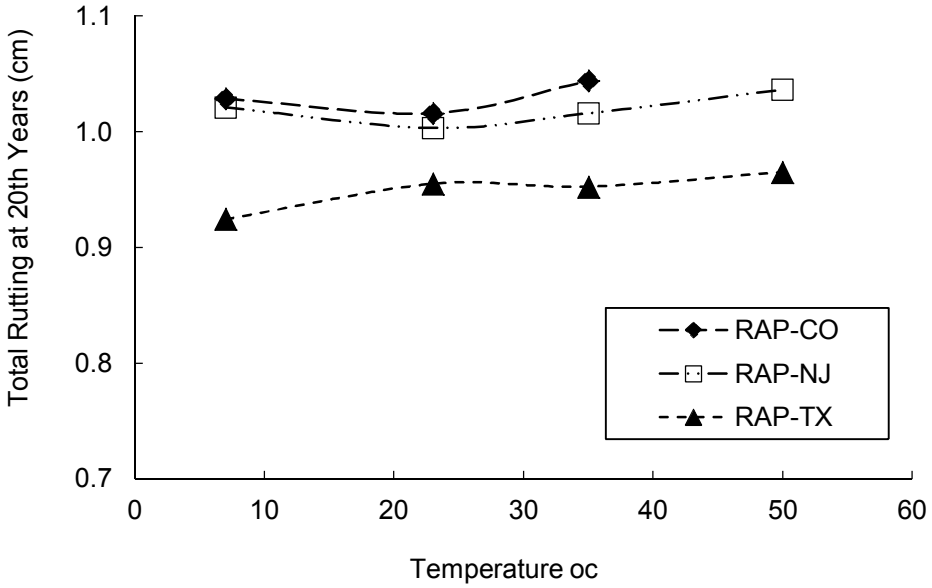

Figure 4.17 Effect of Temperature on Total Rutting after 20 years for Studied Recycled Aggregates and Class 5-MN

APPENDICES

APPENDIX A: HYDRAULIC PROPERTIES OF RECYCLED ASPHALT PAVEMENT AND RECYCLED CONCRETE AGGREGATE

A-1 ABSTRACT

The saturated hydraulic conductivity (k_{sat}) and water characteristic curves (WCCs) of three recycled asphalt pavements (RAPs) and three recycled concrete aggregates (RCAs) were measured. The k_{sat} was determined using a constant-head, rigid-wall, 152-mm-diameter permeameter. The specimens were prepared at 95% of maximum dry density based on modified Proctor testing. The k_{sat} of the RAPs varied from $3.8x10^{-5}$ to $3.7x10^{-4}$ m/s and from $1.6x10^{-5}$ to $2.6x10^{-5}$ m/s for the RCAs. Hazen's equation (1911) tends to over predict k_{sat} for RAPs and RCAs. Hanging columns with large-scale testing cells (305-mm inner diameter and 76-mm height) fitted with air aspirators were used to determine the WCCs. The WCC of each recycled material was fitted using the Fredlund and Xing (1994) model because this model is used in the Mechanistic-Empirical Pavement Design Guide (MEPDG). A hanging column test can measure suction lower than 1 kPa with high accuracy ($\pm$0.02 kPa). The slopes of the WCCs of RAPs were steeper than those of RCAs, although RAPs have higher densities. Compared to Rahardjo et al. (2010), RAPs and RCAs used in this study provided higher air entry suction because the specimens were prepared at higher, compacted density to replicate field conditions. To develop a WCC for RAPs and RCAs over a larger range of suctions, a device such as a pressure plate extractor is recommended.

A-2 INTRODUCTION

The use of recycled material as a base course in pavement construction has widely increased over recent decades. Use of recycled material can reduce global warming potential, energy consumption, and hazardous waste generation (Lee et al., 2010). The use of recycled

material can also provide cost and time savings because the material is generated and reincorporated on site (Bennert et al. 2000).

Among recycled materials, recycled asphalt pavement (RAP) and recycled concrete aggregate (RCA) are commonly used for pavement construction (FHWA, 2008). RAP is a coarse granular material derived from crushing existing asphalt surfaces. RCA is an aggregate obtained from demolition of concrete structures such as roads, runways, and buildings (Guthrie et al., 2007; FHWA, 2008). Studies have confirmed that recycled materials can provide high strength and durability, either as a mixture or as a complete replacement for conventional aggregate (Blankenagel and Guthrie, 2006). However, the hydraulic properties of RAPs and RCAs, which affect long-term performance of base course (Cedergren, 1988), have not been thoroughly investigated.

The important hydraulic properties of base course include saturated hydraulic conductivity (k_{sat}) and the water characteristic curve (WCC). The Mechanistic-Empirical Pavement Design Guide (MEPDG) requires k_{sat} as an input for drainage design and the WCC for adjusting the modulus for base and subgrade for structural pavement design (NCHRP, 2004). However, the WCCs of RAP and RCA (typically, coarse aggregate) are difficult to obtain directly because the water content of coarse aggregate can change rapidly at low suction (< 1 kPa), and few methods measure suction, ψ, accurately for ψ < 1 kPa (Li et al., 2009). To accurately characterize the hydraulic properties of large aggregate, specimens should be prepared at field density, and large enough to represent field compaction condition. ASTM D2434-68 recommends that the minimum diameter of a specimen cylinder for granular material should be approximately 8 times of the maximum aggregate size for hydraulic conductivity test.

This study investigated the k_{sat} of three compacted RAPs and three RCAs used as base course with constant-head, rigid-wall, compaction-mold permeameters. The WCCs were measured by hanging columns with large-scale testing cells (304-mm inner diameter and 76-mm

height). The WCC of each recycled material was fit using the Fredlund and Xing (1994) model because this model is used in the Mechanistic-Empirical Pavement Design Guide (MEPDG). The hydraulic properties of RAP and RCA measured in this study are compared to results from the literature for similarly graded, coarse aggregate.

A-3 HYDRAULIC PROPERTIES OF COARSE GRANULAR MATERIAL

A-3.1 Saturated Hydraulic Conductivity

Saturated hydraulic conductivity (k_{sat}) is the property that defines the ability of water to flow through saturated soil. The k_{sat} of granular material is mainly influenced by particle size and grain size distribution. Various empirical relationships have been proposed to predict k_{sat} of coarse-grained soil (e.g., Hazen, 1911; Kenny et al., 1984; Sherard et al., 1984). Hazen (1991) proposed the relationship between k_{sat} and effective diameter (D_{10}) for uniformly graded, loose sand as:

$$k_{sat} = 0.01 c_1 D_{10}^2 \quad \text{(Eq. A-1)}$$

where the unit of k_{sat} is m/s, c_1 is a constant related to particle shape (0.4 to 1.2), and D_{10} is the 10^{th} percentile for particle size in units of mm.

A-3.2 Water Characteristic Curve

A WCC describes the relationship between water content or degree of saturation and ψ, where $\psi = u_a - u_w$ (u_a is pore air pressure and u_w is pore water pressure). The ψ corresponding to the intersection of the two sloping lines at low suction of the WCC is defined as the air-entry suction (ψ_a) (Fredlund and Rahardjo, 1993). Although the drying path and wetting path of the WCC might be different due to hysteresis, measurement of the wetting path is difficult and only the drying curve is typically measured, especially for granular material (Hillel, 1980).

Numerous fitting equations have been proposed to describe the WCC (e.g., Brooks and Corey, 1964; van Genuchten, 1980; Fredlund and Xing, 1994). Among those models, the Fredlund and Xing equation provides a sigmoid curve suitable for different type of soil for matric suction from 0 to 1 GPa. The model requires four fitting parameters as defined by:

$$\theta = C(\psi)\frac{\theta_s}{\left\{ln\left[e+(\psi/a_f)^{b_f}\right]\right\}^{c_f}} \quad \text{(Eq. A-2)}$$

$$C(\psi) = \left[1 - \frac{ln\left(1+\frac{\psi}{h_{rf}}\right)}{ln\left(1+\frac{1\,000\,000}{h_{rf}}\right)}\right] \quad \text{(Eq. A-3)}$$

where θ is volumetric water content, θ_s is saturated volumetric water content, ψ is suction in kPa, and a_f, b_f, c_f and h_{rf} are fitting parameters. $C(\psi)$ is the adjusting function used to force θ to zero at 1 GPa.

A-4 MATERIALS

Three RAPs and three RCAs were collected from different states across the US (Bozyurt, 2011). The RAPs and RCAs were named according to the source state. Index tests were conducted on each recycled material. Grain size distribution and classification were determined according to ASTM D422. Specific gravity (G_s) and percent absorption were determined per AASHTO T85. Compaction tests were conducted using modified Proctor effort according to ASTM D1557.

Results of index tests on the RAPs and RCAs are summarized in Table A-1. The RAPs and RCAs are broadly graded, including classifications of SM, SP, SW, and GM according to the Unified Soil Classification System (USCS). The G_s of RAPs are lower than conventional aggregates because RAPs are comprised of asphalt, which has low G_s. The grain size distributions of the tested materials are presented in Figure A-1. RAPs have a lower percentage

of fines than RCAs. RAPs are hydrophobic materials, while RCAs are hydrophilic materials (Rahardjo et al., 2010). Thus, percent absorption tends to be higher in RAPs as compared to RCAs. Percent absorption of RAPs ranged between 1.5 and 3.0, while RCAs had percent absorption ranging from 5.0 to 5.8. Compaction curves for RAPs and RCAs are presented in Figure A-2. Both RAP and RCA are sensitive to the molding water content. RAP has higher maximum density than RCA and lower optimum water content.

Table A-1 Properties of RAPs and RCAs

Properties	RAP			RCA		
	Colorado	New Jersey	Wisconsin	Colorado	California	MnROAD
USCS designation	SP	GW	SP	SM	SW	SP
Specific gravity, G_s	2.4	2.49	2.46	2.63	2.63	2.71
Maximum dry unit weight (kN/m^3)	20.6	20.3	20.2	18.9	19.8	19.7
Optimum water content (%)	5.7	6.4	7.7	9.3	10.9	11.2
Percent fines	0.7	0.7	0.5	12.82	3.05	2.32
Percent absorption	3	2.1	1.5	5.8	5	5

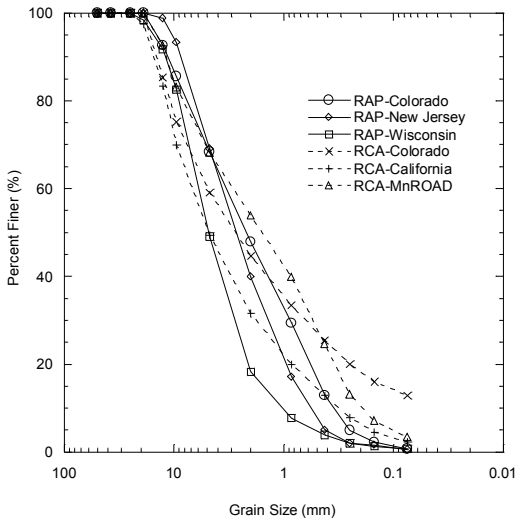

Figure A-1. Grain-Size Distributions

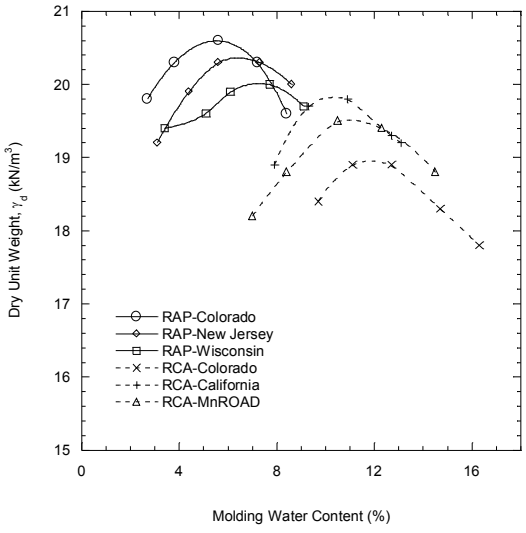

Figure A-2. Modified Proctor Compaction Curves

A-5 METHODS

A-5.1 Hydraulic Conductivity Measurement

Hydraulic conductivity was conducted following ASTM D5856, measurement of hydraulic conductivity of porous material using a rigid-wall, compaction-mold permeameter. The specimens were compacted in 152-mm-diameter compaction molds at 95% of the maximum dry density as shown in Table A-1. Tap water was used for all tests. The flow rate of an empty cell was checked for compliance in head loss. If the flow rate of an empty cell is lower than 10 times the flow rate of the cell with the specimen, the head loss from the specimens can be considered to be negligible (Daniel, 1994). The head was kept constant with a Marriott bottle. The hydraulic gradients were less than 5 because a high hydraulic gradient can wash fines from the sample. The ratio of outflow to inflow was measured to confirm saturation of the specimens.

A-5.2 WCC Measurement Using Large-Scale Hanging Column Test

A hanging column test combined with an air aspirator was used to determine the WCCs for the RAPs and RCAs. Figure A-3 presents the schematic of the hanging column test. The test equipment includes four main parts: testing cell, outflow column, manometer, and the hanging column. The hanging column test can measure the WCC precisely at ψ < 1 kPa with high accuracy ($\pm$0.02 kPa; i.e., $\cong$ 2-mm height of water). The lowest ψ which can be measured with this setup is 0.05 kPa. The highest ψ for the hanging column test is approximately 80 kPa due to the limitation of water cavitation. However, ceiling height also limits the ψ applied, or 25 kPa in this study. Suction higher than 25 kPa was supplied to the specimens using an air aspirator.

Testing followed ASTM D6836 method A. Large-scale cylinder specimens of 305-mm inner diameter and 76-mm height were prepared to simulate a base course layer in the field (Figure A-4). A 1-bar porous ceramic plate was used in the testing cell. Rubber gaskets were installed to prevent air flow intrusion.

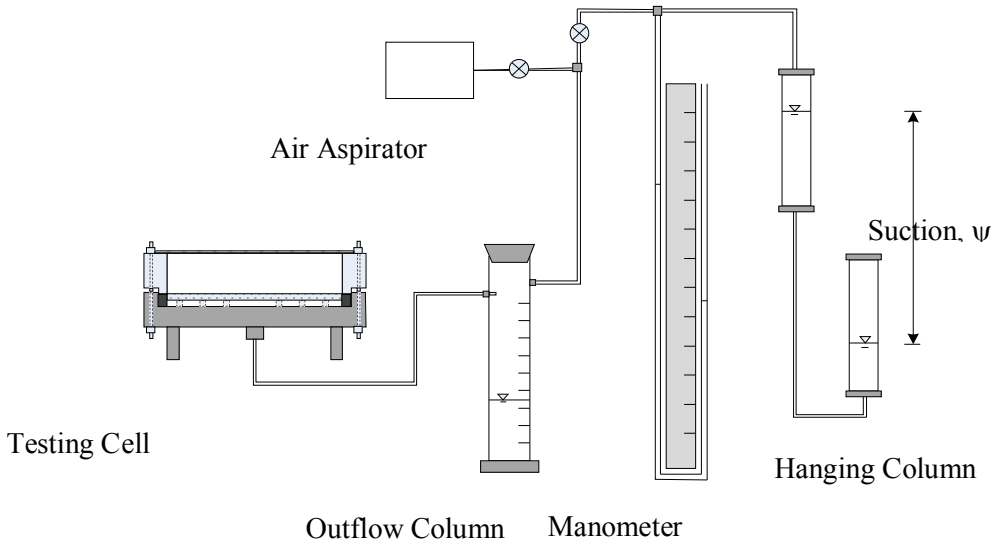

Figure A-3 Schematic of Hanging Column Apparatus

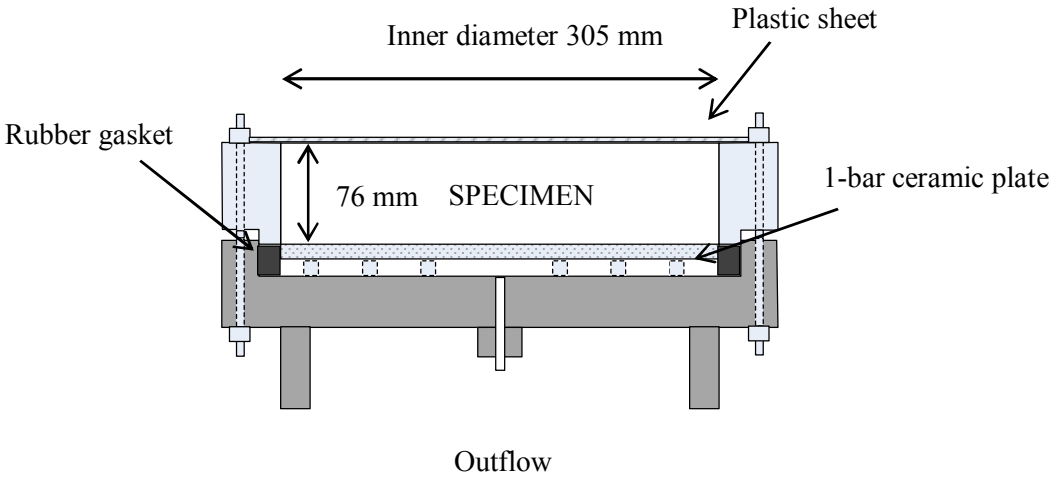

Figure A-4 Schematic of Large-Scale Testing Cell

The specimens were prepared at θ_s calculated from the desired dry unit weight and measured G_s. Specimens were compacted in the testing cell to 95% of maximum dry density. A shaking table was used during compaction to ensure the specimen reached the target density. De-aired, distilled water was used for specimen preparation.

A-6 RESULTS

Average k_{sat} determined from five replicate tests are summarized in Table A-2. The average k_{sat} of the RAPs ranged between $3.8x10^{-5}$ to $3.7x10^{-4}$ m/s, while k_{sat} of the RCAs ranged between $1.6x10^{-5}$ and $2.6x10^{-5}$ m/s. A statistical chart presenting the maximum and minimum values, and the percentiles at 75, 50 (median), and 25 for k_{sat} is depicted in Figure A-5. The measured k_{sat} varied within a narrow range (maximum k_{sat}/minimum k_{sat} <2) for each replicate test for RAP and RCA, which indicates consistency of method. Figure A-6 presents the relationship between effective diameter (D_{10}) and k_{sat} for the recycled materials. Increasing D_{10} tends to increase k_{sat} for RAPs, but does not show significantly increasing k_{sat} for RCAs. The Hazen (1911) prediction for k_{sat} (Eqn. (1)) was developed by using c_1 = 0.4 and 1.2 for the lower and upper bounds, respectively. RAPs and RCAs have lower k_{sat} for the same D_{10}. In comparison to the loose, uniformly graded aggregate for which the Hazen empirical equation was developed, the recycled materials of this study are compacted and more broadly graded; thus, this widely used predictor of k_{sat} is not applicable for these recycled materials.

Table A-2 Average (k_{sat}) of RAPs and RCAs

Description	RAP			RCA		
	Colorado	New Jersey	Wisconsin	Colorado	California	MnROAD
D_{10} (mm)	0.35	1.00	0.56	0.073	0.31	0.08
Measured k_{sat} (m/s)	$3.8x10^{-5}$	$3.7x10^{-4}$	$5.2x10^{-5}$	$1.6x10^{-5}$	$1.9x10^{-5}$	$1.8x10^{-5}$

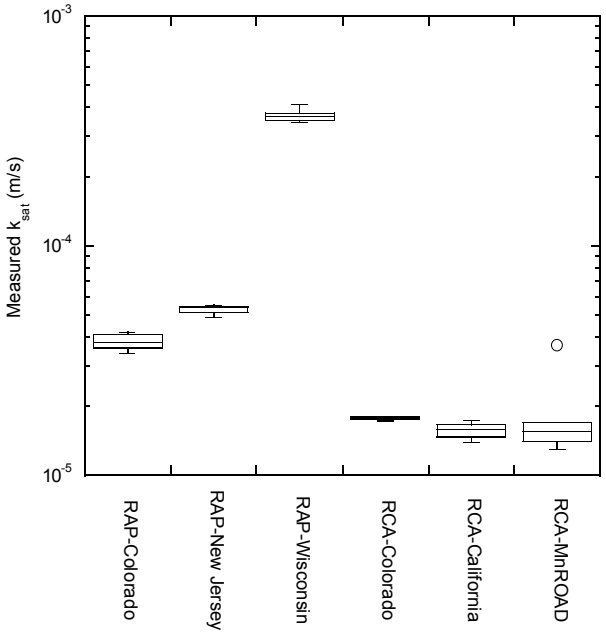

Figure A-5. Statistical Chart for k_{sat} of RAPs and RCAs

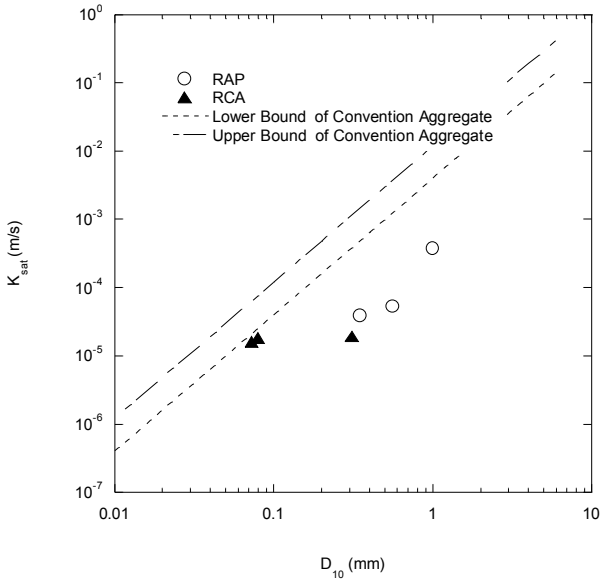

Figure A-6. K_{sat} versus D_{10} for RAPs and RCA

The hanging column test combined with an air aspirator used in this study measured suction between 0.05 and 75 kPa for RAP and RCA, with high accuracy for low suction measurements (±0.02 kPa). Measured WCCs of the RAPs and RCAs are presented as Figure A-7. The ψ_a of the RAPs range from 0.1 to 1.1 kPa, and from 0.5 to 3.0 kPa for the RCAs. The slope at the desorption part of the WCC is greater for the RAPs in comparison to the RCAs. Residual water content (θ_r) represents the water content at the dry state of the WCC for which an increase in ψ does not correspond to an appreciable change in θ. The θ_r of RAPs was obtained for RAP-New Jersey and RAP-Wisconsin. However, the θ_r of RAP-Colorado and the RCAs were indeterminate in this study. Extending the ψ measurement to a higher range (> 80

kPa) from another test method (e.g., pressure plate extractor) is recommended if a full-range WCC of RAP and RCAs is desired or necessary.

The data from each measured WCC was fit to the Fredlund and Xing (1994) model as presented by Eqns (2) and (3) using least square methodology. As shown in Figure A-7, the Fredlund and Xing model provides good fits for the recycled materials evaluated in this study. The a_f parameter might be related to ψ_a of the WCC, while the b_f and c_f parameters influence the slope of WCC at low and high ψ, respectively. The higher the b_f, the greater the slope on the desorption portion. The h_{rf} parameter used to adjust θ became zero at 1 GPa. The fitting parameters for the Fredlund and Xing model are summarized in Table A-3.

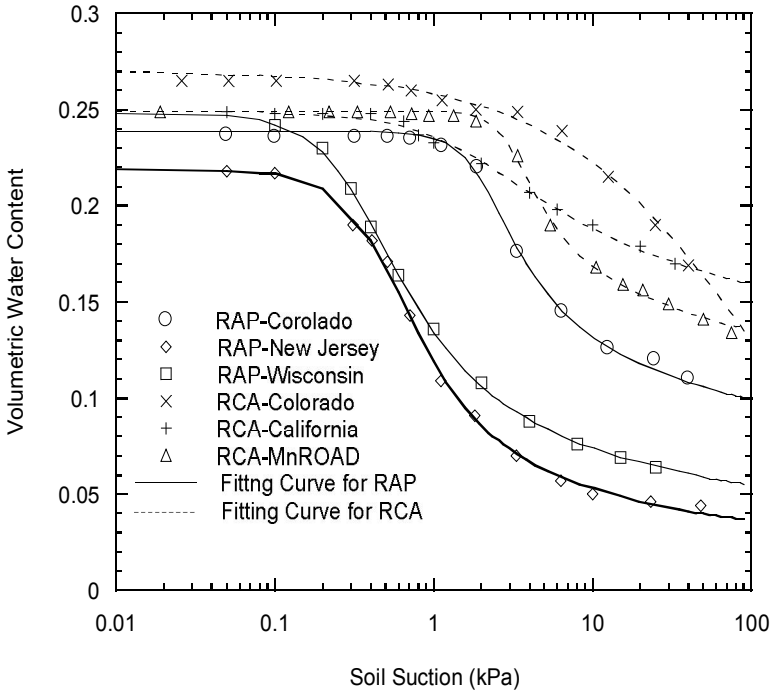

Figure A-7. Measured WCC Data Fitted to Fredlund and Xing (1994) Model

Table A-3 WCC Parameters for RAPs and RCAs

Description		RAP			RCA		
	Symbol	Colorado	New Jersey	Wisconsin	Colorado	California	MnROAD
Saturated θ, Porosity	θ_s, n	0.24	0.22	0.25	0.27	0.25	0.25
Air Entry Suction, kPa	ψ_a	1.1	0.2	0.1	3	0.5	1.7
Fredlund and Xing fitting parameters							
Best fit	a_f (kPa)	1.8	0.4	0.3	4.1	1.4	2.8
	b_f	3.5	2.4	2.1	1.2	1.2	4.7
	c_f	0.3	0.7	0.6	0.4	0.2	0.2
	h_{rf} (kPa)	97	97	100	6197	5596	6047

Table A-4 Comparison of ψ_a of RAPs and RCAs to Reference Data

Materials	USCS Classification	Dry Density (Mg/m3)	ψ_a (kPa)	Reference
RAPs	GW, SP	1.94-1.97	0.1-1.1	This study
RCAs	SP, SP, SM	1.83-1.92	0.5-3.0	
RAPs	GP, SP	1.53-1.67	0.01-0.03	Rahardjo et al. (2010)

Air-entry suctions for RAPs and RCAs from this study were compared to those from Rahardjo et al. (2010) in Table A-4. The ψ_a of the RAPs and RCAs measured in this study are greater than those of RAPs and RCAs conducted by Rahardjo (2010). The RAPs and RCAs used in this study were compacted to realistic field conditions and thus have higher density than the comparable reference data.

A-7 SUMMARY AND CONCLUSIONS

This study presents the hydraulic properties (k_{sat} and WCC) of compacted RAPs and RCAs obtained from different states across the USA that have been used as base course for highway construction. The k_{sat} of the RAPs ranged from $3.8x10^{-5}$ to $3.7x10^{-4}$ m/s and from $1.6x10^{-5}$ to $2.6x10^{-5}$ m/s for the RCAs. The k_{sat} was proportional to the effective diameter (D_{10}) for

RAPs, but does not provide a strong relationship for RCAs. Hazen's (1911) equation for conventional aggregate tends to over predict k_{sat} for both RAPs and RCAs.

A hanging column test combined with an air aspirator can generate suction between 0.05 and 75 kPa for a recycled base, providing high accuracy for low suction measurements ($\pm$0.02 kPa). Fredlund and Xing's (1994) equation provides a good fit for the WCCs of RAPs and RCAs. Compared to Rahardjo et al. (2010), RAPs and RCAs used in this study provided higher ψ_a because the specimens were prepared at higher, compacted density. Extension of ψ measurements using devices such as a pressure plate extractor or sensors would be recommended if the full-range WCC for RAPs and RCAs is desired.

A-8 ACKNOWLEDGEMENTS

The material evaluated in this study was provided from the TPF-5(129) Recycled Unbound Materials Pool Fund administered by the Minnesota Department of Transportation. We thank Professor Tuncer B. Edil for his input**.** The grain size analyses were provided by Ozlem Bozyurt, a graduate student in the Department of Civil and Environmental Engineering (CEE). The compaction curves were prepared by Dr. Young-Hwan Son, Assistant Professor, Department of Rural Systems Engineering, College of Agriculture and Life Sciences, Seoul National University.

A-9 REFERENCES

AASHTO T85. (2010). "Standard method of test for specific gravity and absorption of coarse aggregate."

ASTM D1557. (2009). "Standard method for laboratory compaction characteristics of soil using modified effort (56,000 ft-lb/ft^3 (2,700 kN-m/m^3))."

ASTM D2434-68. (2006). "Standard test method for permeability of granular soils (Constant Head)."

ASTM D422. (2007). "Standard test method for particle-size analysis of soils."

ASTM D5856. (2007). “Measurement of hydraulic conductivity of porous material using a rigid-wall, compaction-mold permeameter.”

ASTM D6836. (2008). “Standard test method for determination of the soil water characteristic curve for desorption using hanging column, pressure extractor, chilled mirror hygrometer, or centrifuge.”

Bennert, T., Papp, W.J., Maher, J.A., and Gucunski, N. (2000). “Utilization of construction and demolition debris under traffic-type loading in base and subbase applications.” *Transport. Res. Rec.*, No. 1350, Washington, D.C., 33–39.

Blankenagel, B.J., and Guthrie, W.S. (2006). “Laboratory characterization of recycled concrete for use as pavement base material.” *Transport. Res. Rec.*, No. 1952, Washington, D.C., 2006, 21–27.

Bozyurt, O. (2011). “Behavior of recycled pavement and concrete aggregate as unbound road base.” MS Thesis, University of Wisconsin-Madison, WI

Brooks, R.H. and Corey, A. T. (1964). “Hydraulic properties of porous media.” Hydrology Paper No.3, Colorado State University.

Cedergren, H. R. (1988). “Why all important pavement should be well drained.” *Transport. Res. Rec.*, No. 1188, Washington, D.C., 56-62.

Daniel, D. E. (1994). “State-of-the-art: Laboratory hydraulic conductivity tests for saturated soils.” In: *Hydraulic conductivity and waste contaminant transport in soil*. Edited by Daniel, D.E. and Trautwein, S.J., Philadelphia: ASTM, 30-77.

FHWA (2008). “User guidelines for byproducts and secondary use materials in pavement construction,” *FHWA Report FHWA-RD-97-148*, FHWA, VA.

Fredlund, D.G. and Rahardjo, H., (1993). *Soil mechanics for unsaturated soils*, Wiley, New York.

Fredlund, D.G., and Xing, A.,(1994). “Equation for the soil-water characteristic curve.”,” *Can. Geotech. J.*, 31(4), 521-532.

Guthrie, W.E.S., Cooley, D., and Eggett, D.L. (2007). “Effects of reclaimed asphalt pavement on mechanical properties of base materials.” *Transport. Res. Rec.*, No. 2005, Washington, D.C., 44–52.

Hazen, A. (1911). ‘‘Discussion of “Dam foundations” by A.C. Koenig.’’ *Trans. Am. Soc. Civ. Eng.,* 73, 199–203.

Hillel, D. (1980). *Fundamental of soil physics*. Academic Press, Inc., San Diego, CA.

Kenney, T., Lau, D., and Ofoegbu, G., (1984). “Permeability of compacted granular materials.” *Can. Geotech. J.*, 21(4), 726-729.

Lee, J.C., Edil, T.B., Tinjum, J.M., and Benson, C.H. (2010). “Qualitative assessment of environmental and economic benefits of recycled materials in highway construction.” *Transport. Res. Rec.*, Washington, D.C., No. 1952, 138-142.

Li, X., Zhang, L.M., and Li, J. H. (2009). “Development of a modified axis translation technique for measuring SWCCs for gravel soils at very low suctions,” *Geotech. Test. J.*, 32(6), 1-11.

NCHRP (2004). “Guide for Mechanistic-Empirical Design of pavement structures: part 2 – Design Inputs.” *ARA, Inc.*, ERES Consultants Division, Champaign, IL.

Rahardjo, H., Vialvong, K., and Leong, E.C. (2010). “Water characteristic curves of recycled materials” *Geotech. Test. J.*, 34(1), 1-8.

Schlicht, P.D., Benson, C.H., Tinjum, J.M., and Albright,W.H. (2010). “In-service hydraulic properties of two landfill final covers in northern California**.”** *Proceeding of GeoFlorida 2010*, ASCE, FL, Feb, 20-24, 2867-2877.

Sherard, J.-L, Dunnigan, L.-P., and Talbot, J.-R. (1984). “Basic properties of sand and gravel filters*.” J. Geotech. Eng.,* ASCE, 110(6), 684-700.

van Genuchten, M. (1980), “A close-form equation for predicting the hydraulic conductivity of Unsaturated soils,” *Soil. Sci. Am. J.*, 44, 892-898.

APPENDIX B: EFFECT OF MATRIC SUCTION ON RESILIENT MODULUS OF COMPACTED AGGREGATE BASE COURSES

B-1 ABSTRACT

This research was conducted to investigate the effect of matric suction on resilient modulus of unbound aggregate base courses. The study characterized the water characteristic curves and resilient modulus vs. matric suction relationships of aggregate base courses that were compacted at different water contents and between 98% and 103% of the modified Proctor density. The soil-water characteristic curve (SWCC) and the relationship between resilient modulus (M_r) and matric suction (ψ) were established for different unbound granular and recycled asphalt pavement materials. This relationship is important for predicting changes in modulus due to changes in moisture of unbound pavement materials. Resilient modulus tests were conducted according to the National Cooperative Highway Research Program (NCHRP) 1-28A procedure at varying water contents, and the measured SWCC was used to determine the corresponding matric suction. Three reference summary resilient moduli (SRM) were considered: at optimum water content, optimum water content + 2 and optimum water content - 2. The Bandia and Bargny limestones are characterized by a higher water-holding capacity explaining why the modulus of limestone was more sensitive to water content than for basalt or quartzite. Limestones tend to be more sensitive to changes in water content and thus to matric suction. The shape of the SWCC depends on the particle size distribution and the cementation properties from dehydration of the aggregates. Material properties required as input to the Mechanistic-Empirical Pavement Design Guide (M-EPDG) to predict changes in resilient modulus in response to changes in moisture contents in the field were determined for implementation in the M-EPDG process. Results show that the SRM was more correlated with matric suction than with compaction water content (for resilient modulus test). The two empirical

models to predict SWCC such as the Parera et al. (2005) and the M-EPDG (NCHRP 2004) models tend to underestimate the SWCC and cannot provide reasonable estimation. SRM normalized with respect to the SRM at the optimum water content varied linearly with the logarithm of the matric suction. Empirical relationships between SRM and matric suction on semi-logarithmic scale were established and are reported.

B-2 INTRODUCTION

Pavements are largely constructed on unsaturated, unbound aggregate layers and, through the life cycle of the pavement, perform as an unsaturated system. The negative soil pressure (termed suction due to the simultaneous presence of air and water in the soil fabric) plays an important role in pavement performance. One approach to design pavement is to maintain the substructure in an unsaturated condition to maintain high strength and stiffness of the supporting base layers. However, many current pavement design methods are based on empirical predictions, and soil inputs often assume that the subgrade and base layers are saturated. Pavement material properties such as resilient modulus and shear strength are greatly influenced by moisture content (Lekarp et al. 2000). Water entering the pavement system contributes to loss of load carrying capacity due to a reduction of strength and stiffness in base and subgrade. However, soil suction is not routinely quantified in geotechnical engineering practice.

Resilient modulus (Mr) is the key mechanical property for calculating the response of pavements under traffic loading according to the Mechanistic-Empirical Pavement Design Guide (M-EPDG). In the field, however, resilient modulus is sensitive to changes in water content corresponding to changes in matric suction. Several researches suggested that the modulus of unsaturated soils is strongly influenced by matric suction and a good correlation was also observed between modulus and matric suction (Sauer and Monismith 1968; Edil et al. 1981; Yang et al. 2005). The matric suction was found to be a fundamental parameter in characterizing

the moisture state and was proposed as a parameter to reflect the influence of soil type and fabric, compaction, climatic variations, and fluctuations of groundwater table on the mechanical behavior of soils better than compaction moisture content or degree of saturation alone. Finally, they suggested the use of the soil matric suction as the basic soil moisture parameter in addition to the compaction moisture content for pavement subgrade performance evaluation (Edil et al. 1981 and Edil et al. 2007).

The impact of temporal variations in moisture on modulus is considered in the Mechanistic-Empirical design through an environmental adjustment factor, F_{ev}. The Enhanced Integrated Climatic Model (EICM) implemented in the Mechanistic-Empirical Pavement Design Guide (M-EPDG) provides moisture, suction and temperature as a function of time, at any location in the unbound layers from which F_{ev} is determined. In unbound layers of the pavement structure, moisture is the variable that can significantly affect the modulus of unbound materials. All other conditions being equal, the higher the moisture content the lower the modulus (NCHRP 2004).

The National Cooperative Highway Research Program (NCHRP) developed an equation to predict change in modulus with respect to moisture content as follows:

$$\log \frac{M_r}{M_{r,opt}} = a + \frac{b-a}{1+EXP\left(\ln\frac{-b}{a} + k_m\left(S - S_{opt}\right)\right)} \qquad \text{(Eq. B-1)}$$

where $M_r/M_{r,opt}$ is the resilient modulus ratio; M_r is the resilient modulus at a given time; $M_{r,opt}$ is the resilient modulus at a reference condition; a is the minimum of log ($M_r/M_{r,opt}$); b is the maximum of log ($M_r/M_{r,opt}$); k_m is a regression parameter; and (S-S_{opt}) is the variation in degree of saturation expressed as a decimal.

After compaction, the reference degree of saturation, S_{opt}, changes with time to an equilibrium state, S_{eq}. This degree of saturation at equilibrium is calculated by the Enhanced

Integrated Climatic Model (EICM) implemented in the M-EPDG using the depth of the groundwater table and the SWCC (NCHRP 2004). Therefore, the value of S_{eq} does not depend directly on the value of the degree of saturation in the reference state, S_{opt}. The objective of this research is to determine the parameters of the SWCC that are input parameters in the mechanistic design approach as well as the change in modulus as function of matric suction determined from the SWCC. In this study, resilient moduli (Mr) of four coarse aggregates used as unbound base course were determined at different water content corresponding to different matric suctions. For each sample, matric suction was measured from its SWCC determined separately and using the compaction water content (or degree of saturation) measured from the resilient modulus test, regardless of the specimen density because when specimens are well compacted, the resilient modulus is not very density-sensitive (Vuong 1992, Thom and Brown 1988, Brown and Selig 1991, Ba et al. 2011). These data were used to define empirical correlations between summary resilient modulus and degree of saturation or soil suction.

B-3 SOIL-WATER CHARACTERISTIC CURVE EQUATIONS

The SWCC (Figure B-1) describes the relationship between the volumetric water content (or degree of saturation) and soil suction. This relationship is essential to describe the behavior of unsaturated soils. The SWCC describes the amount of water retained in soil for a given value of matric suction. This is a hydraulic property that is highly dependent on the distribution of pores in soil and thus on soil structure and texture. This curve is defined mainly by the saturation water content of the sample (θ_s), the air-entry pressure (ψ_a) corresponding to the break in the curve near the saturated water content, and the residual water content (θ_r) corresponding to the asymptote of the SWCC at low degrees of saturation (Tinjum et al. 1997). The water content to saturation depends on the nature, the density and the porosity of the material. Residual water content is the point where the removal of water from the soil structure becomes significantly more difficult and requires significantly more energy (Fredlund et al. 2011). The residual water

content depends mainly on the amount of fines in soil (Zapata et al. 2000). The air-entry pressure is the critical suction value representing the threshold between saturated and unsaturated conditions and depends on pore size distribution in soil structure (Roberson and Siekmeier 2002). Granular material tends to have a low air-entry pressure due to the large pores in its structure.

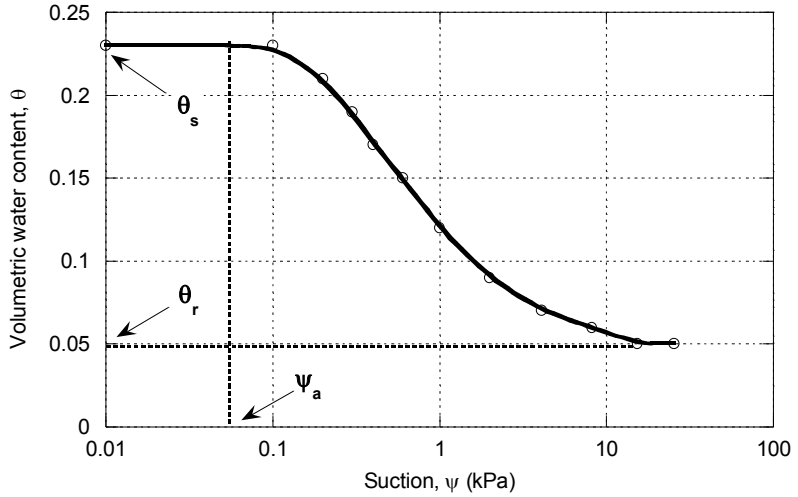

Figure B-1 Typical Soil-Water Characteristic Curve (SWCC) for aggregate

Various equations have been proposed to represent the SWCC. Commonly used models include the van Genuchten (1980) and Fredlund and Xing (1994) equations. Fredlund and Xing (1994) proposed the following relationship, which has been implemented in the M-EPDG to model the state of water content with respect to soil suction (Eq. B-2):

$$\theta_w = \left[1 - \frac{\ln\left(1+\frac{\psi}{h_r}\right)}{\ln\left(1+\frac{1.45\times10^5}{h_r}\right)}\right] \times \left[\frac{\theta_{sat}}{\left[\ln\left[e+\left(\frac{\psi}{a_f}\right)^{b_f}\right]\right]^{c_f}}\right] \qquad \text{(Eq. B-2)}$$

where a_f (kPa), b_f, c_f, and h_r (or h_{rf} (kPa)) are fitting parameters; θ_{sat} is volumetric water content at saturation; θ_w is volumetric water content; and ψ is matric suction (kPa). These input parameters allow the Enhanced Integrated Climatic Model (EICM) (NCHRP 2004) to automatically generate the SWCC at any water content of the material.

The van Genuchten (1980) model is extensively referenced in the literature and used in engineering practice because of its simplicity in determining the model parameters, which could lead to adoption by NCHRP for a future version of the M-EPDG (Eq. B-3):

$$\frac{\theta_w - \theta_r}{\theta_s - \theta_r} = \frac{1}{\left[1 + \left(\frac{\psi}{\alpha}\right)^n\right]^m} \quad \text{(Eq. B-3)}$$

where θ_r, α, n and m are model parameters. The "pivot point" of the curve, α, represents the point of entry of air into the sample, n represents the slope of the curve with respect to the "pivot point", and m depends on the portion between the "pivot point" and the inflection point of the lower part of the curve. According to van Genuchten et al. (1991), m is linked to n by the following equation:

$$m = 1 - n^{-1} \quad \text{(Eq. B-4)}$$

In this study, the SWCCs were determined following the drainage path due to the difficulty to follow the humidification path, but in the field the material is subjected to wet and dry cycles and never becomes saturated.

B-4 TEST MATERIALS AND PROCEDURES

B 4.1 Materials

Resilient modulus tests were conducted on aggregate base courses collected from locations within Senegal and the United States of America (USA): Bakel Black Quartzite (GNB),

Bakel Red Quartzite (GRB), Diack Basalt (BAS), Bandia Limestone (BAN), Bargny Limestone (BAR), Minnesota Class 5, Texas Recycled Asphalt Pavement (Texas RAP) and Colorado Recycled Asphalt Pavement (Colorado RAP). Grain size distributions of the materials tested are shown in Figure B-2. Compaction characteristics and some physical and mechanical characteristics are presented in Table B-1. Aggregate used in base courses must be tough to resist the effects of traffic and the environment. The Micro-Deval test provides a measure of abrasion resistance and durability of mineral aggregates through the actions of abrasion between aggregate particles and between aggregate particles and small steel balls in the presence of water is a good indicator of the quality of aggregates that will be exposed to water. Bandia Limestone exhibits higher Micro-Deval loss and thus generates fines during the compaction procedure. Bargny Limestone exhibits less Micro-Deval loss but higher percent fines and is less coarse than Bandia Limestone. Class 5 is classified as silty sand and presents low percent fines.

Repeated load triaxial testing (NCHRP 1-28A protocol) was used to determine Mr of these aggregates. Test specimens used to determine resilient modulus were prepared around optimum water content ± 2 and at dry unit weights ranging from 98% to 103% of the maximum dry unit weight using modified Proctor effort (ASTM D1557-09). Specimens of each aggregate type were prepared by impact compaction using a modified Proctor hammer in accordance with Procedure A of the impact compaction procedure. The number of blows per layer was adjusted as necessary to achieve the target dry unit weight. To be closer to the in situ conditions, tests were conducted without limiting the maximum aggregate size (31.5 mm) during the Mr and SWCC specimen preparation.

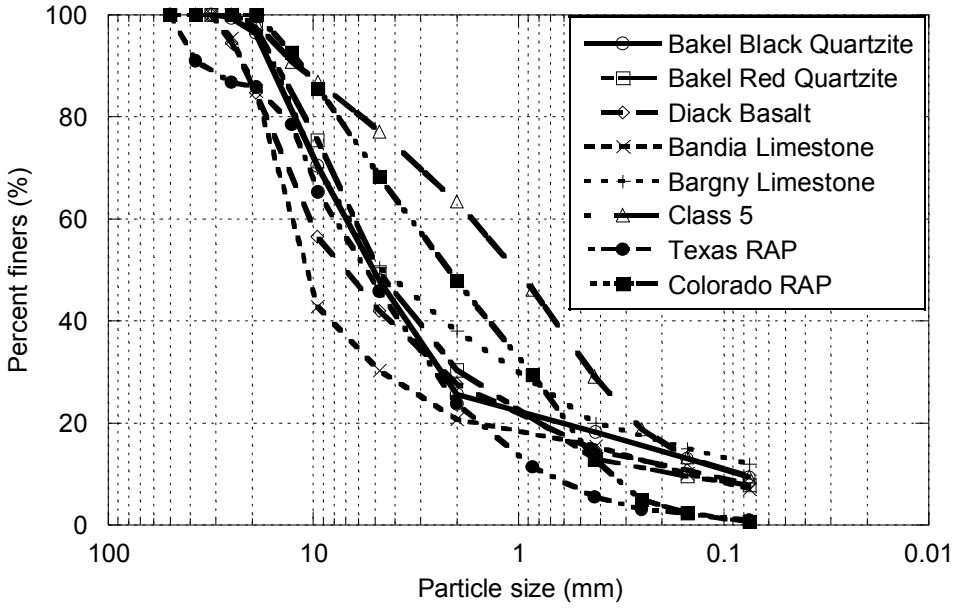

Figure B-2 Particle-Size Distribution for the Aggregates Tested

Table B-1 Physical and Mechanical Properties of the Aggregates

Materials	ρ_{dmax} (kg/m^3)	w_{opt} (%)	G_s	MDE (%)	USCS	D_{10}	D_{20}	D_{30}	D_{50}	D_{60}	D_{90}	% Fines
Bakel Red Quartzite	2140	5.5	2.65	3.07	GW	0.14	0.70	2.00	5.0	6.20	16.00	7.743
Bakel Black Quartzite	2150	4.5	2.65	4.16	GW	0.08	0.60	2.40	5.0	6.5	17.00	9.409
Diack Basalt	2420	4.2	2.95	5.66	GP	0.18	0.80	2.5	7.0	10.00	23.00	7.127
Bandia Limestone	2065	7.6	2.56	40.0	GP	0.20	2.00	5.00	10.2	14.00	22.00	7.401
Bargny Limestone	2015	9.2	2.55	18.6	GW-GM	0.06	0.04	1.00	5.0	6.20	17.00	12.00
Class 5	2217	8.9	2.57	11	SW-SM	0.08	0.28	0.45	1.0	1.80	12.00	9.49
Texas RAP	2239	8.0	2.34	16	SW	0.80	1.50	2.50	5.5	8.00	35.00	0.99
Colorado RAP	2283	5.7	2.23	-	SP	0.40	0.60	0.90	2.2	3.10	11.50	0.69

Symbols: ρ_{dmax} = modified Proctor maximum dry density, w_{opt} = modified Proctor optimum water content, G_s = specific gravity, MDE = Micro Deval (with water), USCS = Unified Soil Classification System

B-4.2 Resilient Modulus Test Procedure

Cyclic loading triaxial tests were performed using a MTS closed-loop servo-electro-hydraulic testing system (Figure B-3), which is capable of applying repeated loads in haversine waveform with a wide range of load duration. The axial deformations were measured by Linear Variable Differential Transducers (LVDTs) mounted inside the triaxial cell. The specimens were submitted to cyclic loading triaxial tests according to the NCHRP 1-28A (NCHRP 2004) test protocol, which was used to establish the 30 loading sequences. The loading involves conditioning, which attempts to establish steady-state or resilient behavior, through the application of 1000 cycles of 207-kPa deviator stress at 103.5-kPa confining pressure. The cycles are then repeated 100 times for 30 loading sequences with different combinations of deviator stress and confining pressure. The Mr is calculated as the mean of the last five cycles of each sequence from the recoverable axial strain and cyclic axial stress. It is an elastic modulus defined as ratio between the applied deviatoric stress, σ_d (= σ_1 - σ_3) and the recoverable strain, ε_r (Eq. B-5).

$$M_r = \frac{\sigma_d}{\varepsilon_r} \qquad \text{(Eq. B-5)}$$

A number of factors (including loading conditions, water content, soil suction, void ratio, grain size, plasticity, and soil structure) affect resilient modulus. Of these factors, stress level is the most important parameter and a number of models were developed to predict the Mr of granular materials. The bulk stress model (Seed et al. 1967) is simple, extremely useful and widely accepted for analysis of stress dependence of granular material stiffness (Lekarp et al. 2000). For this research study, a summary resilient modulus (SRM) was calculated using this model and calculated with θ = 208 kPa (Eq. B-2).

$$M_r = k_1\left(\frac{\theta}{P_a}\right)^{k_2} \quad \text{(Eq. B-6)}$$

Where θ is the bulk stress; P_a is the atmospheric pressure (P_a = 101.6 kPa); k_1 and k_2 are the material properties determined from regression analyses.

The Mr of unbound granular materials from Senegal has been studied by Fall et al. (2007), Ba et al. (2011), and Ba et al. (2012). According to Ba et al. (2012), the compaction water content has less effect on Bakel Quartzites and Diack Basalt than on Bandia and Bargny limestones because Quartzite and Basalt are cohesionless materials and allow water to drain during the compaction procedure.

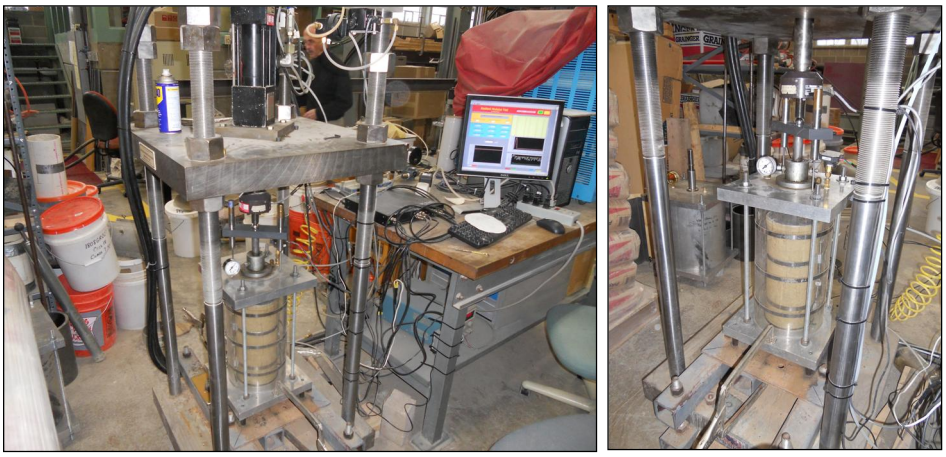

Figure B-3 Photo of the Repeated Loading Machine Illustrating the Resilient Modulus Test (from the UW-Madison, USA)

B-4.3 Soil Suction Measurement in Granular Materials

During testing for the SWCC, suction was applied via a hanging column in which the difference in level of the reservoirs provides the suction. This test is described in ASTM D 6836 - Method A. A schematic diagram of the hanging column and the testing cell is presented in Figure B-4. The test equipment includes four main parts: testing cell, hanging column, outflow tube, and manometer. The hanging column test can apply low suction (ψ < 1 kPa) with high accuracy ($\pm$0.02 kPa). The highest ψ the hanging column can apply is around 80 kPa due to the limitation of water cavitation. However, ceiling height also limits the ψ applied (25 kPa in this study). Suction higher than 25 kPa was supplied to the specimens using an air aspirator (as described in Nokkaew et al. 2012).

Specimens were compacted in the testing cell between 95% and 98% of the maximum dry unit weight. A shaking table was used during compaction to ensure the specimen reached the target density. Prior to testing, the specimen was saturated with de-aired water as well as the ceramic plate and all connecting pipes. The procedure involves applying different suctions by adjusting the elevation of the reservoirs until the difference in elevation corresponds to the desired suction. The amount of water collected by the graduated outflow tube is measured regularly and used to calculate the amount of water retained by the sample.

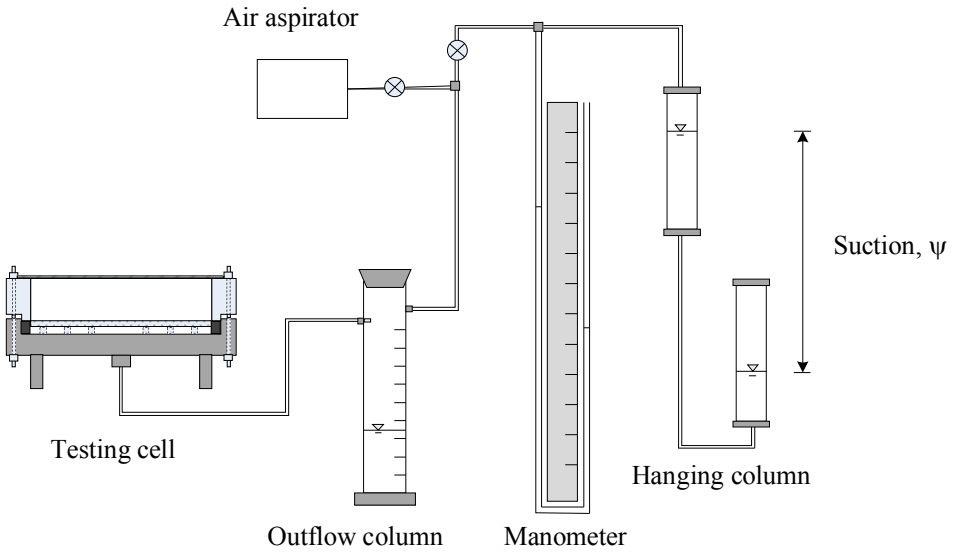

Figure B-4 Schematic of hanging column apparatus

B-5 TEST RESULTS AND ANALYSIS

B-5.1 Analysis and Interpretation of Soil-Water Characteristics Curves

Matric suction is a component of water potential and theoretically represents, in the case of non-cohesive materials, the attraction of water molecules to the solid soil particles (adhesive forces). The movement of water in unsaturated soils is mainly governed by matric suction (Likos and Lu 2004). The shape of the SWCC is a function of the distribution and shape of the pores in the porous media. In turn, the distribution and shape of the pores are mainly determined by grain size, grain shape, and soil structure. In the initial state, when the soil is saturated, all pores are filled by water. As the drainage of the sample commences, the pores begin to drain the water under the effect of gravity. Thus, the pressure approaches the air-entry value, which represents the point of transition between the saturated and unsaturated state.

The Bakel Quartzite aggregates are characterized by rapid drainage beginning from the lowest levels of suction (Figure B-5.a), which is evident from the continuous decrease of the

volumetric water content of the material. This behavior is typical of well-graded granular materials (Zapata et al 2000).

The Diack Basalt experiences a dramatic drop ("collapse") of the volumetric water content when suction passes 0.1 kPa (Figure B-5.b). This behavior is observed in granular materials that are poorly graded (Fredlund and Xing 1994) and is due to the simultaneous presence in the soil structure of large pores and narrow pores. The high maximum grain size (D_{max}) of the basalt allows for coexistence of pores of different sizes. Thus, close to saturation, the large pores drain mainly by gravity, which is materialized by the "collapse" of the SWCC. After this "collapse", the remaining water is retained by the smaller pores in the soil matrix and drains slowly with increase in suction. For this type of material, typical SWCC equations do not model well the drainage behavior. However, this occurrence of large and small pores can and does naturally occur and may be accentuated by the phenomenon of segregation (i.e., separation of coarse and fine particles), which is characteristic of certain crushed, granular aggregates. The behaviors described above (i.e., rapid drainage in Bakel Quartzite and gap drainage in Diack Basalt) are characteristic of non-cohesive granular materials. In these materials, water is drained primarily by gravity and a small portion is retained in the soil structure. This explains why the Mr of Bakel Quartzite and Diack Basalt are "less sensitive" to the effect of water content (Ba et al. 2012). Between w_{opt} and w_{opt} + 2, most of the water does not remain in the material, and is drained during compaction and during the Mr testing.

Bandia Limestone is a granular material, not plastic but cohesive (due to hydration of lime) with a SWCC that is S-shaped (Figure B-5.c). In this case, when the suction is low, the water is retained in the material until the air-entry pressure. Thus, the relatively larger pores water requires greater suctions to fully drain as compared to Diack Basalt or Bakel Quartzite.

Bandia Limestone retains more water at high suction, which is evident by the relatively high residual water content.

The Bargny Limestone can be considered as a plastic material, characterized by high water retention and therefore very low *in situ* suction (Figure B-5.d). When compacted, Bargny Limestone has finer particles (more plastic), which results in smaller pores. The volumetric water content varies slightly for suction ranging between 1 kPa and 100 kPa, where all other tested materials demonstrate significant drainage in this range. The two behaviors described above (for Bandia and Bargny limestones) are typical of granular, plastic and fine soil materials. In these soils, much of the water is retained in the soil matrix, thus small pores control the drainage behavior of these materials. This explains why Bandia and Bargny limestones are more sensitive to water content than Diack Basalt or Bakel Quartzite as described in Ba et al. (2012). Limestones retain more water than quartzite and basalt and are therefore more exposed to the effect of water.

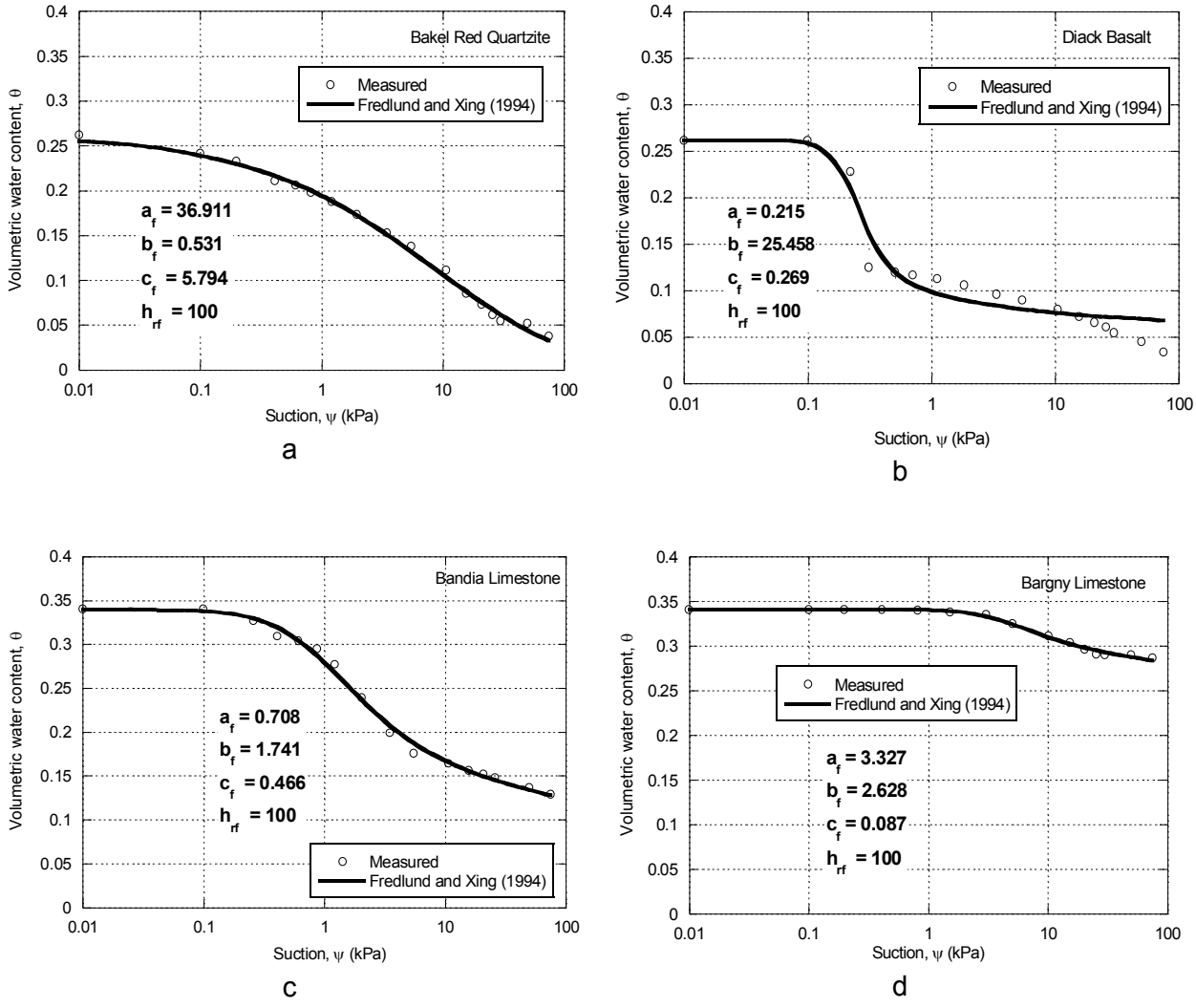

Figure B-5 Soil-Water Characteristic Curves of Some Materials: a) Bakel Red Quartzite, b) Diack Basalt, c) Bandia Limestone, and d) Bargny Limestone

Figure B-6 synthesizes the SWCCs of Bakel Red Quartzite, Bakel Black Quartzite, Diack Basalt, Bandia Limestone, Bargny Limestone, Class 5, Texas RAP, and Colorado RAP. The fits shown are based on the van Genuchten (1980) model. Air-entry pressures, ψ_a (represented as α in Table B-3), of limestones (Bandia and Bargny), Class 5, and Colorado RAP are higher in comparison to those of Bakel Quartzite, Diack Basalt and Texas RAP. Bakel Quartzite, Diack Basalt, and Texas RAP have θ_r values that tend to zero. Bargny Limestone has the higher θ_r. Bandia Limestone, Class 5, and Colorado RAP tend toward the same residual water content, which is higher than those of Bakel Quartzite, Diack Basalt and Texas RAP but below the θ_r of Bargny Limestone. Diack Basalt and Bandia Limestone samples are both classified as GP, exhibit fairly similar particle size distribution and contain fairly similar amount of fines, but the slope of the SWCC of Bandia Limestone sample tends to exhibit less steep as compared to that of Diack Basalt sample. The SWCC of Bargny Limestone also exhibits similar trend but higher air entry suction. This is due to the cohesion and the cementation effect of limestone compared to Bakel Quartzite and Diack Basalt witches are cohesionless aggregates. So, the shape of the SWCC is not only a function of the particle size distribution, but also a function of the cementation properties from dehydration of the aggregates. Table B-2 and B-3 summarize respectively the Fredlund and Xing (1994) and van Genuchten (1980) model parameters for the aggregates tested. The Fredlund and Xing (1994) fitting parameters are given here for engineering practice because this model is implemented in the M-EPDG (NCHRP 2004).

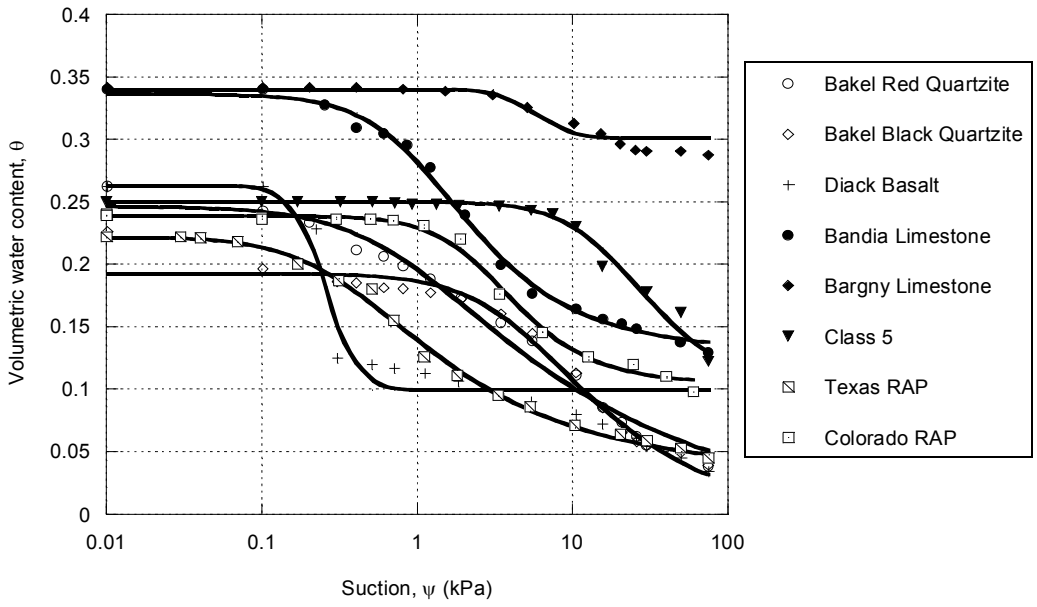

Figure B-6 Soil-Water Characteristic Curves measured and predicted by the van Genuchten (1980) model

Table B-2 Summary of the Fredlund and Xing (1994) Model Parameters for Bakel Quartzite, Diack Basalt, Bandia Limestone and Bargny Limestone

Materials	Fredlund and Xing (1994) model parameters			
	a_f (kPa)	b_f	c_f	h_{rf} (kPa)
Bakel Red Quartzite	36.91	0.53	5.79	100
Bakel Black Quartzite	37	0.57	5.15	100
Diack Basalt	0.215	25.46	0.27	100
Bandia Limestone	0.708	1.74	0.47	100
Bargny Limestone	3.327	2.63	0.09	100

Table B-3 Summary of the van Genuchten (1980) Model Parameters

Materials	van Genuchten (1980) model parameters				
	θ_r	θ_s	α	n	m
Bakel Red Quartzite	0.00	0.25	1.29	1.35	0.26
Bakel Black Quartzite	0.00	0.19	0.21	1.66	0.40
Diack Basalt	0.10	0.26	3.95	10.05	0.90
Bandia Limestone	0.13	0.34	0.96	1.83	0.45
Bargny Limestone	0.30	0.34	0.19	9.66	0.90
Class 5	0.10	0.25	0.05	2.20	0.55
TX RAP	0.04	0.22	2.83	1.50	0.34
CO RAP	0.10	0.24	0.37	2.27	0.56

B-5.2 Estimating the SWCC from the Physical Properties of the Aggregates

Several studies have attempted to predict the SWCC from empirical equations based on correlation relationships between the SWCC and parameters such as soil texture, grain size and plasticity index (Fredlund et al. 1994; Zapata 1999; Parera et al. 2005). From NCHRP Project 9-23 on the effects of environment on pavement structure, Parera et al. (2005) presents a series of equations that describe the SWCC of non-plastic gravels based on the particle size characteristics. These equations relate the Fredlund and Xing (1994) model parameters to the grain size distribution characteristics:

- a_f is expressed as:

$$a_f = 1.14a - 0.5 \quad \text{(Eq. B-7)}$$

where:

$$a = -2.79 - 14.1\log(D_{20}) - 1.9\times10^{-6} P_{200}^{4.34} + \log(D_{30}) + 0.055D_{100} \quad \text{(Eq. B-8)}$$

$$D_{100} = 10^{\left[\frac{40}{m_1}+\log(D_{60})\right]} \quad \text{(Eq. B-9)}$$

$$m_1 = \frac{30}{\left[\log(D_{90}) - \log(D_{60})\right]} \quad \text{(Eq. B-10)}$$

According to Parera et al. (2005), there may exist some extreme cases where the computed value of a_f is negative, which will lead to erroneous results. Therefore, the value of a_f has been limited to 1.0.

- b_f is expressed as follows :

$$b_f = 0.936b - 3.8 \quad \text{(Eq. B-11)}$$

where:

$$b = \left\{5.39 - 0.29\ln\left[P_{200}\left(\frac{D_{90}}{D_{10}}\right)\right] + 3D_0^{0.57} + 0.021P_{200}^{1.19}\right\}m_1^{0.1} \quad \text{(Eq. B-12)}$$

$$D_0 = 10^{\left[\frac{-30}{m_2}+\log(D_{30})\right]} \quad \text{(Eq. B-13)}$$

$$m_2 = \frac{20}{\left[\log(D_{30}) - \log(D_{10})\right]} \quad \text{(Eq. B-14)}$$

- c_f is expressed as follows :

$$c_f = 0.26e^{0.0758c} + 1.4D_{10} \quad \text{(Eq. B-15)}$$

where:

$$c = \log\left(m_2^{1.15}\right) - \left(1 - \frac{1}{b_f}\right) \quad \text{(Eq. B-16)}$$

- The h_f parameter is kept constant: $h_f = 100$

The M-EPDG (NCHRP 2004) proposes the following equations to predict the SWCC from particle size for non-plastic materials:

$$a_f = \frac{0.8627 D_{60}^{-0.751}}{6.895} \text{ in } psi, \qquad \text{(Eq. B-17)}$$

$$b_f = 7.5$$

$$\frac{h_r}{a_f} = \frac{1}{D_{60} + 9.7e^{-4}} \qquad \text{(Eq. B-18)}$$

Eq. B-7 to B-18 are based on the parameters of the soil particle size distribution, which controls the distribution of pores that can be filled with water.

Figure B-7 presents the SWCCs measured and fitted to the Fredlund and Xing (1994) model, and those predicted by empirical models such as the Parera et al. (2005) and M-EPDG (NCHRP 2004) models. Note that all these models predict a dramatic drop ("collapse") of volumetric water content, which is visible only for Diack Basalt, whose maximum particle size (D_{90} = 23 mm) is very high.

For Bakel Quartzites, whose pores are relatively narrower than those of Diack Basalt (possibly due to the smaller maximum grain size and well-graded gradation), this "collapse" is not observed. However, a continuous decrease of the volumetric water content, which cannot be predicted by the two empirical models, is apparent (see Figure B-7 a-b). For relatively high levels of suction (ψ > 25), the θ_r predicted by the M-EPDG empirical model tends to zero, as predicted by the Fredlund and Xing (1994) model. In contrast, the Parera et al. (2005) model predicts higher θ_r, due simply to the fact that this model accounts for the fines content (which

varies between 7 and 12%). In this study, the fines are inert because of the mineralogical nature (quartz and calcite) of the crushed rock (quartzite, basalt and limestone). For the aggregates evaluated in this study (excepted the Bargny Limestone), the fines are marginally involved in the retention of water in the pores.

For Diack Basalt, the Parera et al. (2005) and M-EPDG (NCHRP 2004) models predict the collapse in Figure B-7.c, but the M-EPDG model tends towards zero θ_r, while the Parera et al. (2005) model tends towards relatively higher θ_r. Diack Basalt may retain a little more residual water than Bakel Quartzites due to the presence of ferromagnesian minerals that are more active than quartz; thus, the θ_r does not directly tend towards zero.

Table B-4 summarizes the regression parameters obtained with the two empirical models: Parera et al. (2005) and M-EPDG (NCHRP 2004). Comparing with the measured fitting parameters given in table B-2, both prediction approaches tend to underestimate the SWCC and cannot provide reasonable estimation.

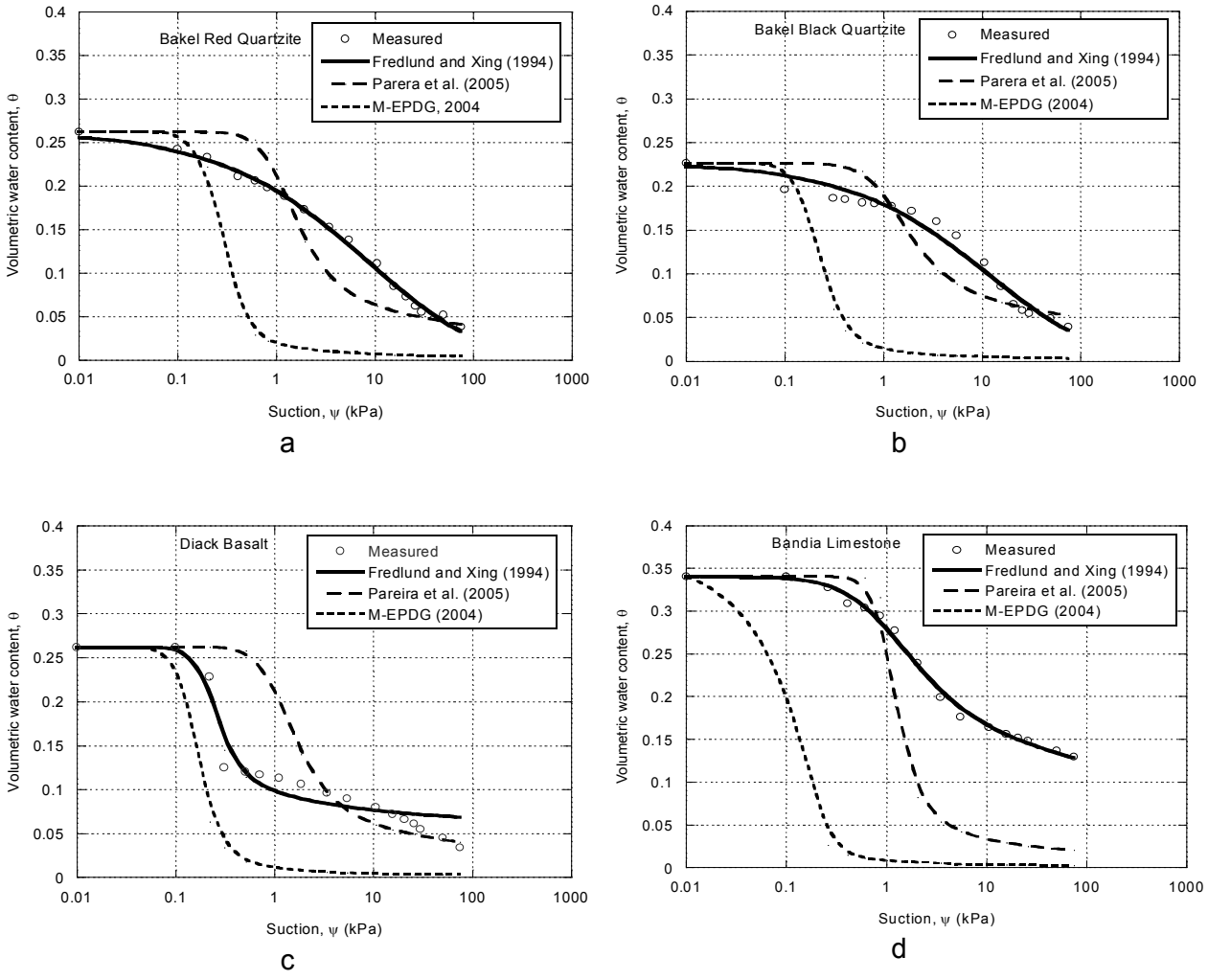

Figure B-7 Soil-Water Characteristics Curves Measured and Predicted by Various Models: a) Bakel Red Quartzite; b) Bakel Black Quartzite; c) Diack Basalt; d) Bandia Limestone

Table B-4 Parameters of the Parera et al. (2005) and MEPDG (NCHRP 2004) Empirical Models

Models	Parameter	Bakel Red Quartzite	Bakel Black Quartzite	Diack Basalt	Bandia Limestone
Parera et al. (2005)	a_f	1.00	1.00	1.00	1.00
	b_f	3.80	3.10	3.80	8.70
	c_f	0.70	0.60	0.70	0.80
	h_f	100.00	100.00	100.00	100.00
M-EPDG (NCHRP 2004)	a_f	0.00	0.00	0.00	0.01
	b_f	7.50	7.50	7.50	7.50
	c_f	1.09	1.12	1.19	1.29
	h_f	0.005	0.004	0.002	0.001

B-5.3 Resilient Modulus as Function of Matric Suction

Table B-5 provides a summary of water content, degree of saturation, matric suction and Summary Resilient Modulus of aggregates from Senegal (quartzite, basalt and limestones). These data were used to study the effect of matric suction on resilient modulus. Figure B- 8 and B-9 show the variation of SRM as a function of degree of saturation, S_r, and ψ, respectively. Empirical relationships are proposed to predict the variation of SRM as a function of S_r or ψ. They show that the SRM of compacted materials is closely related to the ψ. As mentioned by Sawangsurya et al. (2009), a more unique relationship is obtained with matric suction than with water content (or degree of saturation). Gradually, as the ψ increases, the capillary menisci between the solid particles increases, causing an increase in inter-capillary forces and, therefore, the SRM.

Sawangsurya et al. (2009) studied the effect of ψ on the Mr of soils used in working platforms compacted at different water contents and note that the Mr increases with increase in ψ. Sawangsurya et al. (2009) also note that the SRM normalized to the SRM determined at the

optimum water content or saturation varies logarithmically with ψ. Figure B-10 shows the variation of SRM normalized with respect to SRM measured at the optimum water content, depending on the ψ. It indicates that Mr is correlated more to ψ than compaction water content (for resilient modulus test) because ψ depends on the stress state and it is well known that the modulus is controlled by the stress state (Seed et al. 1967; Hicks and Monismith 1970; Uzan 1985). This suggests that for pavement design, defining an equilibrium matric suction is more appropriate than defining an equilibrium water content or degree of saturation (Sawangsurya et al. 2009). An empirical correlation equation (Eq. B-19) of the resilient modulus ratio was developed from the data. All tested materials are combined into only a single regression equation, expressed as follow:

$$\mathrm{MR}_{\mathrm{opt}} = \frac{\mathrm{SRM}}{\mathrm{S}RM_{\mathrm{opt}}} = 0.385 + 0.267 \log \psi \qquad \text{(Eq. B-19)}$$

$$\mathrm{R}^2 = 0.80$$

where MR_{opt} is the resilient modulus ratio at optimum as stipulated in the M-EPDG (NCHRP 2004) for incorporating changes in resilient modulus due to climatic effects in pavement design. This normalization using SRM_{opt} is more practical because resilient modulus is mostly measured at optimum water content according to NCHRP 1-28A protocol. The slope of Eq. B-19 represents the average rate of increase of resilient modulus ratio with increasing suction. Bandia Limestone tends to be more sensitive to changes in water content and thus to matric suction. This normalization is more practical because in the field, moisture conditions do not remain near optimum during the pavement life (Sawangsurya et al. 2009).

Table B-5 Summary of *w*, θ, *Sr* and *SRM* of unbound aggregates from Senegal

Test specimen	Water content, w%	Volumetric water content, θ	Degree of saturation, Sr	Matric suction, ψ (kPa)	Summary resilient modulus, SRM (MPa)
Bakel Red Quartzite	2.84	0.06	0.22	30	200
	5.28	0.11	0.38	18	166
	6.33	0.13	0.46	8	150
Bakel Black Quartzite	2.55	0.05	0.18	33	196
	4.5	0.1	0.33	16	140
	6.1	0.13	0.48	8	130
Diack Basalt	2	0.05	0.16	45	282
	4.23	0.1	0.35	3.5	218
	5.55	0.12	0.49	0.3	200
Bandia Limestone	5.5	0.11	0.46	80	369
	7.6	0.15	0.62	8	204
	9	0.18	0.79	2.7	163
Bargny Limestone	7.75	0.14	0.09	-	215
	8.01	0.15	0.08	-	194
	12.33	0.25	0.14	-	86

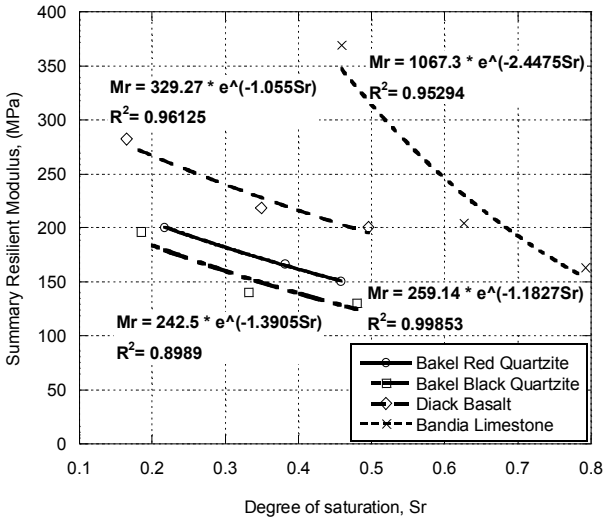

Figure B-8 Resilient Modulus as a Function of Degree of Saturation

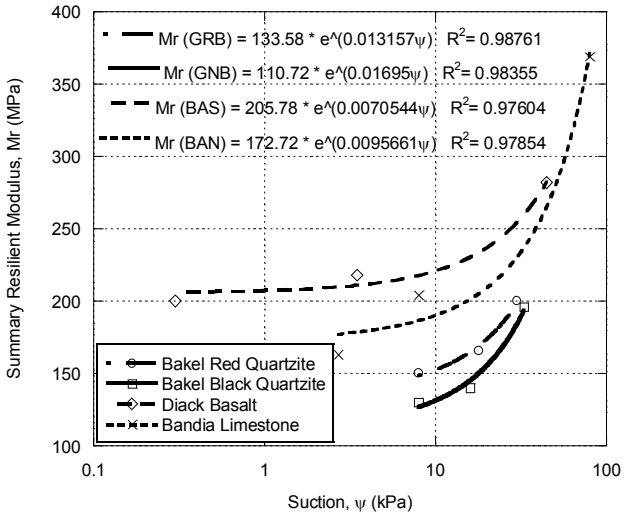

Figure B-9 Resilient Modulus vs Matric Suction on a Semi-Logarithmic Scale

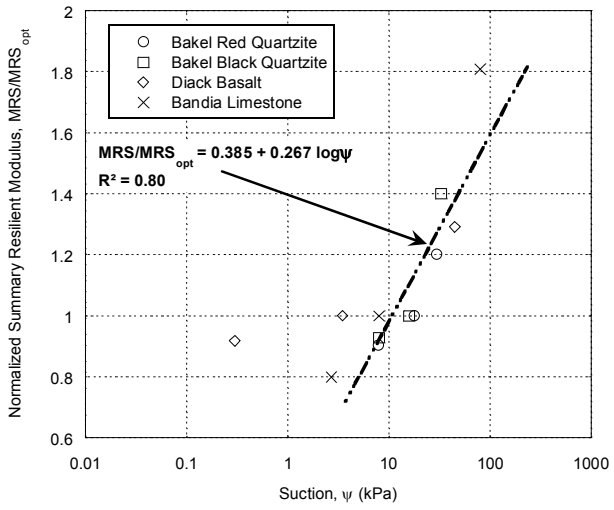

Figure B-10 Normalized Summary Resilient Modulus vs. Matric Suction

B-6 CONCLUSIONS

The results from this study were used to highlight the elastic behavior of aggregates tested as a function of suction, which represents the environmental factors that need to be accounted for in the Mechanistic-Empirical Pavement Design Guide (M-EPDG). The relationship between suction (ψ) and summary resilient modulus (SRM), was developed based on measurement of the SWCC. Bakel Quartzites are characterized by a rapid drainage of water by gravity beginning at very low levels of suction (ψ < 0.1 kPa). The Diack Basalt, by contrast, is characterized by a dramatic drop in the volumetric water content when ψ is close to 0.1 kPa. This "collapse" is due to the coexistence of "large pores" and "small pores". These two behaviors are characteristic of non-cohesive granular materials, where water is drained mainly by gravity, and a small amount is retained by matric suction. The Bandia and Bargny limestones are characterized by a higher water-holding capacity. In these aggregates, much of the water is retained by matric suction and controls material behavior. These two behaviors explain why the modulus of Bandia and Bargny limestones was more sensitive to water content than for Diack Basalt or Bakel Quartzite. The shape of the SWCC depends on the particle size distribution, but depends also on the cementation properties from dehydration of the aggregates. Results show that the SRM was more correlated with ψ than with compaction water content (for resilient modulus test) because *in situ* ψ depends on the stress state, and the modulus also depends on stress state. The two empirical models such as Parera et al. (2005) and M-EPDG (NCHRP, 2004) models tend to underestimate the SWCC and cannot provide reasonable estimation. Empirical equations are proposed to estimate SRM from the ψ. The limestone tends to be more sensitive to changes in water content and thus to matric suction. Fredlund and Xing (1994) and van Genuchten (1980) model parameters for the tested aggregates are reported for implementation in the M-EPDG.

B-7 ACKNOWLEDGEMENTS

Support for this study was provided by the “Entreprise Mapathé Ndiouck SA” (Senegal). The Geological Engineering (GLE) group of the University of Wisconsin-Madison (USA) is also acknowledged for the valuable input in this research study.

B-8 REFERENCES

ASTM D1557 (2009) Standard Method for Laboratory Compaction Characteristics of Soil Using Modified Effort (56,000 ft-lb/ft^3 (2,700 kN-m/m^3). Annual Book of ASTM Standards, ASTM International, West Conshohocken, PA, www.astm.org

ASTM D6836 (2008) Standard test Method for Determination of the Soil Water Characteristic curve for Desorption Using Hanging Column, Pressure Extractor, Chilled Mirror Hygrometer, or Centrifuge. Annual Book of ASTM Standards, ASTM International, West Conshohocken, PA, www.astm.org

Ba M, Fall M, Samb F, Sarr D, Ndiaye M (2011) Resilient Modulus of Unbound Aggregate Base Courses from Senegal (West Africa). Open Journal of Civil Engineering, Vol. 1, No. 1, 2011, pp. 1-6. doi:10.4236/ojce.2011.11001

Ba M, Fall M, Sall OA, Samb F (2012) Effect of Compaction Moisture Content on the Resilient Modulus of Unbound Aggregates from Senegal (West Africa). Geomaterials, Vol. 1, No. 2, pp. 19-23. doi:10.4236/gm.2012.21003

Brown SF, Selig ET (1991) The design of pavement and rail track foundations. Cyclic loading of soils: From theory to design, M. P. O’Reilly and S. F. Brown, eds., Blackie and Son Ltd., Glasgow, Scotland, 249–305

Edil TB, Motan SE and Toha FX (1981) Mechanical Behavior and Testing Methods of Unsaturated Soils. Laboratory Shear Strength of Soil, ASTM STP 740, Philadelphia, PA, pp. 114-129

Edil T, Benson C, Sawangsuriya A (2007) Pavement Design Using Unsaturated Soil Technology. Report N° MN/RC-2007-11, Minnesota Department of Transportation 395 John Ireland Boulevard Mail Stop 330 St. Paul, Minnesota 55155

Fall M, Sawangsuriya A, Benson CH, Edil TB, Bosscher PJ (2007) On the Investigations of Resilient Modulus of Residual Tropical Gravel Lateritic Soils from Senegal (West Africa). Geotechnical and Geological Engineering Journal. Volume 26, Number 1 / February 2008

Fredlund DG, Xing A (1994) Equation for the soil-water characteristic curve. Canadian Geotechnical Journal, Vol. 31, No. 4, pp. 521-532

Hicks RG, Monismith CL (1970) Factors Influencing the Resilient Properties of Granular Materials. Ph.D. Thesis, University of California, Berkeley

Lekarp F, Isacsson U, Dawson A (2000) State of the Art. I: Resilient Response of Unbound Aggregates. Journal of Transportation Engineering, Vol. 126, No. 1, pp. 66-75

Likos WJ, Lu N (2004) Hysteresis of Capillary Stress in Unsaturated Granular Soil. Journal of Engineering Mechanics, Vol. 130, No. 6, June 1, 2004. ©ASCE, ISSN 0733-9399/2004/6-646–655

NCHRP (2004) Guide for Mechanistic-Empirical Design of Pavement Structures. National Cooperative Highway Research Program. *ARA, Inc.*, ERES Consultants Division, Champaign, IL

Nokkaew K, Tinjum JM, Benson CH (2012) Hydraulic Properties of Recycled Asphalt Pavement and Recycled Concrete Aggregate. GeoCongress 2012, ASCE, Oakland, CA 2012, pp. 1476-1486

Perera YY, Zapata CE, Houston WN, Houston SL (2005) Prediction of the Soil-Water Characteristic Curve Based on Grain-Size-Distribution and Index Properties. GSP 130 Advances in Pavement Engineering, ASCE

Roberson R, Siekmeier J (2002) Determining Material Moisture Characteristics for Pavement Drainage and Mechanistic Empirical Design. Research Bulletin. Minnesota Department of Transportation. Office of materials & road research

Sauer EK and Monismith CL (1968) Influence of Soil Suction on Behavior of a Glacial Till Subjected to Repeated Loading. Highway Research Record, No. 215, Washington, D.C., pp. 18-23

Sawangsuriya A, Edil TB, Benson CH (2009) Effect of Suction on Resilient Modulus of Compacted Fine-Grained Subgrade Soils. Transportation Research Record: Journal of the Transportation Research Board, N°. 2101, Transportation Research Board of the National Academies, Washington, D.C., 2009, pp. 82–87. DOI: 10.3141/2101-10

Seed HB, Mitry FG, Monismith CL, Chan CK (1965) Predictions of pavement deflection from laboratory repeated load tests. Rep. No. TE-65-6, Soil Mech. and Bituminous Mat. Res. Lab., University of California, Berkeley, Berkeley, Calif

Thom NH, Brown SF (1988) The effect of grading and density on the mechanical properties of a crushed dolomitic limestone. Proc., 14th ARRB Conf., Vol. 14, Part 7, 94–100

Tinjum JM, Benson CH, Blotz LR (1997) Soil-Water Characteristic Curves for compacted clays. J. Geotech. Geoenviron. Eng., 123(11), 1060-1069

Uzan J (1985) Characterization of Granular Material. Transportation Research Board, Washington, pp. 52-59

van Genuchten M (1980) A close-form equation for predicting the hydraulic conductivity of unsaturated soils. Soil. Sci. Am. J., 44, 892-898

van Genuchten M, Leij F, Yates S (1991) The RETC code quantifying the hydraulic functions of unsaturated soils. Rep. N°. EPA/600/2-91/065, U.S. EPA, Office of Research and Development, Washington, D.C.

Vuong B (1992) Influence of density and moisture content on dynamic stress-strain behaviour of a low plasticity crushed rock. Rd. and Transp. Res., 1(2), 88–100

Zapata CE, Houston WN, Houston SL, Walsh KD (2000) Soil-Water Characteristic Curve Variability. In: C. D. Shackelford, S. L. Houston, and N-Y Chang (eds). Advances in Unsaturated Geotechnics. ASCE – GEO Institute Geotechnical Special Publication, No 99. Also Proceedings of Sessions of Geo-Denver 2000, Aug. 5-8, 2000, Denver, CO. pp. 84-124

Zapata CE (1999) Uncertainty in Soil-Water-Characteristic Curve and Impacts on Unsaturated Shear Strength Predictions. PhD Dissertation, Arizona State University, Arizona, USA

Yang SR, Huang WH and Tai YT (2005) Variation of Resilient Modulus with Soil Suction for Compacted Subgrade Soils. Transportation Research Record, No. 1913, Washington, D.C., pp. 99-106